Remodeling of nucleoprotein complexes by a Type ISP restriction-modification enzyme LlaBIII

A Thesis submitted in partial fulfilment of the requirements

for the degree of

Doctor of Philosophy

By

Sujata S. Gaiwala Sharma

20153388

INDIAN INSTITUTE OF SCIENCE EDUCATION AND RESEARCH, PUNE

2025

Remodeling of nucleoprotein complexes by a Type ISP restriction-modification enzyme LlaBIII

विद्या वाचस्पति की

उपाधि की अपेक्षाओं की आंशिक पूर्ति में प्रस्तुत शोध प्रबंध

A thesis submitted in partial fulfilment of the requirements of the degree of Doctor of Philosophy

द्वारा / By

सुजाता गायवाला शर्मा / **Sujata S Gaiwala Sharma**

पंजीकरण सं. / Registration No.:20153388

शोध प्रबंध पर्यवेक्षक / Thesis Supervisor:

Prof. Saikrishnan Kayarat

भारतीय विज्ञान शिक्षा एवं अनुसंधान संस्थान पुणे

INDIAN INSTITUTE OF SCIENCE EDUCATION AND RESEARCH PUNE

2024

I would like to dedicate my thesis to my precious Nani – my woman of steel

CERTIFICATE

Certified that the work incorporated in the thesis entitled "**Remodeling of nucleoprotein complexes by the Type ISP restriction-modification enzyme LlaBIII**" submitted by **Ms. Sujata S Gaiwala Sharma**, was carried out by the candidate, under my supervision. The work presented here or any part of it has not been included in any other thesis submitted previously for the award of any degree or diploma from any other University or institution.

Date: 16/01/2025

Prof. Saikrishnan Kayarat

Supervisor

DECLARATION

Name – Sujata S Gaiwala Sharma

Registration no. - 20153388

Supervisor – Prof. Saikrishnan Kayarat

Department – Biology, IISER, Pune

Date of joining program – 01 August 2015

Date of presynopsis seminar – 06 December 2024

Title of thesis – Remodeling of nucleoprotein complexes by a Type ISP restriction-modification enzyme LlaBIII

I declare that this written submission represents my idea in my own words and where others' ideas have been included; I have adequately cited and referenced the original sources. I declare that I have acknowledged collaborative work and discussions wherever such work has been included. I also declare that I have adhered to all principles of academic honesty and integrity and have not misrepresented or fabricated or falsified any idea/data/fact/source in my submission. I understand that violation of the above will be cause for disciplinary action by the Institute and can also evoke penal action from the sources which have thus not been properly cited or from whom proper permission has not been taken when needed.

The work reported in this thesis is the original work done by me under the guidance of Prof. Saikrishnan Kayarat.

Sujata S. Gaiwala Sharma

Sujata

Date: 16/01/2024

Registration no. 20153388

Acknowledgements

I would like to express my sincere gratitude to my supervisor Prof. Saikrishnan Kayarat, without his guidance and support, this project would not have reached this level of accomplishment. He was always available to discuss and overcome the challenges of the project by providing valuable inputs in the experiments and critically analyzing the results, which helped immensely in progress of this project. I appreciate his wit, knowledge and expertise in areas of structural biology, molecular biology and protein biochemistry. I have particularly learned a lot from his ability to critically analyze my data and point out interesting facts that I would have easily missed in my analysis. Our discussions have guided me through my PhD and given my project a constructive direction. His guidance has taught me to look at my data in an unbiased way and has been a learning experience on how to be scientifically sound.

I am sincerely grateful to IISER, Pune for giving me the opportunity to work here and providing premium infrastructure for carrying out my research. I thank Bio-managers, who ensured smooth functioning of labs during my Ph.D.

I would like to thank the University Grants Commission (UGC) for providing me the financial support during my Ph.D. tenure. I would also like to specially thank the Women in Science Committee (WISC) 2022-2023 for providing me financial support for four months after my UGC fellowship expired.

I thank my RAC members Dr. Jomon Joseph, Dr. Gayathri Pananghat and Dr. Krishanpal Karmodiya for their regular discussions and expert advice during RAC meetings. I thank Prof. Itzhak Fishov (Emeritus), Ben-Gurion University of the Negev, Israel, for kindly providing us an E. coli strain for our experiments.

I sincerely thank Dr. Gayathri Pananghat, her present and past lab members for their valuable inputs and discussions during the regular combined lab meetings.

I would like to especially thank Dr. Krishanpal Karmodiya and Dr. Mukul Rawat for their help and guidance during the mammalian cell culture experiments.

I thank the support and contributions of my lab members (present and past) throughout the tenure of my Ph.D.

I am grateful for the support of my batchmates Dr. Ankita Sharma and Dr. Shalaka Patil during my tenure here.

Lastly, I would like to thank my family for always being there for me. I thank my Nani for instilling in me the strength that she herself has lived with. I thank my mother, brother and my maternal family for taking me in and giving my life a positive direction from a young age. I would not have achieved anything worthwhile without their unwavering support. I thank my

late father for always having faith in me and enabling me to be an independent woman. I thank my husband's family for being so welcoming, supportive and encouraging in both my personal and professional life. Last but never the least, I thank my husband and son for their unconditional and unfaltering support through thick and thin. I thank them for reminding me every day of the most important things in life and for inspiring me to keep doing better as an individual.

Sujata

Table of contents

List of figures and tables i

Abbreviations iv

Synopsis viii

Chapter 1 – Introduction to restriction modification enzymes, chromatin remodeling complexes and nucleoid associated proteins 1

1.1 Bacteria and the bacteriophages 2

1.2.1 Restriction-modification systems 5

1.2.2 Type I restriction enzymes 7

1.3.1 Chromatin remodelers 9

1.3.2 Proposed mechanisms of nucleosome remodeling 15

1.3.3 The role of ATPase in chromatin remodeling 16

1.4.1 Bacterial nucleoid compaction 17

1.4.2 Nucleoid associated proteins (NAPs) 20

1.5 Aim of this study 21

1.6 Objectives 22

1.7 References 24

Chapter 2 – LlaBIII, a Type ISP RM enzyme, can displace mononucleosomes from their positions on DNA 31

2.1 Introduction 32

2.2 Materials and methods 35

2.2.1 Preparation of DNA substrate 35

2.2.2 Purification of human histones 36

2.2.3 Assembly and purification of octamer..... 37

2.2.4 Purification of LlaBIII..... 37

2.2.5 Reconstitution of nucleosome particles..... 38

2.2.6 Restriction Enzyme Accessibility Assay (REAA)..... 39

2.3 Results..... 39

2.3.1 Purification of human histones and assembly of octamer..... 39

2.3.2 Reconstitution of terminally and centrally placed mononucleosomes..... 42

2.3.3 Displacement of mononucleosomes from DNA by LlaBIII..... 47

2.4 Discussion..... 49

2.5 References..... 51

Chapter 3 – Nucleosome remodeling is exclusively the property of active DNA translocases..... 57

3.1 Introduction..... 58

3.2 Materials and methods..... 60

3.2.1 Preparation of DNA for dinucleosome assembly..... 60

3.2.2 Purification of histones and assembly of histone octamer..... 61

3.2.3 Purification of LlaBIII WT, LlaBIIIR564A and LlaBIII n-..... 61

3.2.4 Purification of EcoP1IE916A 61

3.2.5 Reconstitution of dinucleosome and determination of nucleosome position on the DNA.....61

3.2.6 Restriction enzyme accessibility assay (REAA) with dinucleosome..... 62

3.3 Results..... 62

3.3.1 Preparation of dinucleosome..... 62

3.3.2 REAA with dinucleosome and LlaBIII WT..... 64

3.3.3 REAA with dinucleosome and EcoP1I..... 66

3.3.4 REAA with dinucleosome and LlaBIII n-..... 67

3.3.5 REAA with dinucleosome and LlaBIIIR564A..... 69

3.3.6 REAA with methylated dinucleosome..... 70

3.4 Discussion..... 75

3.5 References..... 78

Chapter 4 – Mechanism of nucleosome remodeling by LlaBIII..... 81

4.1 Introduction..... 82

4.2 Materials and methods..... 83

4.2.1 Preparation of Cy5-labelled DNA substrates for nucleosome assembly..... 83

4.2.2 Mono and dinucleosome assembly..... 84

4.2.3 Electrophoretic mobility shift assay (EMSA) 84

4.2.4 Time dependent REAA with HhaI, NdeI and BamHI..... 84

4.3 Results..... 86

4.3.1 Time dependent remodeling EMSA with mono and dinucleosomes..... 88

4.3.2 Time dependent REAA with dinucleosome - HhaI..... 97

4.3.3 Time dependent REAA with dinucleosome – NdeI 100

4.4 Discussion..... 103

4.5 References..... 105

Chapter 5 – Effect of LlaBIII on protein-DNA interactions in bacterial and mammalian cells..... 107

5.1 Introduction..... 108

5.2 Materials and methods..... 109

5.2.1 Cloning of LlaBIII mutants 109

5.2.2 Methylation assay..... 110

5.2.3 Microscopy..... 110

5.2.4 Culture and transfection of HEK293 cells 111

5.2.5 Fluorescent in-situ hybridization..... 112

5.2.6 Immunoblotting 112

5.2.7 RNA extraction and cDNA synthesis 113

5.2.8 Quantitative real-time PCR 113

5.3 Results..... 113

5.3.1 LlaBIII methylates an adenine in its target site, in vivo 113

5.3.2 Effect of LlaBIII on bacterial nucleoid..... 117

5.3.3 Expression of LlaBIII constructs in HEK293 cells..... 122

5.3.4 Quantitative RT-PCR to monitor changes in transcription from the specific gene loci. 125

5.4 Discussion..... 126

5.5 References..... 131

List of figures and tables

Table 1: DNA oligos used for the study..... vi

Figure 1.1: The life cycle of a bacteriophage..... 3

Figure 1.2: Restriction-modification systems..... 3

Figure 1.3: Restriction-modification (RM) enzyme families and subunit compositions for methyl-transferase activity and DNA cleavage activity..... 5

Figure 1.4: Structure of LlaBIII in complex with a 28 base pair DNA containing the specific target site..... 6

Figure 1.5: Model for loop-independent DNA translocation and DNA cleavage by LlaBIII... 7

Figure 1.6: Classification and hierarchy of helicase like proteins, specifically the superfamily 2 of helicases..... 9

Figure 1.7: Chromatin remodeler families and their ATPase domain organization..... 11

Figure 1.8: Outcomes of chromatin remodeling processes and the chromatin remodelers that perform them..... 12

Figure 1.9: Proposed models for nucleosome remodeling..... 13

Figure 1.10: Mechanistic details of twist defect model..... 14

Figure 1.11: Mechanistic details of loop propagation models..... 15

Figure 1.12: Schematic representation of the bottle brush model for bacterial nucleoid organization..... 18

Figure 1.13: Nucleoid associated proteins..... 19

Figure 1.14: Flow chart elaborating the objectives of this study..... 23

Figure 2.1: Overexpression and purification of human histones H2A, H2B, H3 and H4..... 41

Figure 2.2: Purification of assembled octamer..... 42

Figure 2.3: Design of the mononucleosome substrates..... 43

Figure 2.4: Reconstitution of nucleosomes *in vitro*..... 44

Figure 2.5: Domains of LlaBIII and their enzymatic activities 45

Figure 2.6: Restriction enzyme accessibility assay (REAA) design.....46

Figure 2.7: Nucleosome remodeling by LlaBIII..... 48

Figure 3.1: Design of the dinucleosome..... 63

Figure 3.2: Nucleosome positioning check..... 64

Figure 3.3: REAA with dinucleosome..... 65

Figure 3.4: REAA with dinucleosome and EcoP1IE916A..... 67

Figure 3.5: REAA with dinucleosome and LlaBIII n-..... 68

Figure 3.6: REAA with dinucleosome and LlaBIIIR564A..... 70

Figure 3.7: REAA with methylated dinucleosome..... 73

Figure 4.1: Possible mechanisms for nucleosome displacement by LlaBIII..... 86

Figure 4.2: Nucleosome positions observed on native polyacrylamide gel..... 87

Figure 4.3: Time dependent EMSA with centrally placed mononucleosome and LlaBIII..... 91

Figure 4.4: Time dependent EMSA with dinucleosome and LlaBIII..... 94

Figure 4.5: Graphical representation of the 5'-cy5 labeled dinucleosome construct..... 96

Figure 4.6: Time dependent REAA with HhaI and LlaBIII..... 99

Figure 4.7: Time dependent REAA with NdeI and LlaBIII..... 102

Figure 5.1: MTase activity of LlaBIII WT and mutants in different E. coli..... 115

Figure 5.2: ATPase activity of LlaBIII mutants.....116

Figure 5.3: Effect of LlaBIII mutants on bacterial nucleoid and HU localization.....119

Figure 5.4: Bacterial nucleoid morphology and HU localization..... 120

Figure 5.5: Quantitation of HU localization..... 121

Figure 5.6: Quantitation of HU displacement from the nucleoid..... 122

Figure 5.7: Localization of LlaBIII mutants in HEK293 cells..... 123

Figure 5.8: Immunoblots blots showing full length expression of LlaBIII mutants in HEK293 cells..... 124

Figure 5.9: Quantitative RT-PCR showing gene transcription in LlaBIII mutants' transfected HEK293 cells..... 125

Figure 5.10: Schematic elaborating possible applications of Type I RM enzymes as targeted chromatin remodelers..... 128

Abbreviations

ºC	Degree Celsius
µl	Microliters
µm	Micrometers
µM	Micromolar
nM	Nanomolar
mg	Milligram
mL	Millilitre
ADP	Adenosine diphosphate
ATP	Adenosine triphosphate
bp	Base pair
dsDNA	Double stranded deoxyribonucleic acid
DNA	Deoxyribonucleic acid
Nuc	Nucleosome
DTT	Dithiothreitol
E. coli	Escherichia coli
EDTA	Ethylenediaminetetraacetic acid
EMSA	Electrophoretic mobility shift assay
HsdM	Host specificity for DNA modification
HsdR	Host specificity for DNA restriction
HsdS	Host specificity for DNA specificity

IPTG	Isopropyl β-D-1-thiogalactopyranoside
kDa	Kilodalton
MTase	Methyltransferase
PAGE	Polyacrylamide gel electrophoresis
PCR	Polymerase chain reaction
RM	Restriction-modification
SDS	Sodium dodecyl sulphate
SF2	Superfamily 2
REA	Restriction enzyme accessibility
FISH	Fluorescent *in-situ* hybridization

Table 1: DNA oligos used in the study

Name	Sequence (5'-3')
329F	CGAGGGGTAGGCCGCATCCTAATGACCTAATCAGACCTGAGCCTTCACACCG
329R	CGAATTCGAGCTCGGTACCC
Cy5oligo-498-AdaptorF	CCCGTAGTGCTGTGCTGATAATCAGACCTGAGCCTTC
Cy5-F	TGGACACGACTTGAGCCCTCCTCACTTTCTTCCTCACCCGTAGTGCTGTGCTGA
601R	ACAGGATGTATATATCTGACACG
F1 overlap	GCATCTGCATATGTATCCCGCCCTGGAGAATCCCGG
R1 overlap	GGCGGGATACATATGCAGATGCACAGGATGTATATATC
LBΔN-pHIS-F	CTTTAAGAAGGAGATATACATATGCGTCCAGAAAATGTTGTTG
LB-PHIS-R	CGCAGCAGCGGTTTCTTTACCAGACTCGAGTTATAGTCCCTGTACTA CTCTTG
T7-F	TAATACGACTCACTATAGGG
T7-R	GCTAGTTATTGCTCAGCGG
LB-N1017D-F	CCAATTACTGTAATTATGGGGGATCCACCCTATTCTGCAAAAC
LB-WalkerA-R	GACTAGTAAATGTTGCTCCTGTACCTGGTGC
LBdN-pCMV10-F	ATGACAAGCTTGCCCCCAAGAAGAAGAGAAAGGTGGGCAGAGGCCGTCCAGAAAATGTTGTTG

Table 1 – Oligos used in this study

LBdN-pCMV10-R	GCGCGGATCCCTACTCTTGAATCTCAAATTC
HEXIM1-F	CCAAGAAGAAGCGGCATTGG
HEXIM1-R	ACTGCGTGGTGTTATAGGGC
HIST1H2BC-F	GTGACCAAAGCGCAGAAGAA
HIST1H2BC-R	TGGAAGAGATGCCAGTGTCG
ZXDA-F	TGAAGATGCACCTGCTGACG
ZXDA-R	CCGAAGGGCCGCAGTTTATC
SF3B5-F	AGTCCAAGTACATCGGCACG
SF3B5-R	CTCGCGCTTTGCTCTCATTC
RNF26-F	ATGGCCATCCTCCTTTGGAC
RNF26-R	AGTCCGGATGCAACACAGTC
ZNF830-F	TTAAGAGCGAGCTCCTGTGG
ZNF830-R	ACATCTTGGTCGTCTGCGTC
GAPDH-F	CTGCACCACCAACTGCTTAG
GAPDH-R	GTCTTCTGGGTGGCAGTGAT
SP1-F	GGCTGGCAGATCATCTCTTC
SP1-R	CACAACATACTGCCCACCAG

Table 1 – Oligos used in this study

Synopsis

Chapter 1 – Introduction to restriction modification enzymes, chromatin remodeling complexes and nucleoid associated proteins.

Bacteria are unicellular prokaryotes that are prevalent in nearly all ecosystems on earth. Their occurrence is not without challenges from pathogens such as viruses called bacteriophages. The bacteriophages infect bacteria and take over the bacterial cellular machinery to produce its own copies ultimately killing the bacterial cells. The bacteria have thus evolved various strategies to evade bacteriophage attacks. Some are physiological barriers whereas some are molecular barriers that prevent the phage genetic material to survive in the bacterial cells. One such mechanism involves the restriction-modification (RM) systems which perform two major activities – DNA methylation and DNA cleavage. Broadly these enzymes methylate the bacterial DNA at specific target sites which allows these to be recognized as self-DNA and cleave any foreign DNA that does not possess methylated bases at the specific target sites (Dryden et al., 2001). The RM systems are composed of a methyl-transferase, that methylates the DNA and a restriction endonuclease that nucleolytically cleaves an unmodified DNA. These enzymes have a target recognition domain that recognizes and binds to a specific DNA sequence called target site which allows activation of the methyl-transferase or nucleolytic activity. Restriction enzymes have been categorized into four broad categories - Type I, Type II, Type III and Type IV - based on subunit composition, nucleoside preference, cofactor requirements, preference for methylated or un-methylated target sequence and DNA cleavage tendencies (Loenen et al., 2014a; 2014b).Type ISP is a sub-class of Type I RM enzymes, which is made of a single polypeptide. We have focused on the Type ISP and Type III RM enzymes in this study. Type ISP and Type III RM enzymes are ATP dependent enzymes and utilize ATP for bringing about DNA cleavage. Both these categories of RM enzymes possess a highly conserved ATPase motor domain that can hydrolyze ATP (Lapkouski et al., 2007; Loenen et al., 2014b; McClelland S. E. and Szczelkun, 2004). Upon recognition of a specific unmethylated target site the ATPase motor is activated and ATP is hydrolyzed which allows these enzymes to move on the DNA away from the target site. Both Type ISP and Type III RM enzymes recognize two head-to-head oriented target sites that can be separated by thousands of base pairs of DNA, and cleave the DNA in between the two target sites. While the Type ISP

RM enzymes actively translocate DNA constantly hydrolyzing ATP (Chand et al., 2015; Šišáková et al., 2013; Van Aelst et al., 2015), Type III RM enzymes utilize ATP only in an initial burst, following which they diffuse bi-directionally on the DNA (Ahmad et al., 2018; Tóth et al., 2015). The motor that facilitates the ATP powered movement on DNA belongs to the superfamily 2 (SF2) of helicase-like proteins. Another subfamily of proteins classified under the SF2 helicases are the eukaryotic chromatin remodelers. The chromatin remodelers are multi-subunits complexes that are involved in maintenance of chromatin structure, nucleosome occupancy and histone composition. Depending on the cellular ques, these complexes regulate the nucleosome spacing, allow histone exchange and displace nucleosomes to allow DNA binding proteins to access DNA wrapped around the nucleosomes (Clapier & Cairns, 2009). At the core of the chromatin remodeling complexes is an ATPase motor similar to that of the Type ISP and Type III RM enzymes (Mueller-Planitz, Klinker, & Becker, 2013). As these functionally distinct enzymes share the same evolutionarily conserved ATPase motor which forms the core of these enzymes, we asked whether the RM enzymes can perform nucleosome remodeling similar to the chromatin remodelers. To address this, we decided to test nucleosome remodeling activity of the RM enzymes - LlaBIII, a Type ISP RM enzyme and EcoP1I, a Type III RM enzyme.

Chapter 2 - LlaBIII, a Type ISP RM enzyme, can displace mononucleosomes from their positions on DNA

In order to test whether the Type I and Type III RM enzymes can remodel nucleosomes, we sought to perform *in vitro* nucleosome remodeling studies. Therefore, we prepared stable nucleosome complexes *in vitro*. First, we purified individual human histone proteins (H2A, H2B, H3 and H4) to high degree of purity using the rapid histone purification protocol (Klinker et al., 2014). Here the histones were purified under denaturing conditions throughout the purification process, finally eluted with 15mM Tris Cl and stored as lyophilized powder. For octamer reconstitution, the histone powders were reconstituted with an unfolding buffer containing guanidium hydrochloride and mixed in equimolar ratio. The histone mixture was dialyzed overnight against a buffer containing 2 M NaCl. This allowed the histones to refold into an appropriately folded octamer complex which was then purified through size exclusion chromatography. The fractions containing properly refolded octamer were pooled and

concentrated for further use in nucleosome reconstitutions. Simultaneously the DNA required for nucleosome reconstitution was generated through PCR amplification. The DNA was designed to contain a single LlaBIII target site upstream from a nucleosome positioning sequence called 601or Widom sequence (Lowary & Widom, 1998). This allowed us to design two types of nucleosomes, one with octamer positioned on the terminal end and other with a centrally positioned nucleosome. The nucleosomes were reconstituted through salt dilution method as given by Dyer et al (Dyer et al., 2003). Nucleosome remodeling by the Type I RM enzyme, LlaBIII was tested using the restriction enzyme accessibility (REA) assay. In short, this assay utilizes the presence of the target site for a Type II restriction enzyme (HhaI), in the center of the 601 sequence. As the 601 sequence wraps around the octamer to form a nucleosome, the HhaI site gets sequestered. Thus, HhaI cannot access its target site and cleave the DNA until the octamer is displaced. The DNA fragments formed as a result of HhaI cleavage can be tracked through polyacrylamide gel electrophoresis. When the nucleosome was mixed with HhaI and LlaBIII in absence of ATP, LlaBIII binds to its target site upstream of the nucleosome but cannot translocate DNA and thus cannot affect the nucleosome positions. Upon addition of ATP, LlaBIII translocates DNA directionally and encounters the nucleosome downstream. We saw an increase in HhaI cleaved DNA fragments upon ATP addition indicating LlaBIII could displace nucleosome and allow HhaI access to the DNA wrapped around the octamer. We saw that both the terminally placed nucleosome and the centrally positioned nucleosomes were remodeled efficiently by LlaBIII. Thus, LlaBIII mediated nucleosome remodeling is not hampered by presence of a DNA overhang as that present in case of centrally positioned nucleosome.

Chapter 3 – Nucleosome remodeling is exclusively the property of active DNA translocases

Having shown that LlaBIII, a Type ISP RM enzyme can displace both terminally placed and centrally placed mononucleossomes, we intended to increase the nucleosome substrate complexity. For this we designed a dinucleosome substrate where in the 601 regions were duplicated separated by a 22 bp linker DNA. Both the 5’ and 3’ DNA overhangs were same as those designed for the centrally positioned mononucleosome. A LlaBIII target site was positioned upstream of the first 601 region. Both the 601 regions had the HhaI target sites in the center, whereas target sites for other Type II restrictions enzymes were also present in the

center of the linker DNA (NdeI) and at the beginning of the first 601 region (NotI). The dinucleosome was assembled using the same protocols as used for the mononucleosomes. The quality of the nucleosome positions in the dinucleosome was assessed using the HhaI, NdeI and NotI target sites. The dinucleosome was exposed to these restriction enzymes individually and the cleavage products were analyzed using polyacrylamide gel electrophoresis. If properly assembled, the HhaI target sites were expected to be completely protected due its sequestration in the nucleosomes, the NdeI being present in the linker region would be completely exposed and the NotI site being present just at the beginning of the nucleosome wrap was expected to be partially accessible. The outcomes of our assay with the dinucleosome and these individual enzymes exhibited outcomes consistent with the above given expectations, hence we could conclude that the dinucleosome was optimally assembled and we proceeded with REA assay. The REA assay was performed similar to that performed with mononucleosomes and the HhaI cleavage of dinucleosome DNA upon ATP addition in presence of LlaBIII was assessed through polyacrylamide gel electrophoresis. We saw an increase in DNA cleavage by HhaI indicating nucleosome displacement by LlaBIII upon ATP addition. We also observed appearance of DNA fragments from cleavage at both the HhaI sites, suggesting stepwise displacement of both the nucleosomes. Next, we tested nucleosome remodeling by a Type III RM enzyme called EcoP1I. EcoP1I also communicates between two unmethylated target sites separated by thousands of base pairs to bring about DNA cleavage. Upon target recognition, EcoP1I gets activated by an initial burst of ATP hydrolysis and begins bidirectional diffusion on DNA (Schwarz et al., 2013). When one such diffusing enzyme encounters another activated but target site bound EcoP1I, the nuclease domain of both enzymes gets activated causing each enzyme to cut one DNA strand resulting in a double stranded break in the DNA (Ahmad et al., 2018). EcoP1I diffuses on DNA rather than actively translocate DNA like LlaBIII. Hence, we sought to test the nucleosome remodeling activity of this diffusing enzyme using the same dinucleosome substrate in the REA assay. For the assay we used a nuclease dead but ATPase active mutant, EcoP1I^{E916A}, as EcoP1I has been shown to catalyze the non-canonical single-site DNA cleavage (Ahmad et al., 2018). In the REA assay, EcoP1I^{E916A} was unable to displace nucleosomes even in presence of ATP. This suggested that nucleosome remodeling required an actively translocating enzyme and a diffusing enzyme cannot displace nucleosomes. Additionally, we tested a nuclease truncated version of LlaBIII, LlaBIII n-, for nucleosome remodeling. We found that the truncation of LlaBIII nuclease domain did not affect its

translocation activity and LlaBIII n- could remodel the dinucleosome at par with the wild type protein. An important motif in the LlaBIII motor domain is the motif V which has been identified as a hot spot for cancer causing mutations in canonical chromatin remodelers (Medina & Sanchez-Cespedes, 2008). Mutation of an arginine residue to alanine (R564A) in LlaBIII has been shown to affect its translocation activity but not the ATPase activity (Chand et al., 2020). LlaBIII^{R564A} was also found to be defective in displacement of triplex oligomer (Chand et al., 2020). We thus tested its nucleosome remodeling activity and found that it could displace nucleosomes at par with the wild type enzyme.

Furthermore, we tested the nucleosome remodeling by all of these enzymes with nucleosomes prepared with methylated DNA. In mammalian cells, the nucleosomes are always associated with cytosine methylated DNA. Hence, we sought to check if the cytosine methylation affects nucleosome remodeling by LlaBIII. We found that LlaBIII and its mutants, LlaBIII n- and LlaBIII^{R564A}, were able to efficiently displace nucleosomes even from methylated DNA whereas EcoP1I^{E916A} could not displace even the methylated nucleosomes.

Chapter 4 – Mechanism of nucleosome remodeling by LlaBIII

Our experiments so far have shown that LlaBIII can displace nucleosomes and open up the wrapped DNA to allow DNA binding proteins access to the sequestered DNA sequences. It was unclear how LlaBIII was able achieve this. The canonical remodelers either slide the nucleosomes or eject the nucleosomes from their positions on DNA. So, we decided to investigate if LlaBIII utilizes either of these two mechanisms to displace nucleosomes. For this we used two methods – time dependent electrophoretic mobility shift assay (EMSA) and time dependent REA assay with HhaI and NdeI. The time dependent nucleosome remodeling reactions with LlaBIII were performed in a staggered manner and the reactions for various specific time points were stopped simultaneously with addition of excess unlabeled competitor DNA and ADP. Further the reactions were split into three fractions, one processed for EMSA and two fractions were individually treated with HhaI and NdeI followed by protein denaturation and analysis of DNA cleavage products using polyacrylamide gel electrophoresis. The assays were performed with both centrally placed mononucleosome and dinucleosome as substrates. The nucleosomes have been shown to segregate into distinct bands based on the

octamer occupancy on the DNA (Fan et al., 2003; Manelyte et al., 2014). When a nucleosome sample is resolved on native polyacrylamide gel, based on octamer occupancy, the nucleosome fractions migrate at different speeds. The most terminally positioned nucleosomes migrate the fastest and the most centrally positioned nucleosomes migrate the slowest. Nucleosomes with intermediate octamer occupancy assume intermittent positions accordingly. Using this information, we tested whether LlaBIII ejected the nucleosomes, which would result in direct conversion of the slow migrating centrally positioned species to fast migrating free DNA or LlaBIII slides the nucleosomes, which would result in appearance of many fast-migrating nucleosome species as the octamers are pushed to more terminal positions as the remodeling reaction proceeds. We observed that upon ATP addition, the slow migrating centrally positioned nucleosomes are gradually converted into fast migrating terminally positioned nucleosomes with an increase in free DNA over time. Similar results were seen for nucleosome remodeling with the dinucleosome substrate. This supported the nucleosome sliding mechanism of nucleosome remodeling by LlaBIII.

Secondly, we performed time dependent REA with HhaI and NdeI with the dinucleosome substrate and LlaBIII. If the octamers are directly ejected from the DNA, both the HhaI sites would be opened up instantaneously and the NdeI site would also remain open through the process. Whereas if the octamers are slid, the HhaI sites would be opened up in a stepwise manner whereas the NdeI site would be occluded as the first octamer gets slid over the linker DNA. We found that upon ATP addition there is a sharp rise in DNA cleavage at both the HhaI sites with a simultaneous decrease in cleavage at NdeI site. These observations again supported the sliding model for nucleosome remodeling by LlaBIII

Chapter 5 – Effect of LlaBIII on protein-DNA interactions in bacterial and mammalian cells

Once established, the targeted nucleosome remodeling activity of LlaBIII could be used for targeted chromatin manipulation in mammalian cells. This would also pave the way for use of other actively translocating Type I RM enzymes to be used as tools for targeted chromatin remodeling. Towards this goal we began testing the effect of LlaBIII on nucleoprotein complexes in both prokaryotic cells (*E. coli*) and mammalian cells (HEK 293 cells). In *E. coli*, the histone like protein, HU, has been implicated in maintenance of nucleoid structure and

function. HU and other proteins similar in structure or function are collectively called nucleoid associated proteins (NAPs). These proteins collectively function similar to eukaryotic nucleosomes, and are directly or indirectly involved in nucleoid structure maintenance and gene regulation in bacteria (Dillon & Dorman, 2010). We utilized an *E. coli* strain that expressed HU-GFP fusion from its native promotor in the genome (Abebe et al., 2017). This strain allowed us to visualize HU localization in *E. coli* cells through fluorescence microscopy. For the *in vivo* experiments we used the nuclease truncated LlaBIII, LlaBIII n-. Furthermore, we have found that LlaBIII methylates its target site *in vivo*, in *E. coli* cells. Binding to a methylated target site does not allow DNA translocation by LlaBIII and would therefore prevent its nucleoprotein remodeling activity. Thus, we created a methyltransferase catalytic mutant, LlaBIII$^{n\text{-}m\text{-}a+}$, which could does not methylate the LlaBIII target sites in *E. coli*. Additionally, we also created an ATPase mutant, LlaBIII$^{n\text{-}m\text{-}a-}$, wherein the Walker A motif was mutated such that the enzyme could not hydrolyze ATP even in presence of specific DNA. We transformed the *E. coli* strain expressing HU-GFP with combinations of these mutants. Cells from the overnight grown cultures were harvested and stained with Hoechst dye to stain the nucleoid and visualized through epi-fluorescence microscopy. The nucleoid position and HU-GFP localization was tracked for individual cells and the distance from the cell center and between Hoechst and HU-GFP foci was plotted against the cell length. We found that as compared to control cells, the cells expressing both LlaBIII$^{n\text{-}m\text{-}a+}$ and LlaBIII$^{n\text{-}m\text{-}a-}$ affected HU-GFP localization. In both the transformants, HU was localized in a sub polar region and it did not co-localize with the nucleoid like the control cells. Hence LlaBIII disrupted HU associated with the nucleoid DNA but it is yet to be determined that this effect was the result of LlaBIII DNA translocation and not simply of its competition with HU for DNA binding as the ATPase defective mutant also affected HU localization. The experimental protocols need to be tweaked and effect of LlaBIII expression on HU and nucleoid need to be monitored as soon as the mutants are introduced in the *E. coli* cells. Time dependent, phase wise tracking of HU localization and nucleoid morphology would allow us to better gauge the effects of LlaBIII on HU-nucleoid interaction.

Finally, we aimed to check if LlaBIII could displace nucleosomes in mammalian cells and affect transcription from gene loci in the vicinity of its target sites. So prepared mammalian expression construct carrying LlaBIII$^{n\text{-}m\text{-}a+}$ and LlaBIII$^{n\text{-}m\text{-}a-}$ fused with an N-terminal 3x-FLAG tag and a SV40-NLS sequence in frame with the coding sequence under the control of CMV

enhancer and promotor. HEK293 cells were transfected with these plasmid constructs individually and the cells were harvested 72 hours post transfection and processed for western blotting, fluorescent *in-situ* hybridization (FISH) and total mRNA extraction for qRT-PCR. For western blotting and FISH, we used anti-FLAG antibodies to detect LlaBIII. Western blot analysis confirmed expression of full length LlaBIII mutants. FISH images also confirmed this finding, although we could observe only ~10-15 percent cells expressing LlaBIII. Nevertheless, when expressed LlaBIII was localized in the nucleus of the cells indicating the NLS sequence we had incorporated was functional. Next, we extracted total mRNA from the cell cultures (un-transfected, LlaBIII$^{n\text{-}m\text{-}a^+}$ and LlaBIII$^{n\text{-}m\text{-}a}$) and performed qRT-PCR to analyze effect of LlaBIII expression on gene transcription in these cells relative to un-transfected cells. We selected single exon genes and mapped LlaBIII target sites in the 5'-UTR, upstream region, gene body and 3'-UTR, downstream region. We did not observe any significant change in transcription from the selected gene loci. Either LlaBIII did not affect gene transcription at these loci in spite of presence of multiple target sites in the vicinity or this lack of change in transcription could be attributed to the low transfection efficiency wherein only 10-15 percent of the total cells took up and expressed LlaBIII at significant levels. We harvested total cell population for mRNA extraction, which potentially diluted the effect of LlaBIII expression on gene perturbation. In future experiments, the cells expressing LlaBIII need to be enriched either by using a selectable marker or by expressing fluorescently tagged version of LlaBIII followed by cell sorting. The enriched culture can then be processed for qRT-PCR to track transcription perturbation at specific loci or for high throughput methods such as RNA seq correlated with ChIP seq. These techniques would allow us to correlate LlaBIII translocation with nucleosome occupancy and perturbation of gene transcription.

References

Abebe, A. H., Aranovich, A., & Fishov, I. (2017). HU content and dynamics in Escherichia coli during the cell cycle and at different growth rates. *FEMS Microbiology Letters*, *364*(19), fnx195. https://doi.org/10.1093/femsle/fnx195

Ahmad, I., Kulkarni, M., Gopinath, A., & Saikrishnan, K. (2018). Single-site DNA cleavage by Type III restriction endonuclease requires a site-bound enzyme and a trans-acting enzyme that are ATPase-activated. *Nucleic Acids Research*, *46*(12), 6229–6237. https://doi.org/10.1093/nar/gky344

Campbell, A. (2003). The future of bacteriophage biology. *Nature Reviews Genetics*, *4*(6), 471–477. https://doi.org/10.1038/nrg1089

Chand, M. K., Carle, V., Anuvind, K. G., & Saikrishnan, K. (2020). DNA-mediated coupling of ATPase, translocase and nuclease activities of a Type ISP restriction-modification enzyme. *Nucleic Acids Research*, *48*(5), 2594–2603. https://doi.org/10.1093/nar/gkaa023

Chand, M. K., Nirwan, N., Diffin, F. M., Van Aelst, K., Kulkarni, M., Pernstich, C., Szczelkun, M. D., & Saikrishnan, K. (2015). Translocation-coupled DNA cleavage by the Type ISP restriction-modification enzymes. *Nature Chemical Biology*, *11*(11), 870–877. https://doi.org/10.1038/nchembio.1926

Clapier, C. R., & Cairns, B. R. (2009). The Biology of Chromatin Remodeling Complexes. *Annual Review of Biochemistry*, *78*(1), 273–304. https://doi.org/10.1146/annurev.biochem.77.062706.153223

Clapier, C. R., Iwasa, J., Cairns, B. R., & Peterson, C. L. (2017). Mechanisms of action and regulation of ATP-dependent chromatin-remodelling complexes. *Nature Reviews Molecular Cell Biology*, *18*(7), 407–422. https://doi.org/10.1038/nrm.2017.26

Dillon, S. C., & Dorman, C. J. (2010). Bacterial nucleoid-associated proteins, nucleoid structure and gene expression. *Nature Reviews Microbiology*, *8*(3), 185–195. https://doi.org/10.1038/nrmicro2261

Dryden, D. T. F., Murray, N. E., & Rao, D. N. (2001). Nucleoside triphosphate-dependent restriction enzymes. *Nucleic Acids Research*, *29*(18), 3728–3741. https://doi.org/10.1093/nar/29.18.3728

Dyer, P. N., Edayathumangalam, R. S., White, C. L., Bao, Y., Chakravarthy, S., Muthurajan, U. M., & Luger, K. (2003). Reconstitution of Nucleosome Core Particles from Recombinant Histones and DNA. In *Methods in Enzymology* (Vol. 375, pp. 23–44). Academic Press. https://doi.org/https://doi.org/10.1016/S0076-6879(03)75002-2

Fan, H.-Y., He, X., Kingston, R. E., & Narlikar, G. J. (2003). Distinct Strategies to Make Nucleosomal DNA Accessible. *Molecular Cell*, *11*(5), 1311–1322. https://doi.org/10.1016/S1097-2765(03)00192-8

Klinker, H., Haas, C., Harrer, N., Becker, P. B., & Mueller-Planitz, F. (2014). Rapid Purification of Recombinant Histones. *PLOS ONE*, *9*(8), e104029-. https://doi.org/10.1371/journal.pone.0104029

Kommireddy, V., & Valakunja, N. (2013). Diverse Functions of Restriction-Modification Systems in Addition to Cellular Defense. *Microbiology and Molecular Biology Reviews*, *77*(1), 53–72. https://doi.org/10.1128/mmbr.00044-12

Längst, G., & Becker, P. B. (2004). Nucleosome remodeling: one mechanism, many phenomena? *Biochimica et Biophysica Acta (BBA) - Gene Structure and Expression*, *1677*(1), 58–63. https://doi.org/https://doi.org/10.1016/j.bbaexp.2003.10.011

Lapkouski, M., Panjikar, S., Kuta Smatanova, I., & Csefalvay, E. (2007). Purification, crystallization and preliminary X-ray analysis of the HsdR subunit of the EcoR124I endonuclease from Escherichia coli. *Acta Crystallographica Section F*, *63*(7), 582–585. https://doi.org/https://doi.org/10.1107/S174430910702622X

Loenen, W. A. M., Dryden, D. T. F., Raleigh, E. A., & Wilson, G. G. (2014a). Type I restriction enzymes and their relatives. *Nucleic Acids Research*, *42*(1), 20–44. https://doi.org/10.1093/nar/gkt847

Loenen, W. A. M., Dryden, D. T. F., Raleigh, E. A., & Wilson, G. G. (2014b). Type i restriction enzymes and their relatives. *Nucleic Acids Research*, *42*(1), 20–44. https://doi.org/10.1093/nar/gkt847

Loenen, W. A. M., Dryden, D. T. F., Raleigh, E. A., Wilson, G. G., & Murrayy, N. E. (2014). Highlights of the DNA cutters: A short history of the restriction enzymes. *Nucleic Acids Research*, *42*(1), 3–19. https://doi.org/10.1093/nar/gkt990

Lowary, P. T., & Widom, J. (1998). *New DNA Sequence Rules for High Affinity Binding to Histone Octamer and Sequence-directed Nucleosome Positioning*.

Luijsterburg, M. S., Noom, M. C., Wuite, G. J. L., & Dame, R. Th. (2006). The architectural role of nucleoid-associated proteins in the organization of bacterial chromatin: A molecular perspective. *Journal of Structural Biology*, *156*(2), 262–272. https://doi.org/https://doi.org/10.1016/j.jsb.2006.05.006

Manelyte, L., & Längst, G. (2013). Chromatin Remodelers and Their Way of Action. In D. Radzioch (Ed.), *Chromatin Remodelling* (p. Ch. 1). IntechOpen. https://doi.org/10.5772/55683

Manelyte, L., Strohner, R., Gross, T., & Längst, G. (2014). Chromatin Targeting Signals, Nucleosome Positioning Mechanism and Non-Coding RNA-Mediated Regulation of the Chromatin Remodeling Complex NoRC. *PLOS Genetics*, *10*(3), e1004157-. https://doi.org/10.1371/journal.pgen.1004157

McClelland S. E. and Szczelkun, M. D. (2004). The Type I and III Restriction Endonucleases: Structural Elements in Molecular Motors that Process DNA. In A. M. Pingoud (Ed.), *Restriction Endonucleases* (pp. 111–135). Springer Berlin Heidelberg. https://doi.org/10.1007/978-3-642-18851-0_5

Medina, P. P., & Sanchez-Cespedes, M. (2008). Involvement of the chromatin-remodeling factor BRG1/SMARCA4 in human cancer. *Epigenetics*, *3*(2), 64–68. https://doi.org/10.4161/epi.3.2.6153

Mueller-Planitz, F., Klinker, H., & Becker, P. B. (2013). Nucleosome sliding mechanisms: new twists in a looped history. *Nature Structural & Molecular Biology*, *20*(9), 1026–1032. https://doi.org/10.1038/nsmb.2648

Nodelman, I. M., & Bowman, G. D. (2021). Biophysics of Chromatin Remodeling. *Annual Review of Biophysics*, *50*(1), 73–93. https://doi.org/10.1146/annurev-biophys-082520-080201

Phillips, Z. N., Husna, A.-U., Jennings, M. P., Seib, K. L., & Atack, J. M. (2019). Phasevarions of bacterial pathogens – phase-variable epigenetic regulators evolving from restriction–modification systems. *Microbiology*, *165*(9), 917–928. https://doi.org/https://doi.org/10.1099/mic.0.000805

Schwarz, F. W., Tóth, J., van Aelst, K., Cui, G., Clausing, S., Szczelkun, M. D., & Seidel, R. (2013). The Helicase-Like Domains of Type III Restriction Enzymes Trigger Long-Range Diffusion Along DNA. *Science*, *340*(6130), 353–356. https://doi.org/10.1126/science.1231122

Šišáková, E., Van Aelst, K., Diffin, F. M., & Szczelkun, M. D. (2013). The Type ISP Restriction-Modification enzymes LlaBIII and LlaGI use a translocation-collision mechanism to cleave non-specific DNA distant from their recognition sites. *Nucleic Acids Research*, *41*(2), 1071–1080. https://doi.org/10.1093/nar/gks1209

Tóth, J., Bollins, J., & Szczelkun, M. D. (2015). Re-evaluating the kinetics of ATP hydrolysis during initiation of DNA sliding by Type III restriction enzymes. *Nucleic Acids Research*, *43*(22), 10870–10881. https://doi.org/10.1093/nar/gkv1154

Van Aelst, K., Saikrishnan, K., & Szczelkun, M. D. (2015). Mapping DNA cleavage by the Type ISP restriction-modification enzymes following long-range communication between DNA sites in different orientations. *Nucleic Acids Research*, *43*(21), 10430–10443. https://doi.org/10.1093/nar/gkv1129

Wang, X., Llopis, P. M., & Rudner, D. Z. (2013). Organization and segregation of bacterial chromosomes. *Nature Reviews Genetics*, *14*(3), 191–203. https://doi.org/10.1038/nrg3375

Zhang, Y., Smith, C. L., Saha, A., Grill, S. W., Mihardja, S., Smith, S. B., Cairns, B. R., Peterson, C. L., & Bustamante, C. (2006). DNA Translocation and Loop Formation Mechanism of Chromatin Remodeling by SWI/SNF and RSC. *Molecular Cell*, *24*(4), 559–568. https://doi.org/https://doi.org/10.1016/j.molcel.2006.10.025

Chapter 1 – Introduction to restriction modification enzymes, chromatin remodeling complexes and nucleoid associated proteins

Introduction

1.1 Bacteria and the bacteriophages

Bacteria are prokaryotic unicellular organisms that inhabit nearly every environment on earth, from ambient surroundings like garden soil or forest floor to extreme conditions of the acidic hot water springs or subzero temperatures of Antarctica (Capece et al., 2013; Rothschild & Mancinelli, 2001; Seckbach et al., 2013). The extensive prevalence of bacteria is not without challenges for bacterial survival. In all the environments where bacteria are found, bacteriophages are also common (Geslin & Prieur, 2006; Mya et al., 2004; Prigent et al., 2005; Säwström et al., 2008; Suttle, 2005). The bacteriophages are viruses that infect bacteria; they hijack and utilize the bacterial cellular machinery for production of their own copies (d'Herelle, 1961; Sharma et al., 2017). The bacteriophages adsorb onto the bacterial membrane and transfer its genetic material across the bacterial membrane. Once inside the cell the viral components begin to transcribe and translate the viral proteins required for replication of its genetic material (DNA/RNA) and the proteins that make up the viral capsid. Once sufficient viral particles are assembled, the bacterial membrane bursts open to release the mature viral particles in the cellular milieu (lytic cycle) (Fig. 1). These mature viral particles can now infect other bacterial cells in the vicinity and begin the process again. Another infection mechanism used by the phages involves integration of the viral genome into the bacterial genome so that the virus can propagate with its host bacteria (lysogenic cycle) (Fig.1).

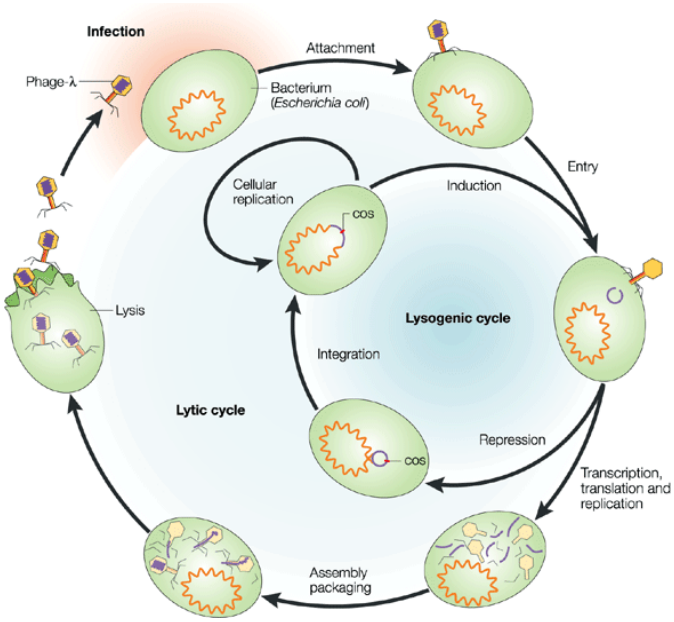

Figure 1.1: Adapted from (Campbell, 2003). The life cycle of a bacteriophage. Bacteriophage attaches to the bacterial cell surface and injects its genetic material inside the cell leaving the capsid (protein shell) outside. The phage can enter into two different cycles – the lytic or the lysogenic cycle. In the lytic cycle the bacterial DNA replication and protein synthesis machinery is hijacked to replicate the viral genetic material and produce its capsid proteins. The phage genetic material gets packaged into the capsids and the cell bursts open to release the mature phages in the environment where it can infect other bacterial cells. In a lysogenic cycle phage replication is suppressed and the phage DNA gets integrated into the bacterial genome. In this state it can replicate indefinitely with the bacterial replication until it gets excised and the lytic cycle is triggered.

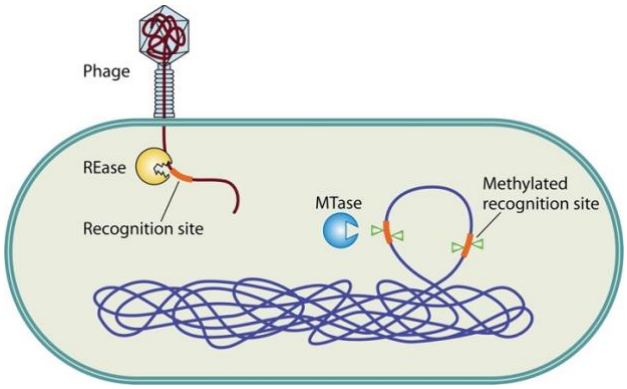

Figure 1.2: Adapted from (Kommireddy & Valakunja, 2013). Restriction-modification systems – Bacterial defense against bacteriophages. The restriction enzyme recognizes unmethylated phage DNA and cleaves it while the methyl-transferase methylates the bacterial genomic DNA thereby protects it from DNA cleavage.

While the viruses have evolved to invade and hijack bacteria, the bacteria too have co-evolved various defense mechanisms to evade the attack by the bacteriophages. There are bacterial defense mechanisms present at every stage of viral infection process (Abedon, 2012; Labrie et al., 2010). These include phage encounter blocks such as bacterial capsules that act as physical barriers to keep phage particles away from the bacterial cell surface. The phages that reach the bacterial surface can face an adsorption block, wherein, the specific receptors that are necessary for phage binding to the surface may be absent or modified. Next, there are penetration blocks that inhibit injection of the genetic material in the bacterial cell. Upon successful infection of a bacterial cell there can be multiple ways to contain the infection. In some cases, the self-destructing pathways are activated that kill the infected bacteria thereby prohibiting further propagation of phage. Alternately, the viral proteins and nucleic acids can be specifically targeted to save the infected cell. The restriction-modification systems and the CRISPR-Cas system are the two DNA endonuclease-based enzyme systems that target the invading phage DNA. While the CRISPR-Cas systems form a pseudo-adaptive immune system of bacteria, the restriction-modification (RM) systems are a major component of the innate immune system of bacteria (Abedon, 2012). The RM enzymes are widespread and ever evolving class of enzymes that protect self-DNA whereas recognize and cleave foreign DNA (phage DNA).

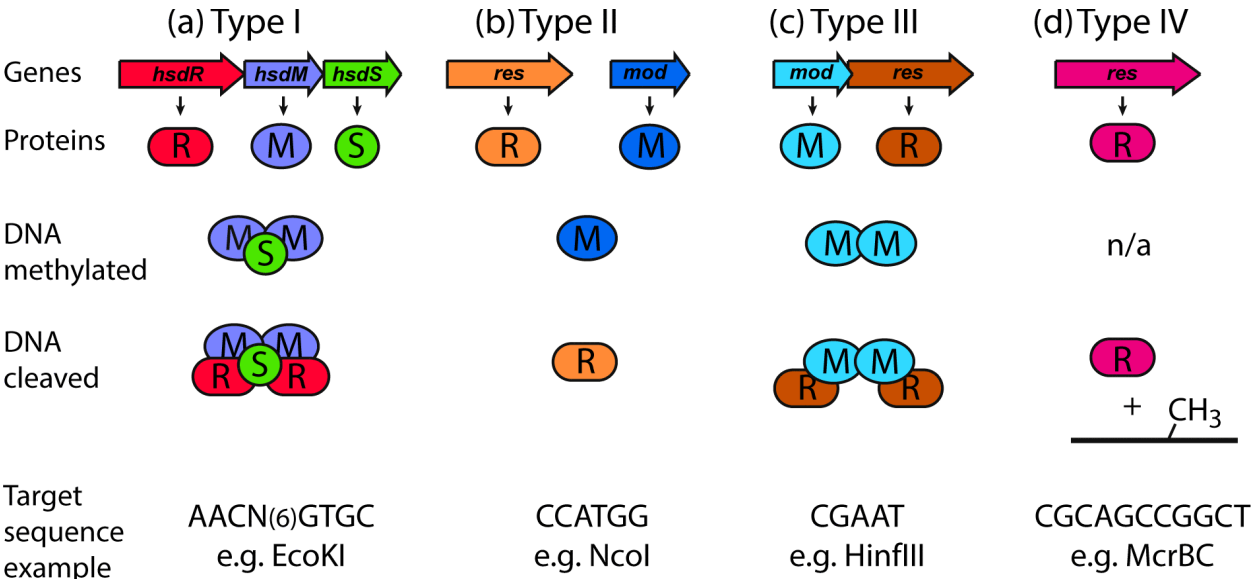

Figure 1.3: Adapted from (Phillips et al., 2019). Restriction-modification (RM) enzyme families and subunit compositions for methyl-transferase activity and DNA cleavage activity. Type I, II and III RM enzymes cleave unmethylated DNA substrates whereas Type IV restriction enzymes cleave methylated DNA substrates.

1.2.1 Restriction-modification systems

Restriction-modification enzymes are enzyme complexes that protect bacterial DNA and cleave foreign DNA. The RM systems are composed of a restriction unit that cleaves DNA within or away from a specific target sequence and a modification unit that methylates a DNA base within the target sequence (Fig. 2). Based on subunit composition, nucleotide preference, cofactor requirements, preference for methylated or un-methylated target sequence and DNA cleavage tendencies, the RM systems are classified into four categories – Type I, Type II, Type III and Type IV (Loenen et al., 2014a; 2014b) (Fig. 3). The Type II restriction enzymes are nucleoside 5'-triphosphate (NTP) independent enzymes that recognize short, mostly palindromic sequences and in presence of cofactor- $Mg2^{+}$, cut within or very close to the recognition site (Perona, 2002; A. Pingoud & Jeltsch, 2001). These are the restriction enzymes that are most commonly used for *in vitro* DNA manipulations in everyday molecular biology applications, example, HindIII, EcoRI, etc. The other three categories of RM enzymes, Type I, Type III and Type IV, are NTP dependent

enzymes. These enzymes derive energy from NTP hydrolysis to catalyze DNA cleavage near or thousands of base pairs away from their target site. The Type IV enzymes, also known as modification dependent restriction systems (MDRS), recognize methylated DNA sequences and utilize ATP or GTP for communication between enzymes units and DNA cleavage (Bourniquel & Bickle, 2002; Dryden et al., 2001; Nirwan et al., 2019; Tumuluri et al., 2021). Whereas, the Type I and Type III enzymes recognize and cleave unmethylated DNA while utilizing energy from ATP hydrolysis for communication between target sites separated by thousands of base pairs. Enzymes from both these categories communicate between the two target sites through ATP dependent movement on DNA. The Type I and Type III enzymes are both powered by a common conserved ATPase motor domain and function similarly to some extent.

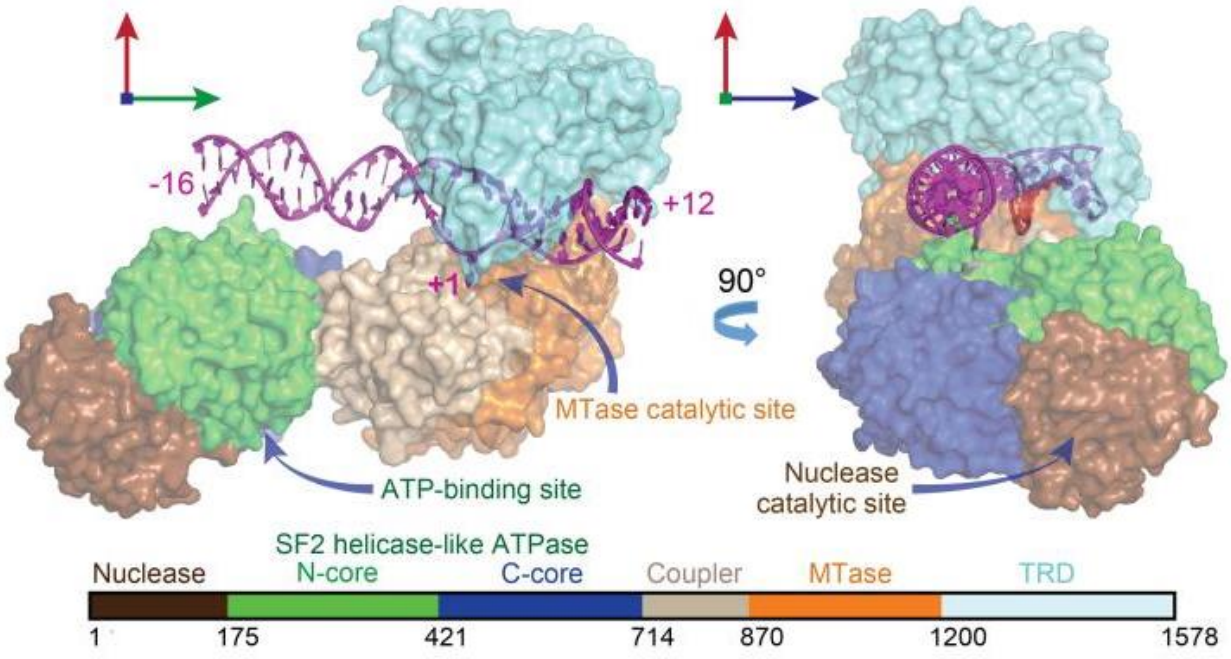

Figure 1.4: Adapted from (Chand et al., 2015). Structure of LlaBIII in complex with a 28 base pair DNA containing the specific target site. The domain organization shows an N-terminal nuclease, a SF2 helicase-like ATPase connected via a coupler domain to the methyl-transferase and a C-terminal target recognition domain (TRD). PDB accession number - 4XQK.

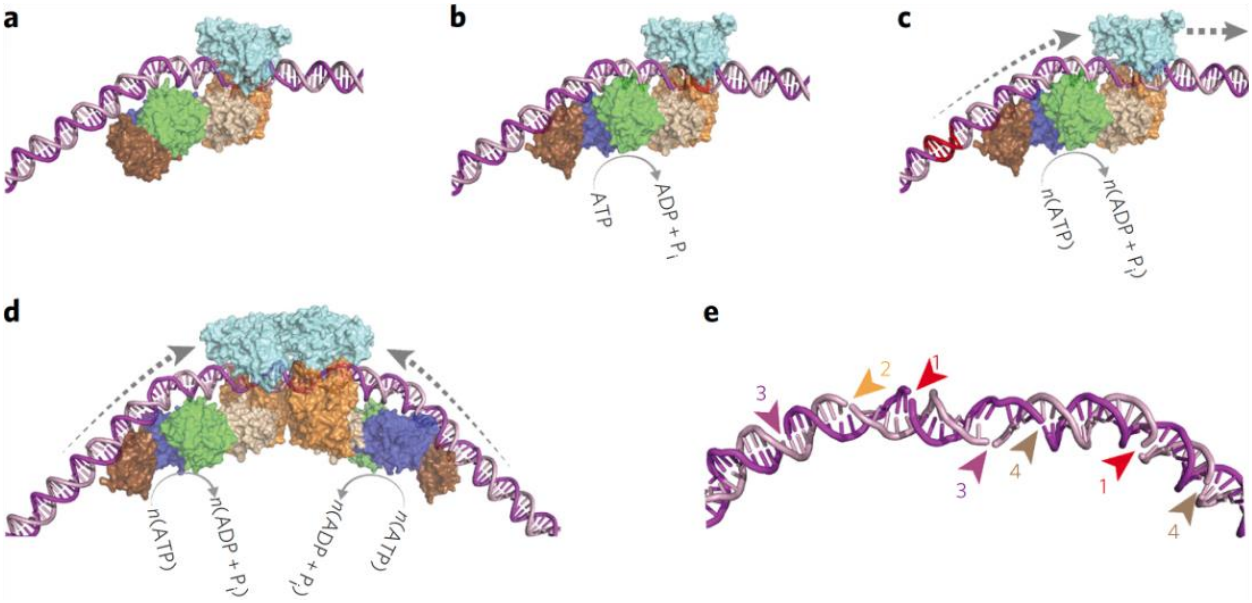

Figure 1.5: Adapted from (Chand et al., 2015). Model for loop-independent DNA translocation and DNA cleavage by LlaBIII. (a) Pre-initiation complex where nuclease is in an inactive conformation. (b) ATPase activation leads to change in conformation which releases the grip on TRD. (c) The enzyme moves downstream from the target site (red) (d) Convergence of two translocating enzymes brings the nucleases in close proximity. (e) The nicking of one DNA strand by each of the two enzymes leads to DNA shredding. Numbers are the order of the nicking events

1.2.2 Type I restriction enzymes

Historically, the Type I RM enzymes were the first RM systems to be discovered and characterized (Arber & Dussoix, 1962; Dussoix & Arber, 1962a). These enzymes were found to be responsible for the phenomenon called – 'host-controlled variation' in bacterial viruses. They were discovered as factors that limit or promote the propagation of bacteriophages obtained from one bacterial strain on other bacterial strains. This incompatibility was later discovered to be caused due to the presence or absence of specific DNA methylation mark on the obtained phage genomes and the presence or absence of restriction enzymes, that are sensitive to these methylation marks, present in the target bacterial strain. EcoKI and EcoR124 are two of the most extensively studied Type I RM enzymes (Loenen et al., 2014a; 2014b). The Type I enzymes initially discovered were found to be pentameric complexes that could form two independent, enzymatically active subcomplexes.

The genes coding for these RM systems are designated with prefix *hsd* for **h**ost **s**pecificity **d**eterminant. Three genes known as *hsdS* for specificity, *hsdM* for methyltransferase, *hsdR* for restriction, code for the three subunits that assemble into a complete pentameric enzyme complex. Two methyltransferase subunits associate with the specificity subunit to form an active methyltransferase capable of recognition of specific DNA sequence and catalysis of methyl group transfer from the cofactor S-adenosyl methionine (SAM) to the specific Adenine base in the target DNA sequence (Dryden et al., 2001; Kennaway et al., 2009, 2012). Two restriction subunits make contacts with the methyltransferase to form the pentameric complex. The restriction subunit contains a PD-(D/E)-XK motif that catalyzes DNA cleavage and an ATPase motor with RecA-like fold that allows ATP hydrolysis to power the DNA translocation activity (Lapkouski et al., 2007, 2009; Loenen et al., 2014b). The Type I RM enzymes are further classified into various sub-types based on gene complementation studies. Included among these are the Type ISP RM enzymes which are the **s**ingle **p**olypeptide enzymes that contain all the RM domains in a single polypeptide. A prototype of these is LlaBIII (Fig. 4), a Type ISP RM enzyme isolated from *Lactococcus lactis* subsp. *cremoris* W56 (J. Kong & Josephsen, 2002), and will be further discussed in detail in the subsequent chapters.

In brief, the Type ISP RM enzymes are molecular motors that translocate DNA in an ATP dependent manner. Unlike the other Type I RM enzymes that remain bound to their target sites as they loop in the DNA, the Type ISP enzymes translocate DNA without looping. Upon target recognition the enzyme moves away from the target site and physically converge to bring about double stranded break in the DNA duplex (Chand et al., 2015; Van Aelst et al., 2015) (Fig. 5). These single polypeptide enzymes hydrolyze ATP at a rapid rate utilizing one ATP for every base translocated and move at speeds of ~300bp/s (Šišáková et al., 2013). The ATPase motor hydrolyses ATP and converts the chemical energy from ATP hydrolysis into mechanical energy for active DNA translocation by the Type ISP enzyme. This ATPase motor contains a highly conserved ATPase domain found in many varied families of proteins included under the Superfamily 2 of helicases. Another closely related family of proteins that possess the same conserved ATPase motor at their core are the chromatin remodelers (Snf2 like) (Fig. 6).

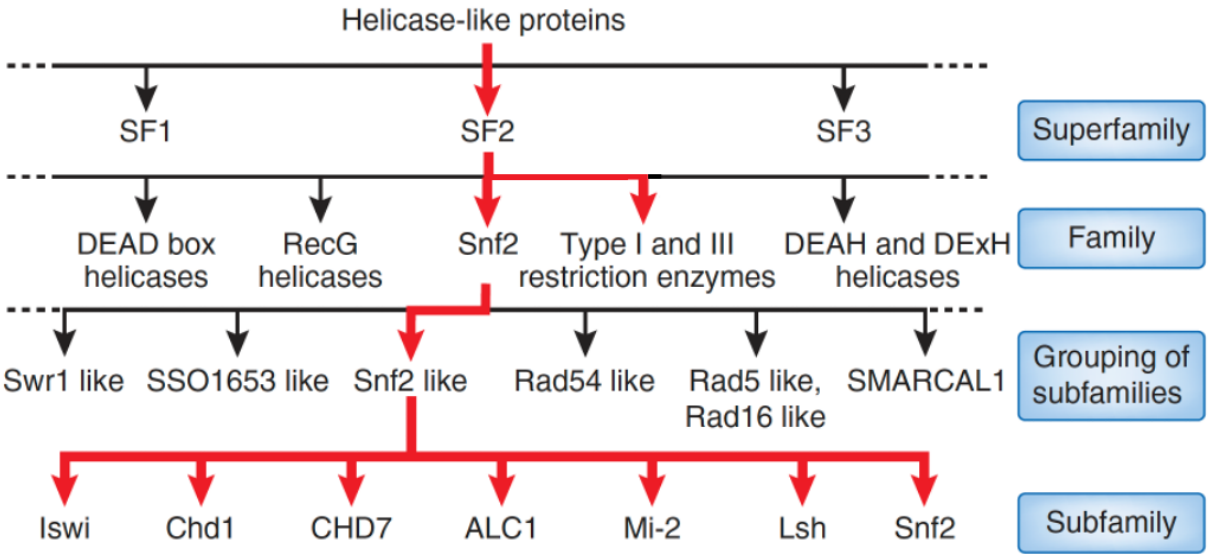

Figure 1.6: Adapted from (Mueller-Planitz, Klinker, & Becker, 2013). Classification and hierarchy of helicase like proteins, specifically the superfamily 2 of helicases. The chromatin remodelers (Snf2 like) are closely related to the Type I and Type III restriction enzyme family.

1.3.1 Chromatin remodelers

In a eukaryotic cell, the genome is maintained in the form of chromatin, in a condensed state to accommodate rather sizeable genetic material inside the tiny space in the nucleus. Multiple DNA condensing mechanisms are at work to achieve this feat. A prominent mechanism involves assembly of nucleosomes that contain an octamer of histone proteins (H2A, H2B, H3 and H4) at the core and 1.65 turns of DNA wrapped around this core. Details of this structure and how it is maintained are discussed in following chapters. The nucleosomes thus form the basic unit of a chromatin. A difficulty that arises due to this structure is the accessibility of the DNA sequence contained in the DNA wrap as the geometry of the nucleosome DNA and its interactions with octamer prevents binding of DNA binding proteins (DBP). To enable DBP to gain access to the nucleosome DNA a special class of enzymes exist known as the chromatin remodelers. These multi-subunit complexes can sense the cellular signals and accordingly open up or close off the nucleosome DNA at specific locations on the genome, such that DBPs can gain access to that DNA sequence. Additionally, the chromatin remodelers perform many functions pertaining the

nucleosome placement and composition (Clapier et al., 2017; Clapier & Cairns, 2009). These are further elaborated below.

The chromatin remodelers are a class of ATP powered complexes that in response to a cellular signal, rearrange, eject or modify nucleosomes at a specific region of the chromatin (Clapier & Cairns, 2009). These enzymes are multi-subunit complexes that contain a SF2 family ATPase at the catalytic core and contain various accessory domains and proteins that facilitate the specialized nucleosome repositioning and modification activity (Singleton & Wigley, 2002). The ATPase is highly conserved and belongs to the Snf2 family of Superfamily 2 helicases (Fig. 6) (Gorbalenya & Koonin, 1993; Singleton et al., 2007). The Snf2 family of helicases have been classified into 24 subfamilies based on the differences in the ATPase subunit (Flaus et al., 2006). Within the 24 subfamilies, the ATPases that act on nucleosome substrates are referred to as chromatin remodelers. The core ATPase contains two tandem RecA-like folds (DExx and HELICc) and seven conserved helicase motifs, that participate in ATP binding and hydrolysis (Eisen et al., 1995; Flaus et al., 2006). Additionally, there are specialized domains and motifs within the motor subunit that make each of these ATPases unique and allow them to perform their distinctive functions (Flaus et al., 2006) (Fig. 7). The distinction is further augmented by the numerous accessory subunits that allow these remodelers to respond to specific cellular requirements for nucleosome modification and rearrangement at specific genomic locations in the chromatin (Manelyte & Längst, 2013).

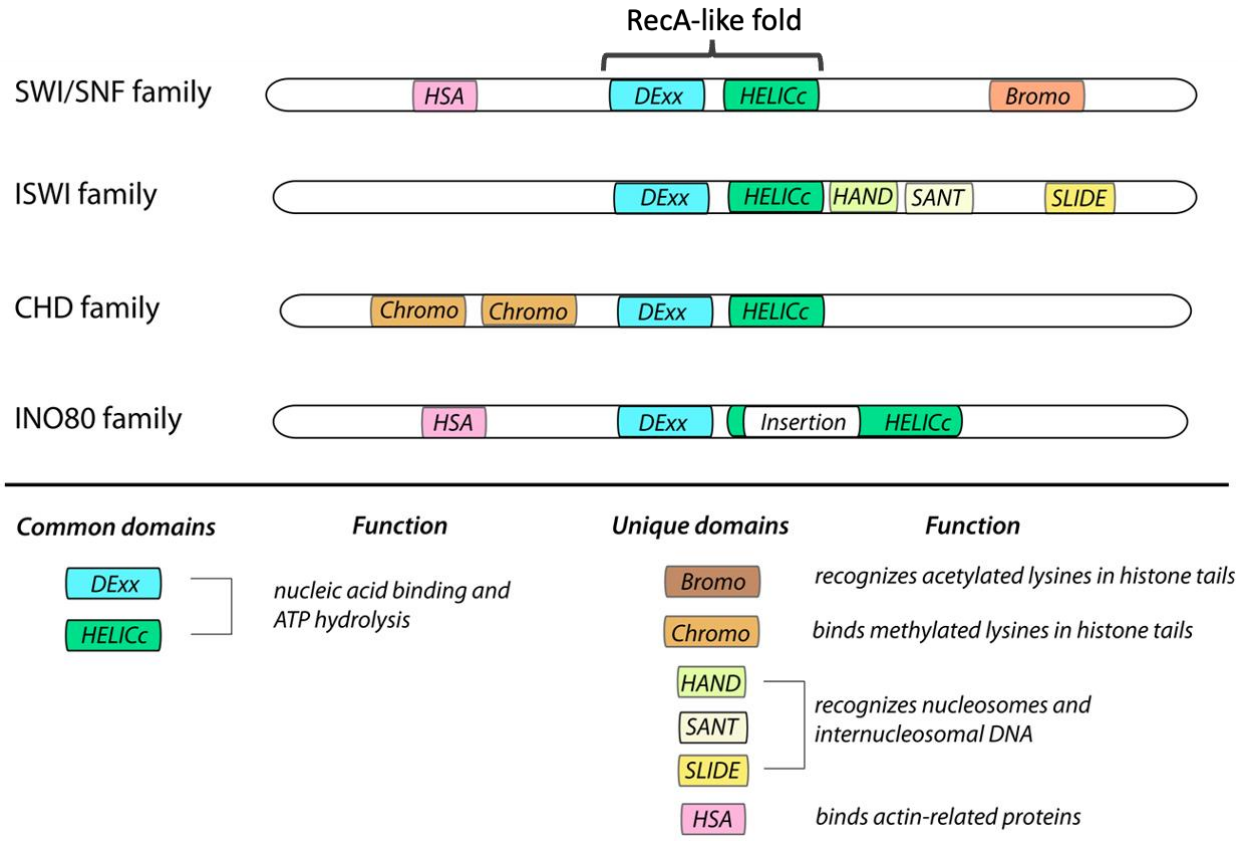

Figure 1.7: Adapted from (Manelyte & Längst, 2013). Chromatin remodeler families and their ATPase domain organization. The conserved RecA-like fold containing ATPase domain is common to all. The unique domains impart specialized functions that distinguish each chromatin remodeler family.

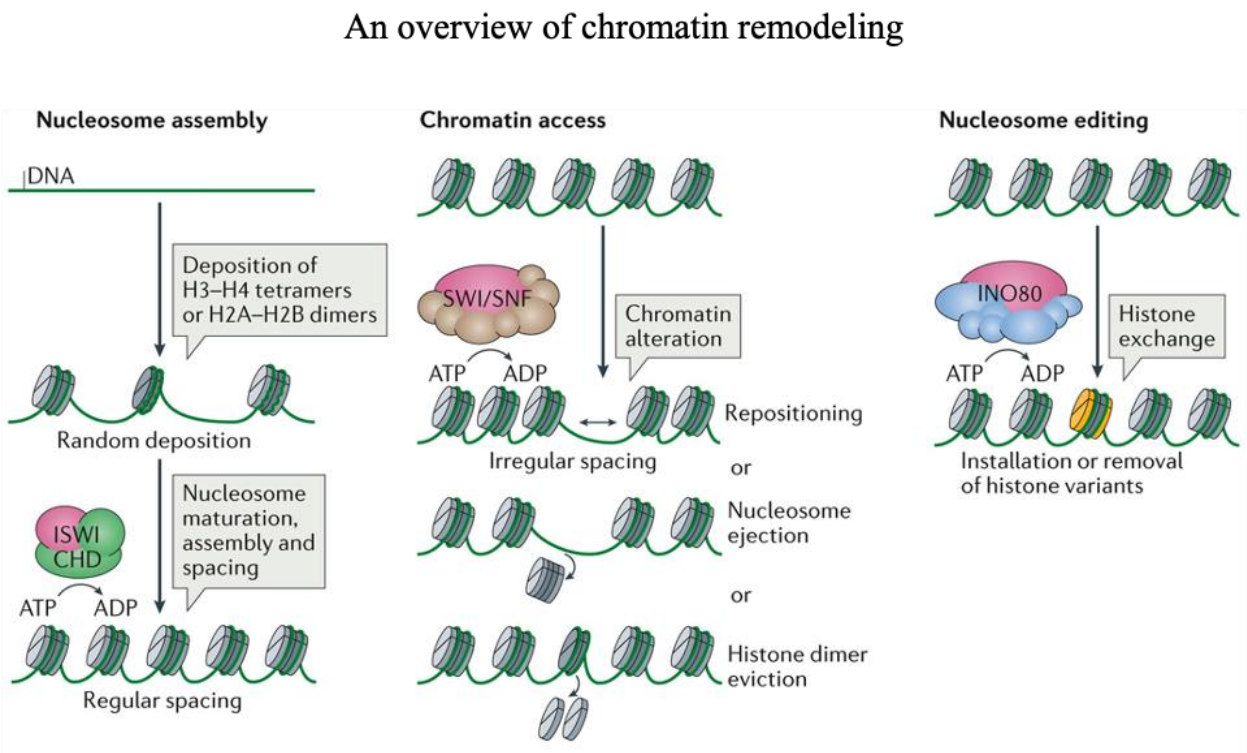

Figure 1.8: Adapted from (Clapier et al., 2017). Outcomes of chromatin remodeling processes and the chromatin remodelers that perform them. The ATPase subunits of all remodelers are depicted in pink and the additional subunits are depicted in green (imitation switch-ISWI and chromodomain helicase DNA-binding-CHD), brown (switch/sucrose non-fermentable-SWI/SNF) and blue (inositol requiring-INO80). Chromatin remodelers can assist in nucleosome assembly, alter chromatin access to DNA binding proteins or modify assembled nucleosomes through histone dimer exchange. The ISWI and CHD family remodelers can enable regular spacing of existing nucleosomes on a DNA and also assist in random deposition of histones and in nucleosome maturation. SWI/SNF family remodelers can alter chromatin access by nucleosome sliding, eviction or histone dimer exchange. Whereas the INO80 family are involved in histone exchange wherein histone variants may be either incorporated or replaced.

The chromatin remodelers are essential for chromatin structural and functional regulation. The four most extensively studied families of chromatin remodelers are, switch/sucrose non-fermentable (SWI/SNF), imitation switch (ISWI), chromodomain helicase DNA-binding (CHD),

and INOsitol requiring 80 (INO80) (Fig. 7 and 8). Each of these remodeler families perform a unique set of functions guided by the spatial and temporal ques in the cell. The helicase motor containing tandem repeats of RecA-like folds can interact with nucleic acids either through phosphodiester backbone interactions or through hydrophobic interactions with the bases in the nucleic acids. The helicase, while functioning as the DNA repair enzyme may read the DNA bases as its function necessitates detection of the base sequence whereas when speed and processivity are important, for example during DNA replication, the helicase does not interact with the bases (Singleton & Wigley, 2002). Chromatin remodelers act on the nucleosomes in a sequence independent manner and depend on the cellular signals that are detected by specific subunits or domains in the remodeling complex to determine the site and mode of nucleosome remodeling. Once bound they alter the chromatin architecture at the given location by one of the following ways; by nucleosome sliding, nucleosome eviction, nucleosome unwrapping, or exchange of histone octamers. The conserved SF2 ATPase facilitates all of these functions as it forms the catalytic core in all the remodelers.

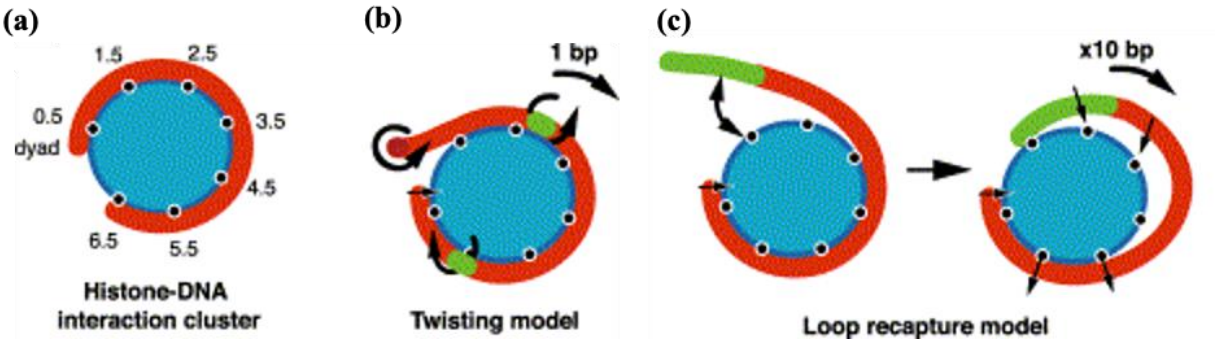

Figure 1.9: Adapted from (Längst & Becker, 2004). Proposed models for nucleosome remodeling. (a) Graphical representation of nucleosome architecture showing super helix locations (SHL) that form histone-DNA interaction clusters. (b-c) Graphical representation of nucleosome remodeling models (b) the twist defect model and (c) the loop recapture/ loop propagation model

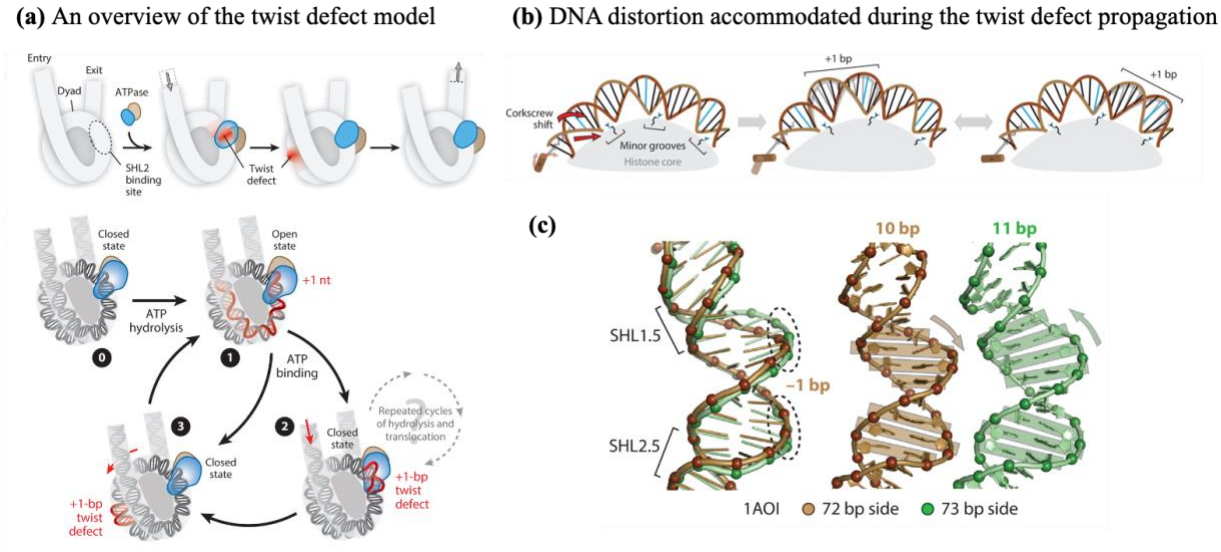

Figure 1.10: Adapted from (Nodelman & Bowman, 2021). Mechanistic details of twist defect model. (a) A graphical representation of the twist defect model and the possible pathways that can lead to nucleosome remodeling. The chromatin remodeler which is the ATPase catalyzes the movement of DNA via a twist defect from the super helix location 2 (SHL2). The DNA is taken in from the entry side, transiently moves through the nucleosome until it leaves from the exit side of the nucleosome. (b) Mechanism of twist defect propagation. The corkscrew movement of the duplex causes the DNA segment between two minor grooves to adsorb an extra base pair – a twist defect. Corkscrew movement of next segment allows propagation of the twist defect and thereby translation of DNA across the nucleosome. (c) Changes in the DNA geometry upon incorporation of a twist defect. SHL2 of two sides of a nucleosome with asymmetrical distribution of DNA in both halves is compared. The defect is staggered over both the DNA strands to accommodate the extra base pair.

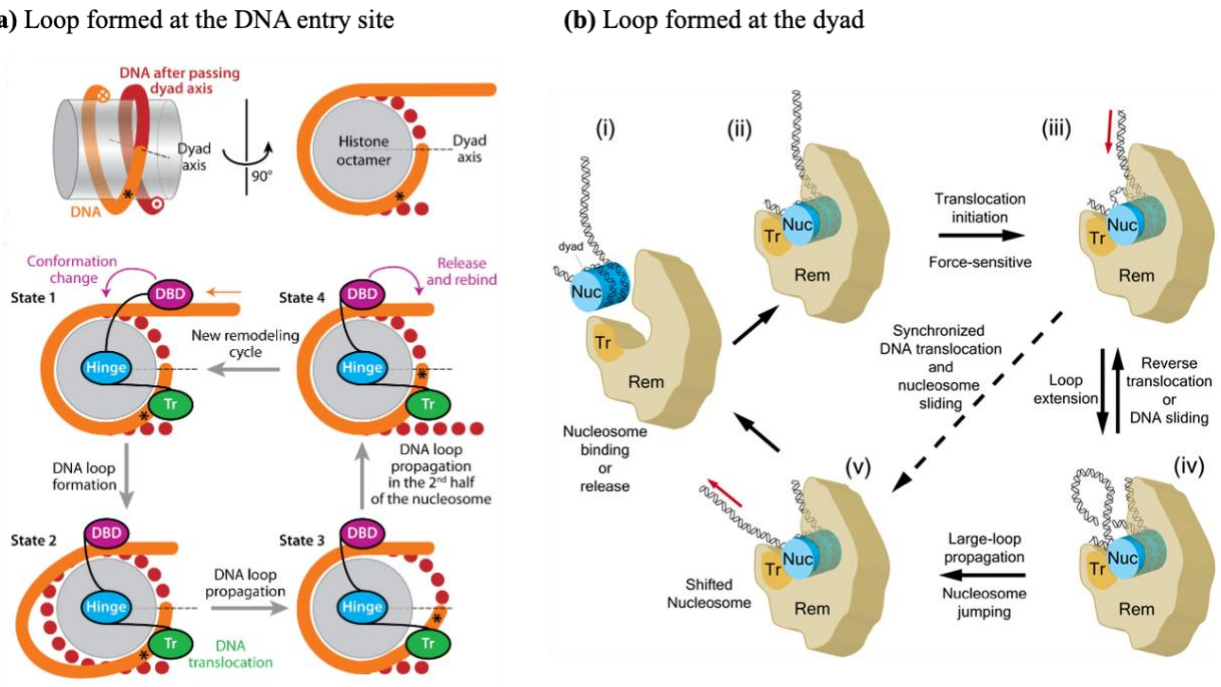

Figure 1.11: Adapted from (Clapier & Cairns, 2009) and (Zhang et al., 2006). Mechanistic details of loop propagation models. (a) Loop propagation model in which the bulge/loop is incorporated at the entry site. The DNA binding domain of the remodeler bound at the nucleosome edge cooperates with the translocase domain bound at the super helix location 2 (SHL2) to create a loop at the entry site. The translocase propagates the loop past SHL2 and out through the exit side to achieve DNA translocation. (b) In this model the loop is incorporated directly at the SHL2 by the remodeler which also propagates the loop further to achieve translocation.

1.3.2 Proposed mechanisms of nucleosome remodeling

There are two proposed models for nucleosome remodeling which are extensively discussed in literature (Nodelman & Bowman, 2021) (Fig. 9). First proposed model is the twist diffusion model where the DNA conformation is changed by the remodeler such that it gives rise to a change in the helicity and step size of the DNA which in turn allows for accommodation of an extra base pair in the DNA wrap around the octamer. This corkscrew movement in DNA is propagated throughout the nucleosome until it exits from the other end of the nucleosome and it gets shifted by a base pair (Fig. 10). In this model, most of the DNA octamer interactions are preserved throughout the

process without causing major changes in the nucleosome structural integrity. Whereas, in the second model proposed, known as the bulge or loop propagation model, nucleosome structure is proposed to undergo a significant conformational change. It is proposed that the remodeling complex actively introduces a bulge in the nucleosome DNA which is propagated through the nucleosome until it exits the other end of the DNA wrap thereby shifting the nucleosome by the number of base-pairs as the bulge (Fig. 11). The bulge or loop propagation breaks protein-DNA interactions through the nucleosome structure which are reformed once the loop passes. In literature, there are examples supporting and opposing both the proposed models. In the loop formation model the loop may be fed into the nucleosome from one end and propagated until it exits from the other end (Fig. 11a) or a loop can be actively formed at the nucleosome dyad which is further propagated to shift the nucleosome (Fig. 11b). In the latter case a major challenge would be the negative supercoiling that arises as a result of internal loop generation which can lead to breaks in the DNA to dissipate the tension. Although nucleosome shifts are not accompanied by DNA damage making the model improbable. Also, the remodelers have been observed to move in ~1 base-pair steps which is not in line with the loop propagation model but supports the twist diffusion model. The twist defect model depends upon the helical nature of DNA and its cork screw movement. Therefore, there are challenges for this model as well. There have been studies in which the DNA structures such as hairpins and protein blocks were incorporated on the nucleosome DNA and these were shown to not hinder nucleosome remodeling. Although the mechanistic details are yet unclear, it seems likely that the various remodelers are biochemically similar only to a certain level and may vary in mechanistic details depending upon their functions, accessory domains and subunits.

1.3.3 The role of ATPase in chromatin remodeling

The ATPase domain in chromatin remodelers possess the basic biochemical activity of the complete complex and have been shown to be functional by itself (McKnight et al., 2011a; Mueller-Planitz, Klinker, Ludwigsen, et al., 2013). In yeast Chd1, the C-terminal DNA binding domain was found to be dispensable for nucleosome remodeling. Chd1 lacking its DBD was able to shift the terminally positioned nucleosomes to a more central position similar to the full-length

protein, although the truncated remodeler was slower and required higher enzyme concentrations for the remodeling reaction (McKnight et al., 2011a). It was concluded that the ATPase domain of Chd1 can independently alter the nucleosome occupancy on a DNA but requires the DBD for determining the direction of nucleosome sliding. Another study done with *Drosophila* ISWI, a chromatin remodeler, also demonstrated that its DBD (Hand-Sant-Slide domain) is not essential for nucleosome remodeling activity but rather required for increasing the specificity and affinity to the nucleosomes (Mueller-Planitz, Klinker, Ludwigsen, et al., 2013). The ATPase domain in all the remodelers is highly conserved but it is not completely interchangeable. Swapping the ATPase domains of Isw2 and Snf2 renders both of the remodelers inactive (Dechassa et al., 2012). Whereas in case of BRG1 and SNF2H, the ATPases of the human chromatin remodeling complexes - SWI/SNF and ISWI, swapping the ATPase domains supports the *in vitro* nucleosome remodeling but cannot regulate all the target promoters like the wild-type complex. The ATPase domains are thus not totally interchangeable *in vivo* (Fan et al., 2003). This study also highlights the central role of the ATPase domains in determining the outcome of nucleosome remodeling as the chimeric proteins tend to behave similar to the remodeler to which the ATPase domain belongs. Hence, the ATPase domains in the chromatin remodelers are independent and biochemically similar, but not redundant and may still have functional characteristics that differ substantially.

1.4.1 Bacterial nucleoid compaction

Compaction of genetic material inside a cell is a universal problem for all living organisms and bacteria also face this challenge. The size of the bacterial genome and the bacterial cell are disproportionate and accommodation of the genetic material inside the available cell volume requires condensation of the chromosomal DNA into a compact structure called nucleoid. Condensation packs the linear DNA into a folded, twisted and inter-wound structure that can be accommodated inside the limited space of the bacterial cell. To achieve this the bacteria employs systematic multi-level hierarchical structural compaction mechanisms that condense the DNA into various structural macrodomains in a stepwise manner. The DNA compaction mechanisms are reversible and can also open up the DNA when access is needed for DNA binding proteins for processes such as DNA replication, transcription or repair and recombination. The DNA

compaction into a nucleoid is brought about by many factors including molecular crowding, DNA supercoiling and nucleoid associated proteins or NAPs (de Vries, 2010; Dillon & Dorman, 2010; Hołówka & Zakrzewska-Czerwińska, 2020; Jeon et al., 2017; Joyeux, 2019; Luijsterburg et al., 2006). Although, bacterial genomic DNA compaction is mainly driven by negative supercoiling wherein the DNA underwinding leads to formation of plectonemic loops. These loops condense the linear DNA into condensed branches that spread outwards. This organization of the nucleoid is thus explained via the bottlebrush model, wherein the plectonemic branches form the bristles of the brush (Wang et al., 2013) (Fig. 12a). These condensed wound structures are further stabilized and assisted by NAPs which can also lead to further DNA compaction (Fig. 12b). The NAPs are small basic bacterial proteins that function analogous to the eukaryotic histones and play an important role in the nucleoid structural organization and its regulation. They majorly contribute to bridging, bending and wrapping of DNA in the nucleoid (Dillon & Dorman, 2010; Luijsterburg et al., 2006).

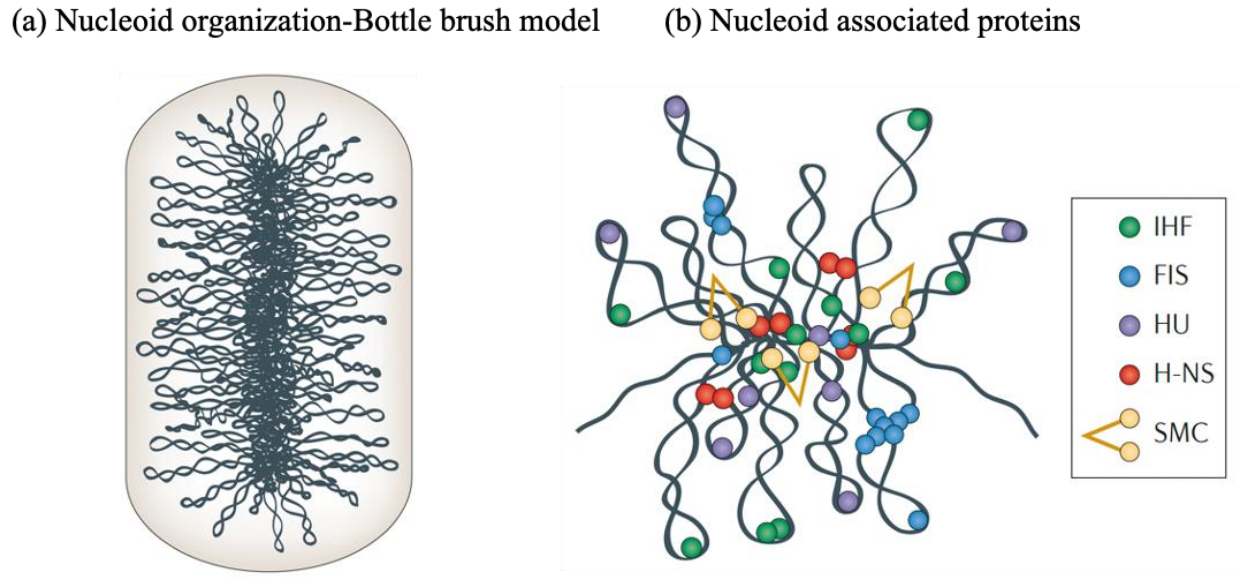

Figure 1.12: Adapted from (Wang et al., 2013). (a) Schematic representation of the bottle brush model for bacterial nucleoid organization. The plectonemes are visualized as the bristles of the brush and the longitudinal axis is made up of densely packed DNA. (b) Graphical representation

of the nucleoid associated proteins – IHF, FIS, HU, H-NS and SMC, and their specific functions – DNA bending, DNA wrapping and DNA bridging.

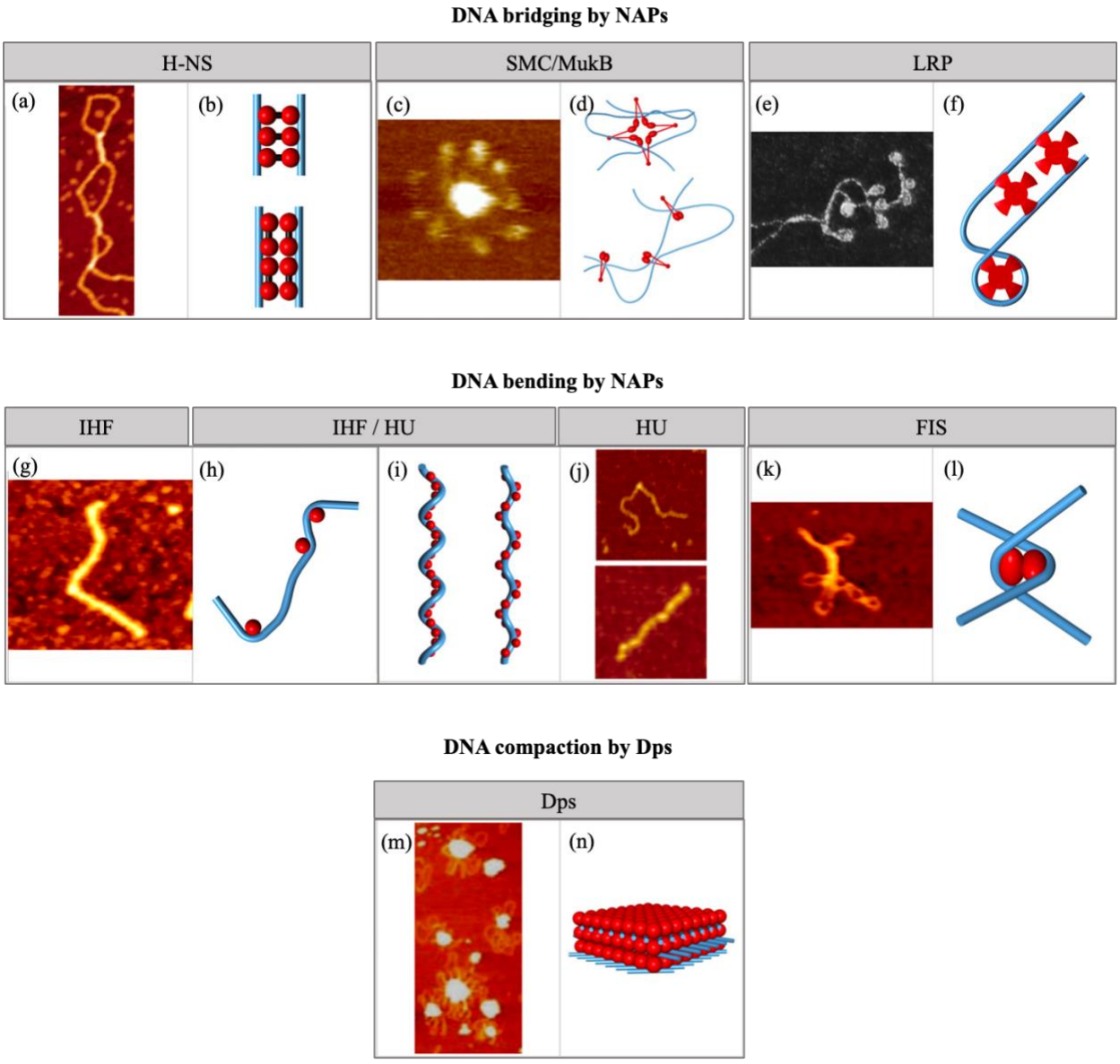

Figure 1.13: Adapted from (Luijsterburg et al., 2006). Nucleoid associated proteins. (a-f) DNA bridging NAPs – (a) SFM image showing DNA bridging and formation of loops by H-NS. (b) Model depicting H-NS mediated DNA bridging. (c) SFM image showing rosette like structure

formed by *B. subtilis* SMC protein in solution (Mascarenhas et al., 2005). (d) Model predicting the SMC-DNA interaction. (e) EM image showing *B. subtilis* LrpC-DNA complex (Beloin et al., 2003) (f) Model depicting DNA bridging and wrapping by Lrp (g-l) DNA bending NAPs – (g) SFM image of IHF with DNA (Dame et al., 2005) (h) Model representing DNA bending by IHF. (i) Model representing formation of protein-DNA filament by IHF at high IHF:DNA ratio. The model also represents the HU-DNA filament formation. (j) SFM images of HU-DNA complexes at (Top) low concentration (Bottom) high HU concentration (rigid filaments) (van Noort et al., 2004). (k) SFM image of Fis-DNA bound to supercoiled plasmid nodes (R. Schneider et al., 2001) (l) Model showing DNA bridging as a result of Fis-Fis interaction. (m-n) Alternative DNA compaction mechanism by Dps. (m) SFM image of Dps-DNA complexes (Ceci et al., 2004). (n) Model representing Dps mediated DNA compaction.

1.4.2 Nucleoid associated proteins (NAPs)

The NAPs are numerous and diverse proteins, and not all very well studied. HU (heat unstable protein), H-NS (histone-like nucleoid structuring protein), Fis (factor for inversion stimulation), IHF (integration host factor), Lrp (leucine responsive regulatory protein), Dps (DNA binding protein from starved cells) and the bacterial SMC (structural maintenance of chromosome) complexes like MukB are examples of the NAPs that have been structurally and functionally been characterized extensively. These proteins vary in their tendency to bind to or to induce specific structural conformations of bacterial DNA and participate in the structural maintenance of the nucleoid architecture. The NAPs – H-NS, Lrp and MukB are involved in bridging of DNA (Fig. 13 a-f) while IHF, HU and Fis are known to induce and/or stabilize bends in the DNA (Dillon & Dorman, 2010; Luijsterburg et al., 2006) (Fig. 13 g-l). Whereas Dps contributes to nucleoid compaction via formation of Dps-DNA sheets that are three-dimensionally packed to form a protein-DNA array (Luijsterburg et al., 2006) (Fig. 13 m-n). The collective action of the NAPs leads to an organization of the nucleoid into various structurally constrained domains. These domains are structurally isolated such that changes in one domain of the nucleoid does not affect another domain thereby maintaining the structural integrity of the nucleoid while allowing necessary DNA related processes to take place. The NAPs function collectively to maintain the

nucleoid structural organization although, most of them are not essential on their own. However, when two or more NAPs are knocked down, a defect is observed in bacterial growth (Luijsterburg et al., 2006). Also, the NAPs are involved in transcriptional regulation either by direct interaction with the transcription factors or the promoters or they can directly or indirectly influence the DNA structure such that it affects transcription of genes in vicinity (Dillon & Dorman, 2010). The NAPs thereby regulate the expression of many genes in bacteria including genes central to the cellular metabolism. The collective function of the NAPs seems to be essential to maintaining homeostasis in the bacterial cell and hence essential for normal growth and proliferation of bacteria. As these proteins function similar to the eukaryotic histones, an enzyme like LlaBIII which is capable of nucleosome displacement may also be able to displace these proteins from the nucleoid. This displacement can be tracked in multiple ways including tracking any of the NAPs microscopically with a fluorescent tag. To study the effects of LlaBIII mediated displacement of NAPs, we tracked HU-GFP in *E. coli*, and the results are discussed in chapter 5.

1.5 Aim of this study:

With this work we aim to determine whether the Type I and Type III RM enzymes, that possess an evolutionarily conserved ATPase motor similar to that of the chromatin remodelers, can perform nucleosome remodeling like the canonical remodelers. To achieve this, the first step we intend to take is to establish the work flow for *in vitro* experiments with nucleosomes. First, we would purify histones and assemble them into octamers. To test the effect of Type I and Type III RM enzymes on nucleosomes, we will prepare nucleosomes using DNA substrates that carry target sites for the selected enzymes. Initially, we mean to use these nucleosomes to test nucleosome remodeling activity of a Type I RM enzyme, LlaBIII. Next, if LlaBIII remodeled mononucleosomes, we intend to test its remodeling activity with a dinucleosome. Also, we would like to find the smallest enzyme construct that would remodel nucleosome for downstream *in vivo* applications. For *in vivo* applications, we would also test the remodeling of nucleosomes assembled on cytosine methylated DNA. Another enzyme that we intend to test is EcoP1I, an example of the Type III RM enzymes. The difference in long range DNA communication via active DNA translocation by LlaBIII and thermal diffusion by EcoP1I would help understand the

nucleosome remodeling process. Ultimately, the overall nucleosome remodeling process of these restriction enzymes would be determined elucidated using a simple biochemical assay. Eventually, the utility of these enzymes to perturb nucleosome occupancy in live mammalian cells and nucleo-protein complexes in bacterial cells would be determined. The objectives to achieve these aims are elaborated below.

1.6 Objectives of this study:

Chapter 2

1. **To purify human histones H2A, H2B, H3 and H4 to high degree of purity and assemble and purify functional octamer for *in vitro* nucleosome reconstitution**
2. **To test whether LlaBIII, a Type ISP RM enzyme and an SF2 family ATPase closely related to the chromatin remodelers, can remodel nucleosome**

Chapter 3

1. **To test the nucleosome remodeling potential of LlaBIII with a dinucleosome substrate**
2. **To find the smallest construct of LlaBIII capable of nucleosome remodeling**
3. **To test whether another closely related SF2 ATPase, a Type III RM enzyme, EcoPI, can remodel nucleosome**
4. **To determine if cytosine methylation of the nucleosome DNA has any effect on the nucleosome remodeling by LlaBIII**

Chapter 4

1. **To determine the mechanism of nucleosome remodeling by LlaBIII**

Chapter 5

1. **To study the effects of LlaBIII expression on the *E. coli* nucleoid by tracking HU, a nucleoid associated protein, relative to the nucleoid**
2. **To study the effects of LlaBIII mediated nucleosome remodeling and its downstream effects on gene expression in mammalian cells**

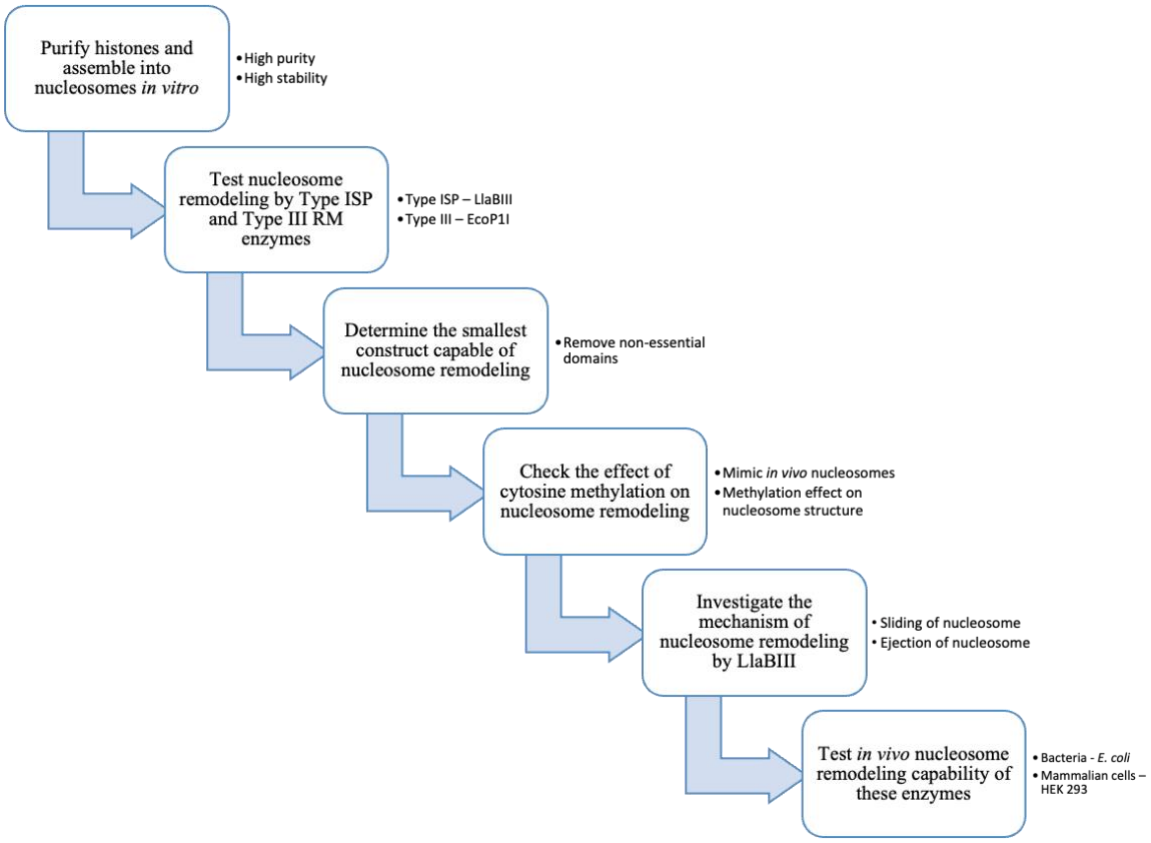

Figure 1.14: Flow chart elaborating the objectives of this study.

1.7 Reference

Abedon, S. T. (2012). Bacterial 'immunity' against bacteriophages. *Bacteriophage*, *2*(1), 50–54. https://doi.org/10.4161/bact.18609

Arber, W., & Dussoix, D. (1962). Host specificity of DNA produced by Escherichia coli: I. Host controlled modification of bacteriophage λ. *Journal of Molecular Biology*, *5*(1), 18–36. https://doi.org/https://doi.org/10.1016/S0022-2836(62)80058-8

Beloin, C., Jeusset, J., Révet, B., Mirambeau, G., Le Hégarat, F., & Le Cam, E. (2003). Contribution of DNA Conformation and Topology in Right-handed DNA Wrapping by the Bacillus subtilis LrpC Protein *. *Journal of Biological Chemistry*, *278*(7), 5333–5342. https://doi.org/10.1074/jbc.M207489200

Bourniquel, A. A., & Bickle, T. A. (2002). Complex restriction enzymes: NTP-driven molecular motors. *Biochimie*, *84*(11), 1047–1059. https://doi.org/https://doi.org/10.1016/S0300-9084(02)00020-2

Campbell, A. (2003). The future of bacteriophage biology. *Nature Reviews Genetics*, *4*(6), 471–477. https://doi.org/10.1038/nrg1089

Capece, M. C., Clark, E., Saleh, J. K., Halford, D., Heinl, N., Hoskins, S., & Rothschild, L. J. (2013). Polyextremophiles and the Constraints for Terrestrial Habitability. In J. Seckbach, A. Oren, & H. Stan-Lotter (Eds.), *Polyextremophiles: Life Under Multiple Forms of Stress* (pp. 3–59). Springer Netherlands. https://doi.org/10.1007/978-94-007-6488-0_1

Ceci, P., Cellai, S., Falvo, E., Rivetti, C., Rossi, G. L., & Chiancone, E. (2004). DNA condensation and self-aggregation of Escherichia coli Dps are coupled phenomena related to the properties of the N-terminus. *Nucleic Acids Research*, *32*(19), 5935–5944. https://doi.org/10.1093/nar/gkh915

Chand, M. K., Nirwan, N., Diffin, F. M., Van Aelst, K., Kulkarni, M., Pernstich, C., Szczelkun, M. D., & Saikrishnan, K. (2015). Translocation-coupled DNA cleavage by the Type ISP restriction-modification enzymes. *Nature Chemical Biology*, *11*(11), 870–877. https://doi.org/10.1038/nchembio.1926

Clapier, C. R., & Cairns, B. R. (2009). The Biology of Chromatin Remodeling Complexes. *Annual Review of Biochemistry*, *78*(1), 273–304. https://doi.org/10.1146/annurev.biochem.77.062706.153223

Clapier, C. R., Iwasa, J., Cairns, B. R., & Peterson, C. L. (2017). Mechanisms of action and regulation of ATP-dependent chromatin-remodelling complexes. *Nature Reviews Molecular Cell Biology*, *18*(7), 407–422. https://doi.org/10.1038/nrm.2017.26

Dame, R. T., van Mameren, J., Luijsterburg, M. S., Mysiak, M. E., Janićijević, A., Pazdzior, G., van der Vliet, P. C., Wyman, C., & Wuite, G. J. L. (2005). Analysis of scanning force microscopy images of protein-induced DNA bending using simulations. *Nucleic Acids Research*, *33*(7), e68–e68. https://doi.org/10.1093/nar/gni073

de Vries, R. (2010). DNA condensation in bacteria: Interplay between macromolecular crowding and nucleoid proteins. *Biochimie*, *92*(12), 1715–1721. https://doi.org/https://doi.org/10.1016/j.biochi.2010.06.024

Dechassa, M. L., Hota, S. K., Sen, P., Chatterjee, N., Prasad, P., & Bartholomew, B. (2012). Disparity in the DNA translocase domains of SWI/SNF and ISW2. *Nucleic Acids Research*, *40*(10), 4412–4421. https://doi.org/10.1093/nar/gks007

d'Herelle, M. F. (1961). Sur un microbe invisible antagoniste des bacilles dysentériques. *Acta Kravsi*.

Dillon, S. C., & Dorman, C. J. (2010). Bacterial nucleoid-associated proteins, nucleoid structure and gene expression. *Nature Reviews Microbiology*, *8*(3), 185–195. https://doi.org/10.1038/nrmicro2261

Dryden, D. T. F., Murray, N. E., & Rao, D. N. (2001). Nucleoside triphosphate-dependent restriction enzymes. *Nucleic Acids Research*, *29*(18), 3728–3741. https://doi.org/10.1093/nar/29.18.3728

Dussoix, D., & Arber, W. (1962). Host specificity of DNA produced by Escherichia coli: II. Control over acceptance of DNA from infecting phage λ. *Journal of Molecular Biology*, *5*(1), 37–49. https://doi.org/https://doi.org/10.1016/S0022-2836(62)80059-X

Eisen, J. A., Sweder, K. S., & Hanawalt, P. C. (1995). Evolution of the SNF2 family of proteins: subfamilies with distinct sequences and functions. *Nucleic Acids Research*, *23*(14), 2715–2723. https://doi.org/10.1093/nar/23.14.2715

Fan, H.-Y., He, X., Kingston, R. E., & Narlikar, G. J. (2003). Distinct Strategies to Make Nucleosomal DNA Accessible. *Molecular Cell*, *11*(5), 1311–1322. https://doi.org/10.1016/S1097-2765(03)00192-8

Flaus, A., Martin, D. M. A., Barton, G. J., & Owen-Hughes, T. (2006). Identification of multiple distinct Snf2 subfamilies with conserved structural motifs. *Nucleic Acids Research*, *34*(10), 2887–2905. https://doi.org/10.1093/nar/gkl295

Gorbalenya, A. E., & Koonin, E. V. (1993). Helicases: amino acid sequence comparisons and structure-function relationships. *Current Opinion in Structural Biology*, *3*(3), 419–429. https://doi.org/https://doi.org/10.1016/S0959-440X(05)80116-2

Hołówka, J., & Zakrzewska-Czerwińska, J. (2020). Nucleoid Associated Proteins: The Small Organizers That Help to Cope With Stress. *Frontiers in Microbiology*, *11*. https://doi.org/10.3389/fmicb.2020.00590

Jeon, C., Jung, Y., & Ha, B.-Y. (2017). A ring-polymer model shows how macromolecular crowding controls chromosome-arm organization in Escherichia coli. *Scientific Reports*, *7*(1), 11896. https://doi.org/10.1038/s41598-017-10421-y

Joyeux, M. (2019). Preferential Localization of the Bacterial Nucleoid. *Microorganisms*, *7*(7). https://doi.org/10.3390/microorganisms7070204

Kennaway, C. K., Obarska-Kosinska, A., White, J. H., Tuszynska, I., Cooper, L. P., Bujnicki, J. M., Trinick, J., & Dryden, D. T. F. (2009). The structure of M.EcoKI Type I DNA methyltransferase with a DNA mimic antirestriction protein. *Nucleic Acids Research*, *37*(3), 762–770. https://doi.org/10.1093/nar/gkn988

Kennaway, C. K., Taylor, J. E., Song, C. F., Potrzebowski, W., Nicholson, W., White, J. H., Swiderska, A., Obarska-Kosinska, A., Callow, P., Cooper, L. P., Roberts, G. A., Artero, J. B., Bujnicki, J. M., Trinick, J., Kneale, G. G., & Dryden, D. T. F. (2012). Structure and operation of the DNA-translocating type i DNA restriction enzymes. *Genes and Development*, *26*(1), 92–104. https://doi.org/10.1101/gad.179085.111

Kommireddy, V., & Valakunja, N. (2013). Diverse Functions of Restriction-Modification Systems in Addition to Cellular Defense. *Microbiology and Molecular Biology Reviews*, *77*(1), 53–72. https://doi.org/10.1128/mmbr.00044-12

Labrie, S. J., Samson, J. E., & Moineau, S. (2010). Bacteriophage resistance mechanisms. *Nature Reviews Microbiology*, *8*(5), 317–327. https://doi.org/10.1038/nrmicro2315

Längst, G., & Becker, P. B. (2004). Nucleosome remodeling: one mechanism, many phenomena? *Biochimica et Biophysica Acta (BBA) - Gene Structure and Expression*, *1677*(1), 58–63. https://doi.org/https://doi.org/10.1016/j.bbaexp.2003.10.011

Lapkouski, M., Panjikar, S., Janscak, P., Smatanova, I. K., Carey, J., Ettrich, R., & Csefalvay, E. (2009). Structure of the motor subunit of type I restriction-modification complex EcoR124I. *Nature Structural & Molecular Biology*, *16*(1), 94–95. https://doi.org/10.1038/nsmb.1523

Lapkouski, M., Panjikar, S., Kuta Smatanova, I., & Csefalvay, E. (2007). Purification, crystallization and preliminary X-ray analysis of the HsdR subunit of the EcoR124I endonuclease from Escherichia coli. *Acta Crystallographica Section F*, *63*(7), 582–585. https://doi.org/https://doi.org/10.1107/S174430910702622X

Le Romancer, M., Gaillard, M., Geslin, C., & Prieur, D. (2007). Viruses in extreme environments. In R. Amils, C. Ellis-Evans, & H. Hinghofer-Szalkay (Eds.), *Life in Extreme Environments* (pp. 99–113). Springer Netherlands. https://doi.org/10.1007/978-1-4020-6285-8_6

Loenen, W. A. M., Dryden, D. T. F., Raleigh, E. A., & Wilson, G. G. (2014b). Type i restriction enzymes and their relatives. *Nucleic Acids Research*, *42*(1), 20–44. https://doi.org/10.1093/nar/gkt847

Loenen, W. A. M., Dryden, D. T. F., Raleigh, E. A., Wilson, G. G., & Murrayy, N. E. (2014a). Highlights of the DNA cutters: A short history of the restriction enzymes. *Nucleic Acids Research*, *42*(1), 3–19. https://doi.org/10.1093/nar/gkt990

Luijsterburg, M. S., Noom, M. C., Wuite, G. J. L., & Dame, R. Th. (2006). The architectural role of nucleoid-associated proteins in the organization of bacterial chromatin: A molecular perspective. *Journal of Structural Biology*, *156*(2), 262–272. https://doi.org/https://doi.org/10.1016/j.jsb.2006.05.006

Manelyte, L., & Längst, G. (2013). Chromatin Remodelers and Their Way of Action. In D. Radzioch (Ed.), *Chromatin Remodelling* (p. Ch. 1). IntechOpen. https://doi.org/10.5772/55683

Mascarenhas, J., Volkov, A. V, Rinn, C., Schiener, J., Guckenberger, R., & Graumann, P. L. (2005). Dynamic assembly, localization and proteolysis of the Bacillus subtilis SMC complex. *BMC Cell Biology*, *6*(1), 28. https://doi.org/10.1186/1471-2121-6-28

McKnight, J. N., Jenkins, K. R., Nodelman, I. M., Escobar, T., & Bowman, G. D. (2011). Extranucleosomal DNA Binding Directs Nucleosome Sliding by Chd1. *Molecular and Cellular Biology*, *31*(23), 4746–4759. https://doi.org/10.1128/MCB.05735-11

Mueller-Planitz, F., Klinker, H., & Becker, P. B. (2013). Nucleosome sliding mechanisms: new twists in a looped history. *Nature Structural & Molecular Biology*, *20*(9), 1026–1032. https://doi.org/10.1038/nsmb.2648

Mueller-Planitz, F., Klinker, H., Ludwigsen, J., & Becker, P. B. (2013). The ATPase domain of ISWI is an autonomous nucleosome remodeling machine. *Nature Structural & Molecular Biology*, *20*(1), 82–89. https://doi.org/10.1038/nsmb.2457

Mya, B., Linda, W., Steven, L., Tom, S., & Forest, R. (2004). Phage Community Dynamics in Hot Springs. *Applied and Environmental Microbiology*, *70*(3), 1633–1640. https://doi.org/10.1128/AEM.70.3.1633-1640.2004

Nirwan, N., Itoh, Y., Singh, P., Bandyopadhyay, S., Vinothkumar, K. R., Amunts, A., & Saikrishnan, K. (2019). Structure-based mechanism for activation of the AAA+ GTPase McrB by the endonuclease McrC. *Nature Communications*, *10*(1), 3058. https://doi.org/10.1038/s41467-019-11084-1

Nodelman, I. M., & Bowman, G. D. (2021). Biophysics of Chromatin Remodeling. *Annual Review of Biophysics*, *50*(1), 73–93. https://doi.org/10.1146/annurev-biophys-082520-080201

Perona, J. J. (2002). Type II restriction endonucleases. *Methods*, *28*(3), 353–364. https://doi.org/https://doi.org/10.1016/S1046-2023(02)00242-6

Phillips, Z. N., Husna, A.-U., Jennings, M. P., Seib, K. L., & Atack, J. M. (2019). Phasevarions of bacterial pathogens – phase-variable epigenetic regulators evolving from restriction–modification systems. *Microbiology*, *165*(9), 917–928. https://doi.org/https://doi.org/10.1099/mic.0.000805

Pingoud, A., & Jeltsch, A. (2001). Structure and function of type II restriction endonucleases. *Nucleic Acids Research*, *29*(18), 3705–3727. https://doi.org/10.1093/nar/29.18.3705

Prigent, M., Leroy, M., Confalonieri, F., Dutertre, M., & DuBow, M. S. (2005). A diversity of bacteriophage forms and genomes can be isolated from the surface sands of the Sahara Desert. *Extremophiles*, *9*(4), 289–296. https://doi.org/10.1007/s00792-005-0444-5

Rothschild, L. J., & Mancinelli, R. L. (2001). Life in extreme environments. *Nature*, *409*(6823), 1092–1101. https://doi.org/10.1038/35059215

Säwström, C., Lisle, J., Anesio, A. M., Priscu, J. C., & Laybourn-Parry, J. (2008). Bacteriophage in polar inland waters. *Extremophiles*, *12*(2), 167–175. https://doi.org/10.1007/s00792-007-0134-6

Schneider, R., Lurz, R., Lüder, G., Tolksdorf, C., Travers, A., & Muskhelishvili, G. (2001). An architectural role of the Escherichia coli chromatin protein FIS in organising DNA. *Nucleic Acids Research*, *29*(24), 5107–5114. https://doi.org/10.1093/nar/29.24.5107

Seckbach, J., Oren, A., & Stan-Lotter, H. (2013). *Polyextremophiles: life under multiple forms of stress* (Vol. 27). Springer Science & Business Media.

Sharma, S., Chatterjee, S., Datta, S., Prasad, R., Dubey, D., Prasad, R. K., & Vairale, M. G. (2017). Bacteriophages and its applications: an overview. *Folia Microbiologica*, *62*(1), 17–55. https://doi.org/10.1007/s12223-016-0471-x

Singleton, M. R., Dillingham, M. S., & Wigley, D. B. (2007). Structure and Mechanism of Helicases and Nucleic Acid Translocases. *Annual Review of Biochemistry*, *76*(1), 23–50. https://doi.org/10.1146/annurev.biochem.76.052305.115300

Singleton, M. R., & Wigley, D. B. (2002). Modularity and Specialization in Superfamily 1 and 2 Helicases. *Journal of Bacteriology*, *184*(7), 1819–1826. https://doi.org/10.1128/jb.184.7.1819-1826.2002

Šišáková, E., Van Aelst, K., Diffin, F. M., & Szczelkun, M. D. (2013). The Type ISP Restriction-Modification enzymes LlaBIII and LlaGI use a translocation-collision mechanism to cleave non-specific DNA distant from their recognition sites. *Nucleic Acids Research*, *41*(2), 1071–1080. https://doi.org/10.1093/nar/gks1209

Suttle, C. A. (2005). Viruses in the sea. *Nature*, *437*(7057), 356–361. https://doi.org/10.1038/nature04160

Tumuluri, V. S., Rajgor, V., Xu, S.-Y., Chouhan, O. P., & Saikrishnan, K. (2021). Mechanism of DNA cleavage by the endonuclease SauUSI: a major barrier to horizontal gene transfer and antibiotic resistance in Staphylococcus aureus. *Nucleic Acids Research*, *49*(4), 2161–2178. https://doi.org/10.1093/nar/gkab042

Van Aelst, K., Saikrishnan, K., & Szczelkun, M. D. (2015). Mapping DNA cleavage by the Type ISP restriction-modification enzymes following long-range communication between DNA sites in different orientations. *Nucleic Acids Research*, *43*(21), 10430–10443. https://doi.org/10.1093/nar/gkv1129

van Noort, J., Verbrugge, S., Goosen, N., Dekker, C., & Dame, R. T. (2004). Dual architectural roles of HU: Formation of flexible hinges and rigid filaments. *Proceedings of the National Academy of Sciences*, *101*(18), 6969–6974. https://doi.org/10.1073/pnas.0308230101

Wang, X., Llopis, P. M., & Rudner, D. Z. (2013). Organization and segregation of bacterial chromosomes. *Nature Reviews Genetics*, *14*(3), 191–203. https://doi.org/10.1038/nrg3375

Zhang, Y., Smith, C. L., Saha, A., Grill, S. W., Mihardja, S., Smith, S. B., Cairns, B. R., Peterson, C. L., & Bustamante, C. (2006). DNA Translocation and Loop Formation Mechanism of

Chromatin Remodeling by SWI/SNF and RSC. *Molecular Cell*, *24*(4), 559–568. https://doi.org/https://doi.org/10.1016/j.molcel.2006.10.025

Chapter 2 – LlaBIII, a Type ISP RM enzyme, can displace mononucleosomes from their positions on DNA

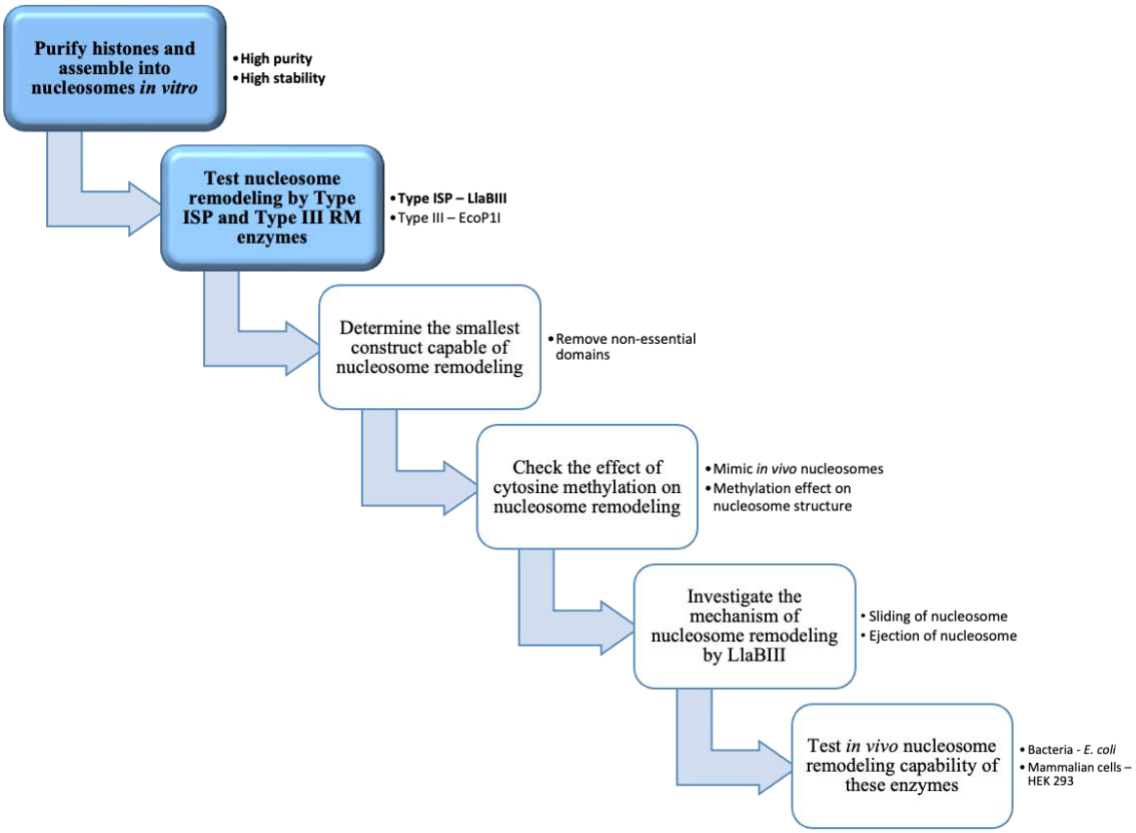

2.1 Introduction

The Type I family of restriction-modification (RM) enzymes are one of the most potent defense systems in bacteria that defend it against invading bacteriophages and potentially dangerous foreign DNA that enter the cell (Arber et al., 1963; Dussoix & Arber, 1962b). These RM enzymes are multi-domain multimeric proteins that recognize specific target DNA sequence, utilize ATP to translocate and cleave DNA at a site away from the target sequence. They can communicate between two target recognition sites in *cis*, which can be separated by thousands of base pairs and cause double stranded breaks approximately midway between two unmethylated target sites (Horiuchi & Zinder, 1972; Loenen et al., 2014b; Studier & Bandyopadhyay, 1988). Also, these enzymes can modify the bacterial DNA by methylation of adenine bases in their target site (Arber & Linn, 1969). This allows the bacterial DNA to be recognized as self-DNA as opposed to the unmethylated foreign DNA. Majority of Type I RM enzymes are pentameric and are composed of fives subunits produced from three genes prefixed as hsd (host specificity determinant), namely *hsdR* (restriction), *hsdM* (modification) and *hsd*S (specificity) (Arber & Linn, 1969; Loenen et al., 2014a). Together these subunits can form two functional enzyme complexes, a methyltransferase that is composed of two modification subunits (HsdM) and one specificity subunit (HsdS) and the restriction-modification complex composed of two restriction subunits (HsdS), two modification subunits (HsdM) and one specificity subunit (HsdS) (Dryden et al., 1997). The HsdS subunit facilitates binding to specific target sequence on the DNA whereas the HsdM subunit possesses the catalytic domains essential for N6-adenine methyl transfer. It utilizes S-adenosyl methionine as a cofactor for methyl transfer. The HsdR subunit comprises of a nuclease domain, a DEAD-box ATPase containing RecA like motor domain (Bird et al., 1998; Davies et al., 1999; Gorbalenya & Koonin, 1991; Murray et al., 1993). The recognition and binding of unmethylated target site activates the enzyme for DNA cleavage. DNA cleavage requires communication between two target sites through DNA translocation/looping (Rosamond et al., 1979; Yuan et al., 1980). ATP and Mg^{2+} are required for translocation/looping and are hence essential for DNA cleavage by these RM enzymes (Eskin & Linn, 1972b, 1972a).

The Type I RM enzymes are classified into five families based on the antibody cross reactivity, complementation tests and amino acid sequence. One such family is the Type I**SP** family which comprises the **s**ingle **p**olypeptide Type I RM enzymes. These enzymes are encoded as a multi-

functional single polypeptide that possesses all four activities, namely target recognition, adenine modification, DNA translocation and nuclease. An example of this family is LlaBIII which was first identified from a plasmid, pJW566 from *Lactococcus lactis* subspecies *cremoris* W56 (Josephsen & Vogensen, 1989). The *Lactococcus lactis* cultures carrying this plasmid were protected from phage mediated cell lysis (Josephsen & Vogensen, 1989; Nielsen, 1998). This plasmid was discovered to harbor a single polypeptide encoded Type I RM enzyme which was named LlaBIII (Josephsen & Vogensen, 1989; J. Kong & Josephsen, 2001, 2002). LlaBIII shares high sequence homology (~90%), in the nuclease, motor and methylase domains, to another Type ISP RM enzyme, LlaGI. The earliest studies were performed on LlaGI, as it was the first single polypeptide enzyme that was identified as a member of the Type I RM enzyme family (Smith et al., 2009a, 2009b; 2009c). The target recognition domain (TRD) of both the enzymes, LlaBIII and LlaGI, recognize a 6 or 7 bp asymmetric DNA sequence respectively. Functionally both the enzymes are so similar that a monomer of each enzyme can coordinate with monomer of other enzyme to bring about DNA cleavage (Van Aelst et al., 2013). Like LlaGI, LlaBIII requires two head-to-head oriented target sites on a DNA to cause a double strand break (Van Aelst et al., 2013). One monomer binds to a target site on the DNA, in presence of ATP and Mg^{2+}, translocates downstream from the target site until it collides with an oncoming enzyme. Upon collision, each of the two monomers cleave one DNA strand to bring about double strand break (Van Aelst et al., 2015). Unlike most of the Type I family RM enzymes, LlaBIII translocates DNA in a unidirectional manner without looping. The enzyme binds the target site and gets activated for DNA translocation. Upon ATP hydrolysis, the enzyme undergoes a conformational change that releases it from the target sites thereby allowing active, directed DNA translocation downstream of the binding site. Analysis of amino acid sequence and structure of Type I enzymes including Type ISP, show presence of DEAD box ATPase motifs and RecA-like fold (Chand et al., 2015; Gorbalenya & Koonin, 1991; Murray et al., 1993). Based on these structural characteristics, the Type I enzymes have been included into the superfamily 2 (SF2) of helicases. This family comprises of many diverse nucleic acid stimulated NTPases that may or may not unwind double stranded (ds) DNA/RNA (Byrd & Raney, 2012; Fairman-Williams et al., 2010; Singleton & Wigley, 2002). Some of these NTPases can translocate single or double stranded nucleic acid while others cannot. The Type I RM enzymes constitute a family of SF2 NTPases that utilize the energy from ATP hydrolysis to translocate dsDNA. Another closely related family of DNA translocases

included in the SF2 helicases is the Swi/Snf family of chromatin remodelers. These are multi-subunit mega-complexes that are involved in nucleosome remodeling in eukaryotic cells. Like LlaBIII, these enzymes contain the conserved ATPase motifs comprising two RecA-like domains that constitute the motor subunit of these complexes (Clapier & Cairns, 2009; Fairman-Williams et al., 2010). The RecA-like domains constitute the motor that converts chemical energy from ATP hydrolysis into mechanical energy for DNA translocation (Dürr et al., 2005a; Grüne et al., 2003; Singleton et al., 2007). The chromatin remodeling complexes powered by the SF2 motor can perform various nucleosome remodeling functions ranging from histone exchange, nucleosome sliding and eviction (Clapier & Cairns, 2009). Many of these complexes are implicated in cellular signaling and can allow DNA binding proteins to access DNA that is wrapped around the nucleosomes or restrict access to DNA by increasing nucleosome occupancy in certain regions on the chromatin. The signals from the cellular network are interpreted by the specialized subunits of these complexes, whereas the nucleosome remodeling process is carried out by the RecA-like motor that forms the core of these complexes. Sequence and structural comparison of LlaBIII and the Swi/Snf family of proteins shows that the core motor domain motifs and folds are highly conserved. This led us to hypothesize that LlaBIII may function in a manner similar to the chromatin remodelers wherein it may be able remodel a nucleosome present downstream of the target site.

To test this hypothesis, we performed *in vitro* nucleosome remodeling assay called the restriction enzyme accessibility assay (REAA) (Fan et al., 2003; Polach & Widom, 1995a). We designed a nucleosome substrate that has a Type II restriction enzyme (HhaI) target sequence in the center of the DNA wrapped around the nucleosome. When unperturbed, occupancy of nucleosome on this DNA restricts the access of HhaI to its target site and the DNA is protected from cleavage. Once the nucleosome is displaced or evicted from this region, the HhaI site is accessible resulting in DNA cleavage leading to emergence of shorter DNA fragments as observed by polyacrylamide gel electrophoresis. We incorporated a LlaBIII target site (5'TnAGCC3') upstream of the nucleosome such that in presence of ATP, LlaBIII can bind and translocate directionally towards the nucleosome. Following incubation, we check for the emergence of cleaved DNA which is an indication of the remodeling activity of LlaBIII.

2.2 Materials and methods

The nucleosomes used in our experiments were prepared *in vitro* by assembling the individual components of the complex in a stepwise manner. Each individual step is described below.

2.2.1 Preparation of DNA substrate

The DNA substrate used for *in vitro* nucleosome preparation was generated by PCR amplification. A 329 bp DNA was generated by amplification from a plasmid encoding the high affinity nucleosome occupancy region Widom (601) sequence (Lowary & Widom, 1998) using primers 329F and 329R.The 329F primer incorporated LlaBIII target sequence upstream of the 601. This fragment was used as template for incorporation of an adaptor sequence using primers Cy5oligo-498-AdaptorF (Cy-F) and 329R. This produced a 320 bp DNA fragment that was used as a template for amplification of the 5'-Cy5 labelled DNA substrates. For terminally placed nucleosome DNA, 265 bp DNA was amplified using primers Cy5-F and 601R. For centrally placed nucleosomes, a 356 bp DNA was generated using primers Cy5-F and 329R. The PCR products were purified using PCR Cleanup Kit (Qiagen, Cat. No. 28106). After purification, the DNA was resolved on a 6% Native polyacrylamide gel, pre-run for 20 minutes. The DNA samples were resolved for 60 minutes at 150V in 1x TBE at room temperature. After the run, the gel was stained with ethidium bromide and visualized on a UV transilluminator. The bands corresponding to the expected DNA size were excised and transferred to a clean 1.5 mL vial. The gel pieces were crushed using a clean micropipette tip and resuspended in autoclaved milliQ. The vials were incubated at 25 °C under shaking conditions, overnight. The vials were then centrifuged at 13000 rpm for 5 minutes to settle the gel pieces and the supernatant was transferred to a fresh vial. Fresh milliQ was added and the process was repeated 2-3 times with 2-hour incubation time. The supernatant collected was simultaneously concentrated using a vacuum concentrator until the supernatant volume was reduced to 50-100 µL. DNA was then purified using a PCR clean up kit. The DNA was eluted in refolding buffer (2 M NaCl, 10 mM Tris pH 7.5, 1 mM EDTA, 10 mM β-mercaptoethanol) and concentration was estimated using NanoDrop™ 2000 (Thermo Scientific). The substrates were stored at -30°C until nucleosomes were reconstituted.

2.2.2 Purification of human histones

The plasmids carrying the human histone encoding genes were acquired from Addgene (Catalog no.42634, 42630, 42633 and 42632). The histones were purified using the Rapid Histone Purification (RHP) protocol as published by (Klinker et al., 2014) with minor changes wherever required. Briefly, the plasmids encoding histones were individually transformed into *E. coli* BL21(DE3). Single colony for each was inoculated in 70 mL LB broth with 100 µg/mL Ampicillin. After 3 hours incubation under shaking conditions at 37°C, 10 mL of this culture was inoculated in 1 L fresh LB broth supplemented with 100 µg/mL Ampicillin. This culture was incubated under shaking conditions at 37°C to a density OD_{600} 0.4-0.8. Histone expression was induced by 0.5mM IPTG and the cultures were further incubated for 3 hours under the same conditions. The cells were then harvested by centrifugation at 4°C and were stored at -80°C.

The buffers for purification were prepared a day in advance, filtered, degassed, and stored at 4°C. The cell pellet thawed on ice before resuspending it in SA buffer (40 mM NaOAc pH-5.2, 1 mM EDTA pH 8.0, 10 mM lysine, 5 mM β-mercaptoethanol) and 200 mM NaCl. Protease inhibitor cocktail (cOmplete™, Roche, commodity code 11836170001) was also added at this step. Urea powder was directly added to the resuspended cells and the volume was made up such that concentration of Urea was ≥ 6 M. The concentrations of all the components were added such that the total volume for resuspended 3 L culture pellet was 35 mL. After most of the urea was dissolved, the suspension was sonicated on ice for 4 cycles of 5 minutes each at 30% amplitude and pulses of 15 second followed by 30 second pauses. The suspension was mixed between the cycles. The lysate was centrifuged at 37000 rpm (Ti45 rotor, Optima XE-100 Ultracentrifuge, Beckman Coulter) for 50 minutes. The supernatant was filtered using 0.45 µm syringe filters before loading onto a HiTrap SP HP column (5 mL; GE Healthcare) that was pre-equilibrated with SAU200 buffer (40 mM NaOAc pH-5.2, 1 mM EDTA pH-8.0, 10 mM lysine, 5 mM β-mercaptoethanol, 200 mM NaCl). The SAU buffers used henceforth all have the same composition except NaCl which was added at varying concentrations specified numerically. The column was then washed with 3 CV SAU250 (250 mM NaCl) and 3 CV of SAU 300 (300 mM NaCl). Elution was done in two steps, where the first step involved a gradient of NaCl, SAU300 to SAU400 (400 mM NaCl) over 5 CV. In the next step a gradient was set up from SAU400 to SAU800 (800 mM NaCl) over 7 CV. The fractions were analysed by SDS-PAGE to locate the bands corresponding

to histones. The fractions with histones were pooled and dialyzed against water with 2 mM β-mercaptoethanol. The protein samples were dialyzed overnight at 4°C and the water was changed once. The protein fractions were recovered from dialysis bags and the Tris pH-8 was added to make the final concentration 15 mM. The sample was centrifuged at 15000 rpm for 20 minutes at 4°C following which it was filtered using a 0.45 µm syringe filter. The filtered protein sample was loaded onto a HiTrap Q HP column (5 mL; GE Healthcare) pre-equilibrated with 15 mM Tris pH-8. The protein does not bind to the column and was present in the flow through which was lyophilized and stored at -30°C.

2.2.3 Assembly and Purification of Octamer

The lyophilized powders of individual histones were separately dissolved in unfolding buffer (7 M Guanidium Hydrochloride, 10 mM Tris pH 7.5 and 10 mM DTT) and protein concentration was estimated. The histones were mixed in equimolar ratio and dialyzed against refolding buffer (2 M NaCl, 10 mM Tris pH 7.5, 1 mM EDTA, 10 mM β-mercaptoethanol) at 4°C overnight. The buffer was changed once during the dialysis. The dialyzed protein was recovered from the dialysis bag and centrifuged at 4°C to remove any precipitates. The protein sample was then applied onto Superdex 200 10/300 column (GE Healthcare) pre-equilibrated with refolding buffer and fractions were analyzed by SDS-PAGE on an 18% polyacrylamide gel. Fractions corresponding to the octamer, molecular weight (109.542 KDa), elute at 12 mL elution volume. These fractions were analyzed by SDS-PAGE and those that showed presence of bands corresponding to all four histones on polyacrylamide gel were pooled and concentrated using Vivaspin2 (Sartorius, commodity code Z614211) sample concentrator at 4000 rpm at 4 °C in Eppendorf centrifuge 5801 R. The protein concentration was estimated by Bradford's assay and the concentrated protein was stored at -80°C.

2.2.4 Purification of LlaBIII

LlaBIII was purified as published by (Chand et al., 2015). Briefly, LlaBIII was overexpressed from a recombinant plasmid in *E. coli* BL21(DE3) by 0.5 mM IPTG mediated protein induction. The cultures were incubated initially at 37°C before the addition of IPTG. Upon reaching the cell density OD_{600} 0.6-0.8 the cultures were shifted to 25°C and IPTG was added. The cultures were

incubated for 5 hours in shaking conditions at 25°C. Cells were harvested by centrifugation and cell pellets were stored at -80°C until protein purification.

The pellet was thawed on ice and resuspended in lysis buffer (50 mM Tris-HCl pH 8.0, 150 mM NaCl, 10 mM MgCl2, 1 mM EDTA and 1 mM DTT). The cells were lysed by 2 cycles of sonication at 60% amplitude with 1second pulse followed by 3 second pauses for 3 minutes. The suspension was mixed once in a 10-minute gap between the two cycles of sonication. The lysate was centrifuged at 37000 rpm (Ti45 rotor, Optima XE-100 Ultracentrifuge, Beckman Coulter) for 50 minutes. The supernatant was fractionated by ammonium sulphate precipitation. The 40%-70% ammonium sulphate precipitate was resuspended in buffer B0 (50 mM Tris pH-8.0, 1 mM EDTA and 1 mM DTT) through gentle swirling. After resuspension, the protein was loaded onto HiPrep Heparin FF 16/10 column (GE Healthcare) pre-equilibrated with buffer B50 (50 mM Tris pH-8.0, 50 mM NaCl, 1 mM EDTA and 1 mM DTT). The protein was eluted by linear gradient 0-100% of buffer B1000 (50 mM Tris pH-8, 1000 mM NaCl, 1 mM EDTA, 1 mM DTT). The fractions were analyzed by SDS-PAGE on a 10% polyacrylamide gel. Fractions with LlaBIII were pooled and dialyzed against buffer B50 for 2 hours at 4°C. The dialyzed samples were centrifuged to remove any precipitates and loaded onto MonoQ 10/100 GL column (GE Healthcare) pre-equilibrated with buffer B50. The protein was eluted by a linear gradient 0-50% of buffer B1000. Fractions were analyzed by SDS-PAGE. Fractions containing purified LlaBIII were pooled and concentrated before loading onto Superdex 200 10/300 column (GE Healthcare) pre-equilibrated with buffer B100 (50 mM Tris-HCl pH 8.0, 100 mM KCl and 1 mM DTT). The fractions containing monomeric LlaBIII were pooled, concentrated, and stored at -80°C.

2.2.5 Reconstitution of nucleosome particles

The nucleosomes were assembled *in vitro* by following the protocol given by (Dyer et al., 2003). Briefly, the histone octamer and 601sequence containing substrate DNA were mixed in various protein:DNA ratios. The volume was made up to 10µL with refolding buffer which contains 2 M NaCl. The mixture was incubated on ice for 30 minutes. After 30 minutes, 10 µL of 10 mM Tris pH-7.5 was added and mixed gently by tapping and again incubated on ice for 1 hour. This process was repeated three more times, stepwise adding 5 µL, 5 µL and 70 µL of 10 mM Tris pH-7.5, thereby diluting the NaCl concentration in a stepwise manner from 2 M to 0.2 M. After the last

incubation on ice for 1 hour the reconstituted nucleosome samples were loaded onto a 6% native polyacrylamide gel that was pre-run at 150 V for 20 minutes at 4°C in 1X TBE. The nucleosome samples were resolved for 90 minutes at 150 V at 4°C in 1X TBE. The gel was then stained with ethidium bromide solution prepared in 1xTBE and imaged on Typhoon Biomolecular Imagers (Amersham).

2.2.6 Restriction Enzyme Accessibility Assay (REAA)

All the REAAs were performed at 37°C in 1x Cutsmart buffer (New England Biolabs, Cat. No. B6004S). 3.75 nM nucleosome and 20 nM LlaBIII were added in the reaction mixture and incubated for 5 minutes on ice following which HhaI (NEB, Cat. No. R0139S) was added to the mix. The reactions were started by addition of 4 mM ATP and incubated at 37°C for 2 hours. At the end of the incubation, the reactions were stopped with 2 µL of 0.5 M EDTA and 0.8 µL of 10% SDS. 2 µL of 2 mg/mL Proteinase K (Invitrogen, Cat. No. AM2546) was added and incubated at 37°C for 30 minutes. The reaction mix was heated at 65°C for 20 minutes before addition of 4 µL ST buffer (100 mM Tris pH-7.5, 40% w/v Sucrose). The samples were resolved on a pre-run 6% native polyacrylamide gel run at 150 V for 50 minutes in 1x TBE at room temperature. Gels were imaged on Typhoon Biomolecular Imagers (Amersham). All the graphs were plotted and statistically analyzed using GraphPad Prism 10 software.

2.3 Results

2.3.1 Purification of human histones and assembly of octamer

The human histones were purified according to the rapid histone purification (RHP) protocol (Klinker et al., 2014).This involved overexpression of untagged histones from a plasmid construct in *E. coli* BL21(DE3) (Fig.2.1a, d, g, j) and purification of the histones from inclusion bodies under denaturing conditions with buffers containing ≥6 M urea. Initially, the histones were purified from the cell lysate by cation exchange chromatography (Fig.2.1b, e, h, k). The cells were lysed and solubilized in urea containing buffer at pH-5.2. At this pH the histones carry a net positive charge and hence bind effectively to the cation exchange column at low salt concentrations while most of the bacterial proteins come out in flow through. The histones were then eluted from the column by an increasing salt gradient. The next step involved removal of the nucleic acids that may have co-

purified with the histones as they bind non-specifically to nucleic acids. For this the histones were further purified by anion exchange chromatography (Fig. 2.1c, f, i, l). Before loading onto the anion exchange column, the purified histones were dialyzed against water to remove the excess salt from the sample as this can deter the nucleic acid binding with the column. The anion exchange column acts as a filter for purified histones wherein the nucleic acid and contaminating proteins bind to this column whereas the histones being positively charged can pass through and was recovered from the flow through. The flow through was lyophilized and the powder was resuspended in a buffer containing guanidium hydrochloride. The histones were mixed in equimolar ratios and were allowed to refold gradually together overnight in a buffer containing 2 M NaCl. This allowed the individual histones H2A, H2B, H3 and H4 to associate, refold and assemble into a functional octamer. The octamers were further purified from the misfolded or incompletely formed protein complexes by size exclusion chromatography (SEC). Based on the size of a complete octamer, it elutes at an elution volume of 12 mL (Fig. 2.2a). The fractions containing all four histone bands (Fig. 2.2b) were pooled, concentrated and the concentration was determined before reconstitution of the nucleosome.

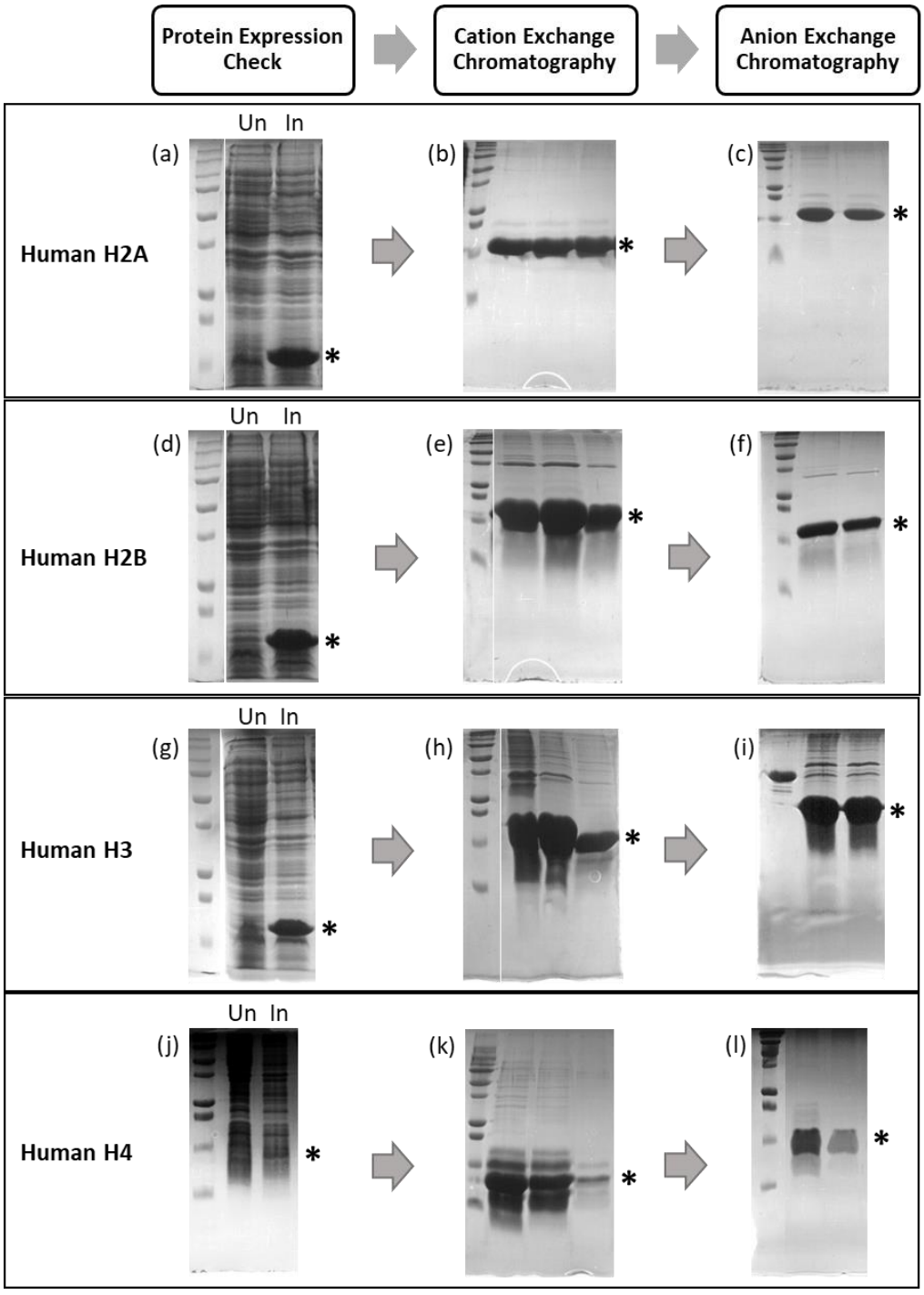

Figure 2.1: Overexpression and purification of human histones H2A, H2B, H3 and H4. (a)(d)(g) and (j) – SDS-PAGE gels showing overexpression of the respective histone proteins in *E. coli* BL21(DE3). Asterisk (*) marks the position of the respective protein bands in the gels. (b)(e)(h) and (k) – SDS-PAGE gels showing fractions from cation exchange chromatography (HiTrap SP

HP, GE Healthcare) containing the respective histone proteins. (c)(f)(i) and (l) - SDS-PAGE gels showing fractions from anion exchange chromatography (HiTrap Q HP, GE Healthcare) containing the respective histone proteins.

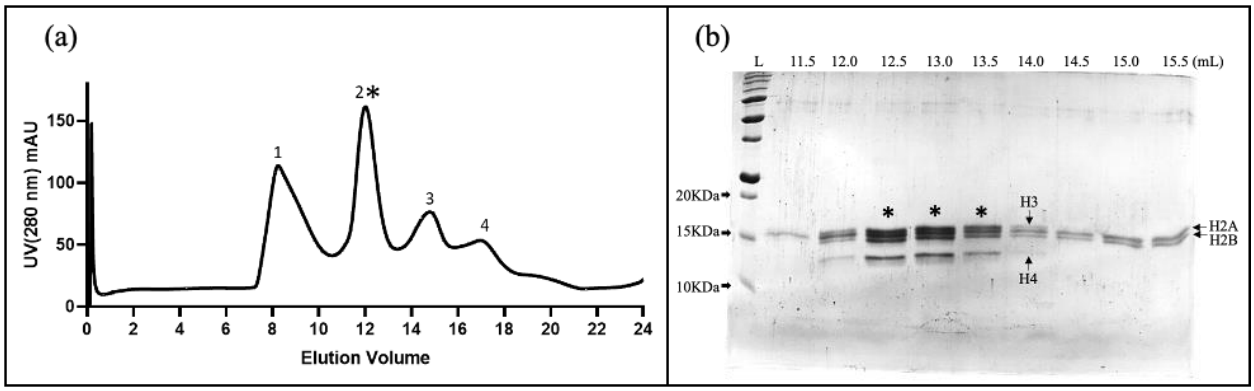

Figure 2.2 Purification of assembled octamer. (a) Elution profile of refolded octamer resolved by size exclusion chromatography (SEC) (Superdex 200 10/300 column, GE Healthcare). 1 – contaminants (high molecular weight) (8.23 mL) 2 – refolded octamer (12.01 mL) 3 – H2A-H2B dimer (14.8 mL) 4 – contaminants (low molecular weight) (17.3 mL). (b) Fractions from SEC resolved by SDS-PAGE. Bands corresponding to each of the four histones are visible in the fractions corresponding to molecular weight of refolded octamer. Asterisk (*) marks the fractions pooled and concentrated for nucleosome reconstitution. N≥3

2.3.2 Reconstitution of terminally and centrally placed mononucleosomes

5'-Cy5 labelled DNA substrates were prepared through PCR amplification and purified to a high degree by extraction from native polyacrylamide gel. The DNA substrates contained a 147 bp high nucleosome occupancy region called the Widom / 601 sequence (Lowary & Widom, 1998). This sequence was incorporated at the 3' terminal in the 265 bp DNA and at the center in the 356 bp DNA leaving a 91 bp overhang at the 3' end of the 601. A LlaBIII binding site (5'TNAGCC3') was incorporated 48 bp upstream from the 601 sequence in both these DNA substrates (Fig. 2.3). At the center of the 601 sequence, there is the target site (GCGC) for cleavage by a nucleotide-independent restriction enzyme, HhaI, that cleaves the DNA within its target site. The DNA substrates and octamers are both prepared in refolding buffer (2 M NaCl, 10 mM Tris pH-7.5, 1 mM EDTA and 10 mM β-mercaptoethanol). The octamer is mixed with the DNA in various

protein:DNA ratios (1:1, 0.5:1, 0.25:1). The nucleosome preparations are analyzed by native PAGE.

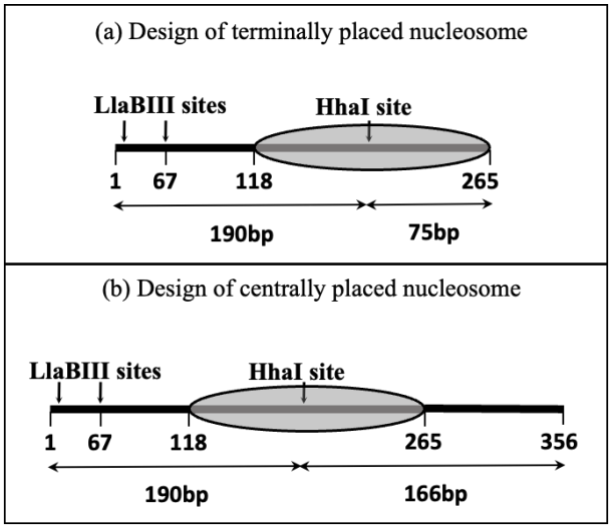

Figure 2.3: Design of the mononucleosome substrates. (a) Cartoon representation of terminally placed mononucleosome (b) Cartoon representation of centrally placed mononucleosome. Substrate design shows the positions of each element on the DNA in base pairs and the fragments that will be generated upon cleavage by HhaI.

The octamers assembled on a DNA are dynamic structures rather than static. When assembled on a DNA fragment longer than 147 bp (length of the core DNA in contact with octamer), the histone octamer tends to adopt various positions on the DNA which migrate with different mobilities on native gel. Several studies have systematically mapped these octamer binding positions on *in vitro* assembled mononucleosomes through gel purification of individual bands followed by micrococcal nuclease digestion and restriction mapping of the resistant DNA fragment (Fig. 2.4a) (Fan et al., 2003; Hamiche et al., 1999a). Presence of the nucleosome positioning sequence increases the probability of the octamer occupying the defined position on the DNA, although other species with different octamer position also exist at any given time and these result in distinct banding pattern observed for the nucleosomes on a native gel. We selected the nucleosome preparations for terminally placed (Fig. 2.4b) or centrally placed (Fig. 2.4c) mononucleosomes that contained minimum unbound DNA for the biochemical assays.

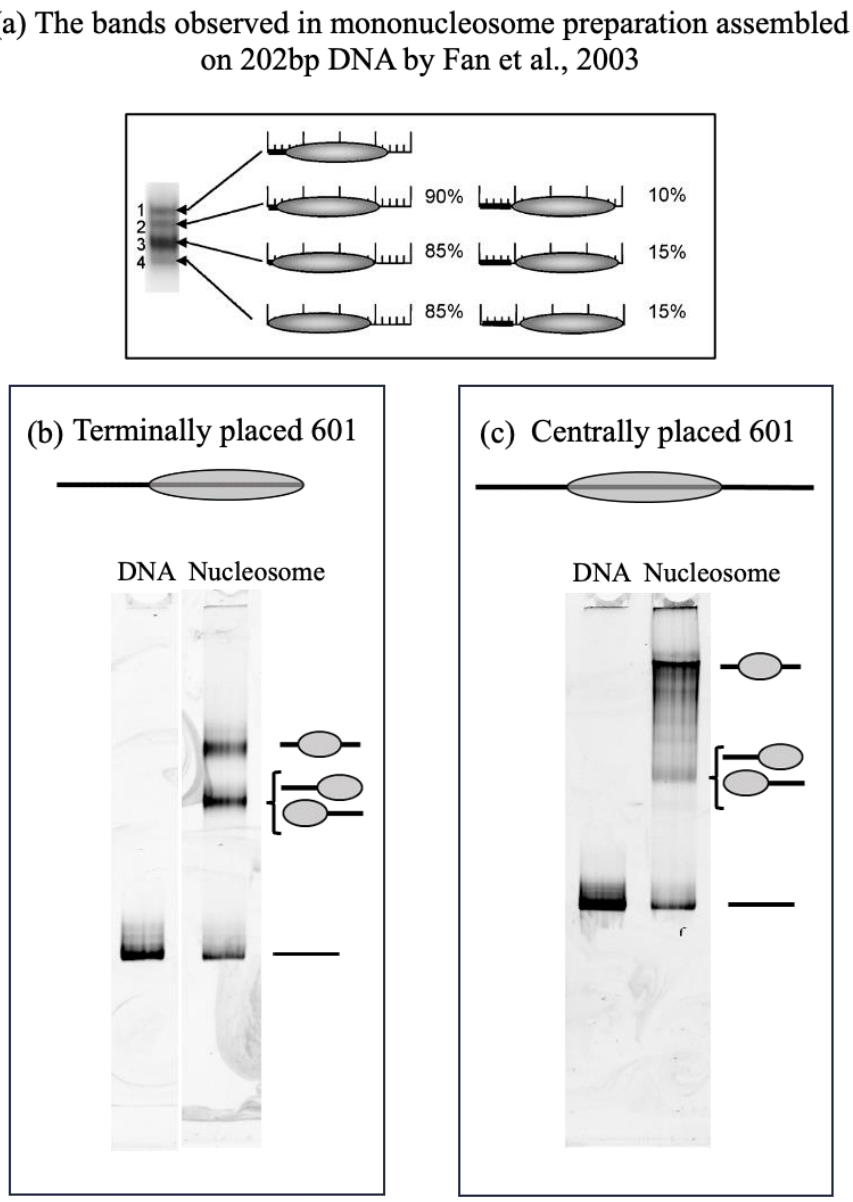

Figure 2.4: Reconstitution of nucleosomes *in vitro*. (a) Adopted from (Fan et al., 2003). Mononucleosome assembled on 202 bp DNA shows four distinctly migrating species, each corresponding to seven distinct octamer positions on the DNA as indicated. Grey ovals represent the octamer and solid black lines represent DNA (b) From this study. Mononucleosome prepared with terminally placed 601 sequence, shows a mix of centrally placed and terminally placed mononucleosomes. (c) Mononucleosome prepared with centrally placed 601 sequence, shows a mix of majorly centrally placed mononucleosomes with minor populations of variably positioned nucleosomes. Both the preparations have some unbound DNA. N=3

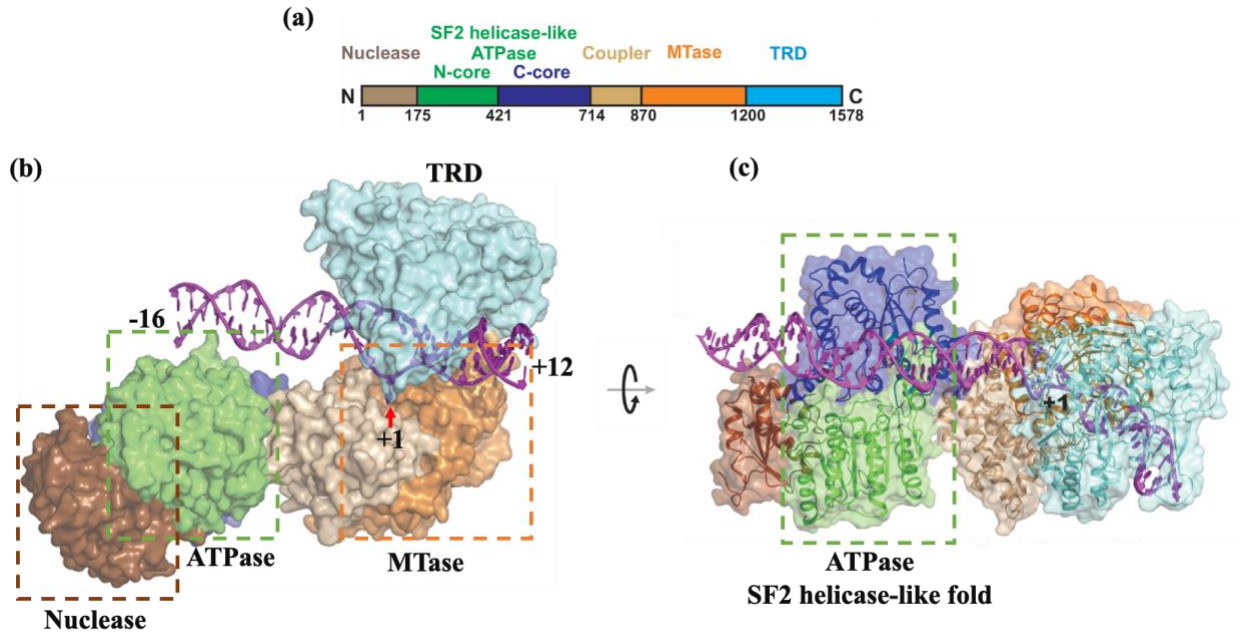

Figure 2.5: Domains of LlaBIII and their enzymatic activities. (a) Domain organization of LlaBIII. Numbers indicate amino acids from N- to C-terminal. (b) Adapted from (Chand et al., 2015). Structure of LlaBIII in complex with a 28 base pair DNA containing the specific target site. The domain organization shows an N-terminal nuclease, a SF2 helicase-like ATPase connected via a coupler domain to the methyl-transferase and a C-terminal target recognition domain (TRD). PDB accession number - 4XQK. (c) Adapted from (Van Aelst et al., 2015). Model of LlaBIII with extended DNA based on 4XQK. The rotated view of LlaBIII shows the two SF2-like ATPase folds, N-core (green) and C-core (dark blue), that constitute the conserved motor domain.

(a) Graphical representation of REA assay

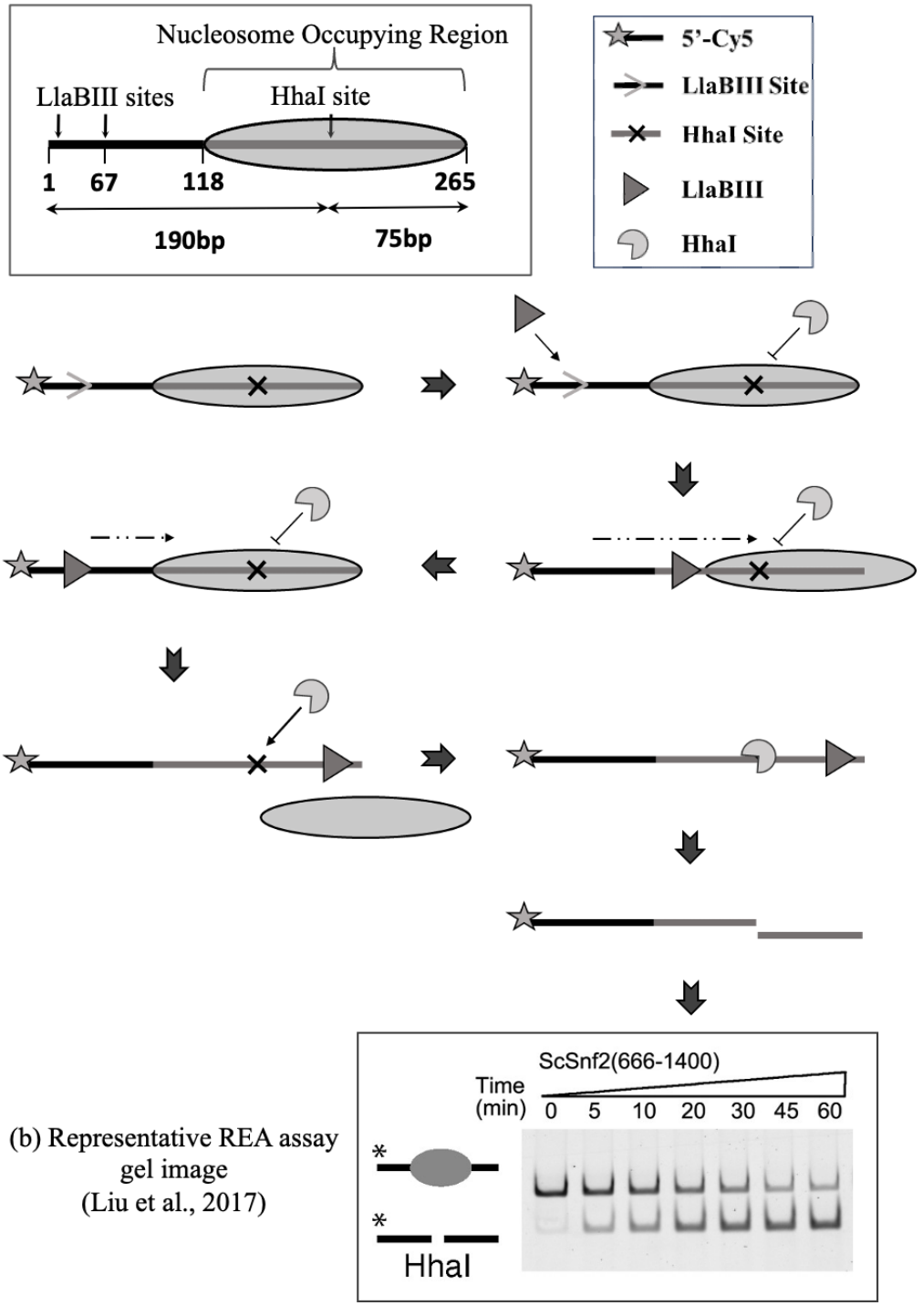

(b) Representative REA assay gel image (Liu et al., 2017)

Figure 2.6: Restriction enzyme accessibility assay (REAA) design. (a) Graphical representation of the REAA with terminally placed mononucleosome as an example. Grey ovals represent the

octamer. (b) Adapted from (Liu et al., 2017). Representative gel image showing the remodeling activity of *Saccharomyces cerevisiae* Snf2 truncated protein over time through REAA. An increase in cut DNA correlates to nucleosome displacement.

2.3.3 Displacement of mononucleosomes from DNA by LlaBIII

The nucleosome remodeling potential of LlaBIII (Fig. 2.5) was tested *in vitro* by the restriction enzyme accessibility assay (REAA) (Polach & Widom, 1995b) (Fig. 2.6). The DNA substrates for preparing the nucleosomes were designed in such a way that there is a LlaBIII target site located 48bp upstream of the 601 sequence (Fig. 2.3). There is another LlaBIII target site located close to the 5' end of the DNA, although this site is too close to the DNA end (11bp) to allow LlaBIII translocation and can be ignored for the purpose of these assays. For the assay, LlaBIII and nucleosome were mixed and incubated for 5 minutes to allow LlaBIII to bind to its target site on the nucleosome DNA. HhaI was added to the mix followed by ATP. When the octamer was bound to the 601 sequence, the HhaI target site on the substrate DNA was occluded and hence the DNA was protected from cleavage by HhaI. LlaBIII utilizes ATP and translocates DNA unidirectionally at a rate ~250 bp/s at 25°C (Šišáková et al., 2013; Smith et al., 2009c; Van Aelst et al., 2013) downstream of the target site towards the nucleosome occupancy region. In the REAA, if LlaBIII displaced the octamer from its position on the DNA, the HhaI site gets exposed, and it can be accessed by HhaI present in the reaction mix. This leads to cleavage of the substrate DNA only when remodeling of the nucleosome happens and can be detected through occurrence of cleaved DNA products of expected size when analyzed by native PAGE. We observed that in absence of LlaBIII or ATP only a small fraction of the substrate DNA that is most likely unbound in the nucleosome preparation is cleaved by HhaI. Whereas, only in presence of LlaBIII and ATP, there is an increase in the HhaI cleavage products, which indicates displacement of octamer by LlaBIII in an ATP dependent manner (Fig. 2.7a). We also tested whether a centrally positioned nucleosome that has an extra 91 bp overhang downstream of the 601 region, poses an obstacle for LlaBIII mediated displacement of the nucleosome. Similar to terminally placed nucleosome, LlaBIII could displace the centrally placed nucleosome from the 601 region (Fig. 2.7c). The fractions of intact and cleaved DNA were quantified for each of the assay conditions tested and plotted as percentage cleaved DNA (Fig. 2.7b, d). For both the terminally placed and centrally placed nucleosomes we saw that just addition of LlaBIII in absence of ATP led to no change in the fraction of DNA

cleaved. Whereas on addition of LlaBIII and ATP, there was a significant increase in the fraction of DNA cleaved indicating nucleosome displacement in an ATP dependent manner.

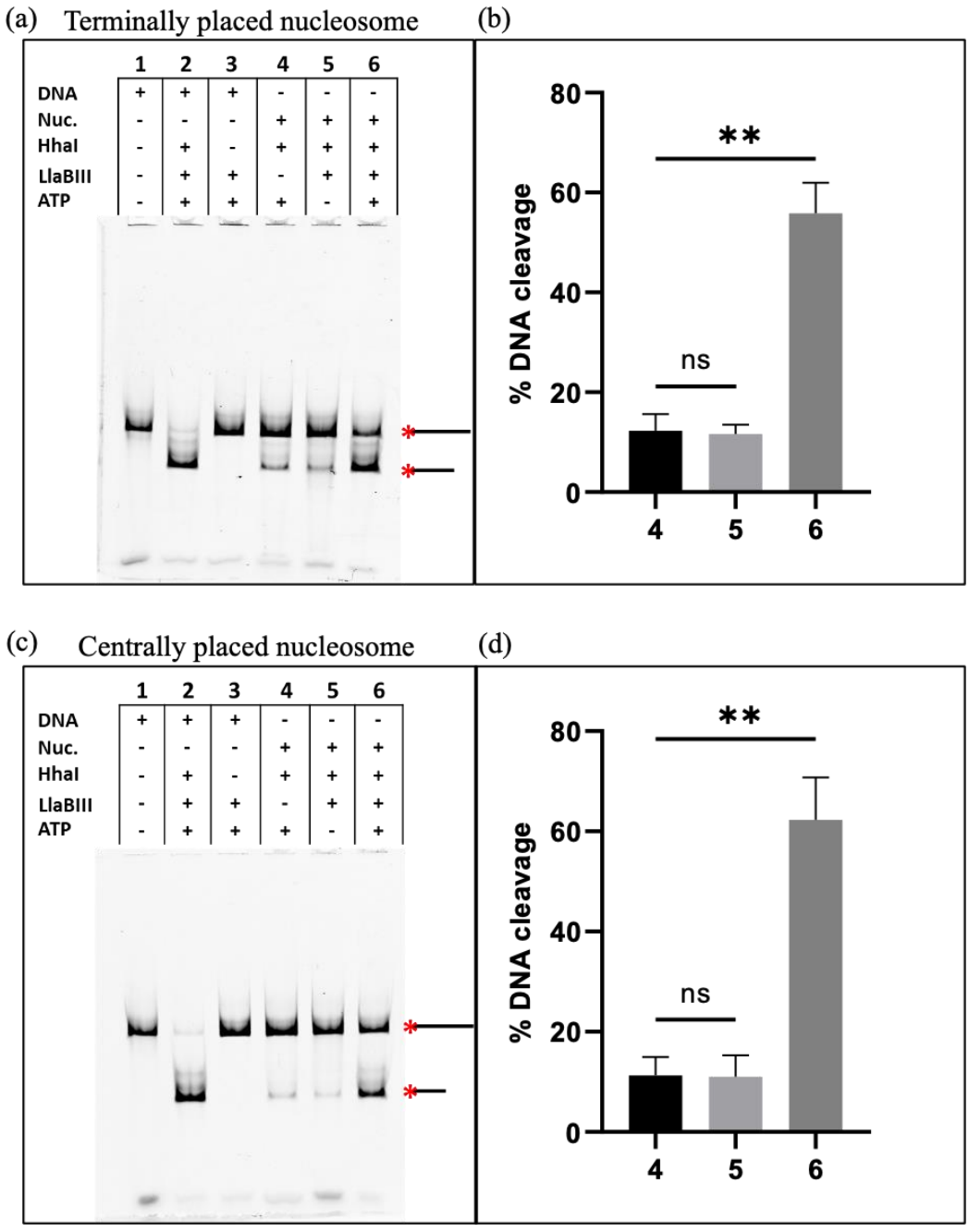

Figure 2.7: Nucleosome remodeling by LlaBIII. (a) REAA with terminally placed nucleosome and LlaBIII. (b) REAA with centrally placed nucleosome. In both the nucleosomes, HhaI site is inaccessible in presence of octamer and hence DNA is protected as seen in lanes 4. LlaBIII in

absence of ATP does not affect the nucleosome as seen in lanes 5. Whereas, in presence of ATP, LlaBIII displaces the octamer and makes the DNA accessible to cleavage by HhaI as observed from lanes 6. The bar plots show the percentage nucleosomal DNA cleaved by HhaI in absence of LlaBIII (4), in presence of LlaBIII (5) and in presence of LlaBIII and ATP (6). N=3 Statistical significance was assessed using the unpaired t-test (*P <0.05, **P <0.01, ***P <0.001). N≥3

2.4 Discussion

The Superfamily 2 of helicases includes both the bacterial defense systems, such as the Type ISP RM enzymes, and the eukaryotic chromatin remodelers, such as the Swi/Snf family (Byrd & Raney, 2012). Every member of these two families of proteins possesses the same conserved ATPase motor domain containing two RecA-like fold subdomains. Although these enzyme complexes perform strikingly different functions, the motor at the core performs the same function, that is, translocation on double stranded DNA. To achieve the varied DNA translocation related cellular functions, accessory domains or subunits are present in the core motor. Here we show that LlaBIII, a prototype of the Type ISP family, can perform the basic functions of the chromatin remodelers like the Swi2/Snf2, by virtue of the conserved and modular motor domain. Like the chromatin remodelers, it can displace nucleosome from its position on a DNA. To demonstrate that the Type ISP RM enzymes can remodel nucleosome, we tested the nucleosome remodeling activity of LlaBIII using the *in vitro* assay - REAA. For this we purified individual histones, assembled an octamer, and reconstituted nucleosome with a DNA containing the LlaBIII target site upstream of the nucleosome. Initially we tested LlaBIII remodeling activity with a terminally positioned nucleosome and found that the enzyme can displace nucleosome only in presence of ATP. This is a direct indication that the remodeling activity is a result of DNA translocation that is powered by ATP hydrolysis by the ATPase motor. Previous studies performed with triplex DNA and magnetic tweezer experiments, have shown that LlaBIII translocates DNA, without looping, in a directional manner (Chand et al., 2015; Šišáková et al., 2013). The rate of translocation has been estimated to be ~300 bp/s with 1-2 ATP hydrolyzed per base pair translocated (Šišáková et al., 2013). Here, we show that although a nucleosome is a far more complex obstacle than a triplex DNA, LlaBIII can break the multiple protein-DNA interactions between the histone octamer and the 601 DNA and efficiently remove octamer from its position. Furthermore, it can not only

remove the octamer present at the termini of the DNA but can also displace a nucleosome positioned in the center of the DNA with a ~91bp extension downstream of the nucleosome.

Our *in vitro* experiments here show that DNA translocating restriction enzyme can function as a nucleosome remodeler. LlaBIII presents the simplest form of nucleosome remodeler wherein it has target recognition and active DNA translocation capabilities, which are the minimum requirements to remodel a nucleosome in a DNA sequences-specific manner. Additionally, there are numerous Type ISP RM enzymes that recognize a specific target sequence and translocate DNA. All these enzymes have the potential to be developed into a targeted chromatin remodeling tool thus providing us with a library of chromatin remodeling enzymes with varying sequence specificities.

2.5 References

Arber, W., Hattman, S., & Dussoix, D. (1963). On the host-controlled modification of bacteriophage λ. *Virology*, *21*(1), 30–35. https://doi.org/https://doi.org/10.1016/0042-6822(63)90300-3

Bird, L. E., Subramanya, H. S., Wigley, D. B., & Sir William, A. (1998). Helicases: a unifying structural theme? In *Current Opinion in Structural Biology* (Vol. 8). http://biomednet.com/elecref/0.959440X00800014

Byrd, A. K., & Raney, K. D. (2012). Superfamily 2 helicases. *FBL*, *17*(6), 2070–2088.

Chand, M. K., Nirwan, N., Diffin, F. M., Van Aelst, K., Kulkarni, M., Pernstich, C., Szczelkun, M. D., & Saikrishnan, K. (2015). Translocation-coupled DNA cleavage by the Type ISP restriction-modification enzymes. *Nature Chemical Biology*, *11*(11), 870–877. https://doi.org/10.1038/nchembio.1926

Clapier, C. R., & Cairns, B. R. (2009). The Biology of Chromatin Remodeling Complexes. *Annual Review of Biochemistry*, *78*(1), 273–304. https://doi.org/10.1146/annurev.biochem.77.062706.153223

Davies, G. P., Kemp, P., Molineux, I. J., & Murray, N. E. (1999). *The DNA Translocation and ATPase Activities of Restriction-deficient Mutants of EcoKI*. https://doi.org/10.1006/jmbi.1999.3081.

Dryden, D. T. F., Cooper, L. P., Thorpe, P. H., & Byron, O. (1997). The in Vitro Assembly of the EcoKI Type I DNA Restriction/Modification Enzyme and Its in Vivo Implications. *Biochemistry*, *36*(5), 1065–1076. https://doi.org/10.1021/bi9619435

Dürr, H., Körner, C., Müller, M., Hickmann, V., & Hopfner, K.-P. (2005). X-Ray Structures of the Sulfolobus solfataricus SWI2/SNF2 ATPase Core and Its Complex with DNA. *Cell*, *121*(3), 363–373. https://doi.org/10.1016/j.cell.2005.03.026

Dussoix, D., & Arber, W. (1962). Host specificity of DNA produced by Escherichia coli: II. Control over acceptance of DNA from infecting phage λ. *Journal of Molecular Biology*, *5*(1), 37–49. https://doi.org/https://doi.org/10.1016/S0022-2836(62)80059-X

Dyer, P. N., Edayathumangalam, R. S., White, C. L., Bao, Y., Chakravarthy, S., Muthurajan, U. M., & Luger, K. (2003). Reconstitution of Nucleosome Core Particles from Recombinant Histones and DNA. In *Methods in Enzymology* (Vol. 375, pp. 23–44). Academic Press. https://doi.org/https://doi.org/10.1016/S0076-6879(03)75002-2

Eskin, B., & Linn, S. (1972a). The Deoxyribonucleic Acid Modification and Restriction Enzymes of Escherichia coli B: II. PURIFICATION, SUBUNIT STRUCTURE, AND CATALYTIC PROPERTIES OF THE RESTRICTION ENDONUCLEASE. *Journal of Biological Chemistry*, *247*(19), 6183–6191. https://doi.org/https://doi.org/10.1016/S0021-9258(19)44780-7

Eskin, B., & Linn, S. (1972b). The Deoxyribonucleic Acid Modification and Restriction Enzymes of Escherichia coli B: III. STUDIES OF THE RESTRICTION ADENOSINE TRIPHOSPHATASE. *Journal of Biological Chemistry*, *247*(19), 6192–6196. https://doi.org/https://doi.org/10.1016/S0021-9258(19)44781-9

Fairman-Williams, M. E., Guenther, U.-P., & Jankowsky, E. (2010). SF1 and SF2 helicases: family matters. *Current Opinion in Structural Biology*, *20*(3), 313–324. https://doi.org/https://doi.org/10.1016/j.sbi.2010.03.011

Fan, H.-Y., He, X., Kingston, R. E., & Narlikar, G. J. (2003). Distinct Strategies to Make Nucleosomal DNA Accessible. *Molecular Cell*, *11*(5), 1311–1322. https://doi.org/10.1016/S1097-2765(03)00192-8

Gorbalenya, A. E., & Koonin, E. V. (1991). Endonuclease (R) subunits of type-I and type-III restriction-modification enzymes contain a helicase-like domain. *FEBS Letters*, *291*(2), 277–281. https://doi.org/https://doi.org/10.1016/0014-5793(91)81301-N

Grüne, T., Brzeski, J., Eberharter, A., Clapier, C. R., Corona, D. F. V, Becker, P. B., & Müller, C. W. (2003). Crystal Structure and Functional Analysis of a Nucleosome Recognition Module

of the Remodeling Factor ISWI. *Molecular Cell*, *12*(2), 449–460. https://doi.org/10.1016/S1097-2765(03)00273-9

Hamiche, A., Sandaltzopoulos, R., Gdula, D. A., & Wu, C. (1999). ATP-Dependent Histone Octamer Sliding Mediated by the Chromatin Remodeling Complex NURF. *Cell*, *97*(7), 833–842. https://doi.org/10.1016/S0092-8674(00)80796-5

Horiuchi, K., & Zinder, N. D. (1972). *Cleavage of Bacteriophage fl DNA by the Restriction Enzyme of Escherichia coli B (DNA endonuclease/mutant DNA/sites of cleavage)* (Vol. 69, Issue 11). https://www.pnas.org

Josephsen, J., & Vogensen, F. K. (1989). Identification of three different plasmid-encoded restriction/modification systems in Streptococcus lactis subsp. cremoris W56. *FEMS Microbiology Letters*, *59*(1–2), 161–166. https://doi.org/10.1111/j.1574-6968.1989.tb03102.x

Klinker, H., Haas, C., Harrer, N., Becker, P. B., & Mueller-Planitz, F. (2014). Rapid Purification of Recombinant Histones. *PLOS ONE*, *9*(8), e104029-. https://doi.org/10.1371/journal.pone.0104029

Kong, J., & Josephsen, J. (2001). *The ability of the plasmid-encoded restriction and modification system LlaBIII to protect Lactococcus lactis against bacteriophages*.

Kong, J., & Josephsen, J. (2002). The ability of the plasmid-encoded restriction and modification system LlaBIII to protect Lactococcus lactis against bacteriophages. *Letters in Applied Microbiology*, *34*(4), 249–253. https://doi.org/https://doi.org/10.1046/j.1472-765x.2002.01089.x

Liu, X., Li, M., Xia, X., Li, X., & Chen, Z. (2017). Mechanism of chromatin remodelling revealed by the Snf2-nucleosome structure. *Nature*, *544*(7651), 440–445. https://doi.org/10.1038/nature22036

Loenen, W. A. M., Dryden, D. T. F., Raleigh, E. A., & Wilson, G. G. (2014a). Type i restriction enzymes and their relatives. *Nucleic Acids Research*, *42*(1), 20–44. https://doi.org/10.1093/nar/gkt847

Loenen, W. A. M., Dryden, D. T. F., Raleigh, E. A., & Wilson, G. G. (2014b). Type I restriction enzymes and their relatives. *Nucleic Acids Research*, *42*(1), 20–44. https://doi.org/10.1093/nar/gkt847

Lowary, P. T., & Widom, J. (1998). *New DNA Sequence Rules for High Affinity Binding to Histone Octamer and Sequence-directed Nucleosome Positioning*.

Murray, N. E., Daniel, A. S., Cowan, G. M., & Sharp, P. M. (1993). Conservation of motifs within the unusually variable polypeptide sequences of type I restriction and modification enzymes. *Molecular Microbiology*, *9*(1), 133–143. https://doi.org/https://doi.org/10.1111/j.1365-2958.1993.tb01675.x

Nielsen, E. W. (1998). Long term use of a cheddar starter and development of phages with homology to its bacteria. *INTERNATIONAL DAIRY JOURNAL*, *8*(12), 1003–1009.

Polach, K. J., & Widom, J. (1995a). Mechanism of Protein Access to Specific DNA Sequences in Chromatin: A Dynamic Equilibrium Model for Gene Regulation. *Journal of Molecular Biology*, *254*(2), 130–149. https://doi.org/https://doi.org/10.1006/jmbi.1995.0606

Polach, K. J., & Widom, J. (1995b). Mechanism of Protein Access to Specific DNA Sequences in Chromatin: A Dynamic Equilibrium Model for Gene Regulation. In *J. Mol. Biol* (Vol. 254).

Rosamond, J., Endlich, B., & Linn, S. (1979). Electron microscopic studies of the mechanism of action of the restriction endonuclease of Escherichia coli B. *Journal of Molecular Biology*, *129*(4), 619–635. https://doi.org/https://doi.org/10.1016/0022-2836(79)90472-8

Singleton, M. R., Dillingham, M. S., & Wigley, D. B. (2007). Structure and Mechanism of Helicases and Nucleic Acid Translocases. *Annual Review of Biochemistry*, *76*(1), 23–50. https://doi.org/10.1146/annurev.biochem.76.052305.115300

Singleton, M. R., & Wigley, D. B. (2002). Modularity and Specialization in Superfamily 1 and 2 Helicases. *Journal of Bacteriology*, *184*(7), 1819–1826. https://doi.org/10.1128/jb.184.7.1819-1826.2002

Šišáková, E., Van Aelst, K., Diffin, F. M., & Szczelkun, M. D. (2013). The Type ISP Restriction-Modification enzymes LlaBIII and LlaGI use a translocation-collision mechanism to cleave non-specific DNA distant from their recognition sites. *Nucleic Acids Research*, *41*(2), 1071–1080. https://doi.org/10.1093/nar/gks1209

Smith, R. M., Diffin, F. M., Savery, N. J., Josephsen, J., & Szczelkun, M. D. (2009a). DNA cleavage and methylation specificity of the single polypeptide restriction-modification enzyme LlaGI. *Nucleic Acids Research*, *37*(21), 7206–7218. https://doi.org/10.1093/nar/gkp790

Smith, R. M., Diffin, F. M., Savery, N. J., Josephsen, J., & Szczelkun, M. D. (2009b). DNA cleavage and methylation specificity of the single polypeptide restriction-modification enzyme LlaGI. *Nucleic Acids Research*, *37*(21), 7206–7218. https://doi.org/10.1093/nar/gkp790

Smith, R. M., Josephsen, J., & Szczelkun, M. D. (2009). The single polypeptide restriction-modification enzyme LlaGI is a self-contained molecular motor that translocates DNA loops. *Nucleic Acids Research*, *37*(21), 7219–7230. https://doi.org/10.1093/nar/gkp794

Studier, F. W., & Bandyopadhyay, P. K. (1988). Model for How Type I Restriction Enzymes Select Cleavage Sites in DNA. *Proceedings of the National Academy of Sciences of the United States of America*, *85*(13), 4677–4681. http://www.jstor.org/stable/31850

Van Aelst, K., Saikrishnan, K., & Szczelkun, M. D. (2015). Mapping DNA cleavage by the Type ISP restriction-modification enzymes following long-range communication between DNA sites in different orientations. *Nucleic Acids Research*, *43*(21), 10430–10443. https://doi.org/10.1093/nar/gkv1129

Van Aelst, K., Šišáková, E., & Szczelkun, M. D. (2013). DNA cleavage by Type ISP Restriction-Modification enzymes is initially targeted to the 3′-5′ strand. *Nucleic Acids Research*, *41*(2), 1081–1090. https://doi.org/10.1093/nar/gks1210

Werner Arber, B., & Linn, S. (1969). *DNA MODIFICATION AND RESTRICTION1,2,a 700*. www.annualreviews.org

Yuan, R., Hamilton, D. L., & Burckhardt, J. (1980). DNA Translocation by the Restriction Enzyme from E. coli K. In *Cell* (Vol. 20).

Chapter 3 – Nucleosome remodeling is exclusively the property of active DNA translocases

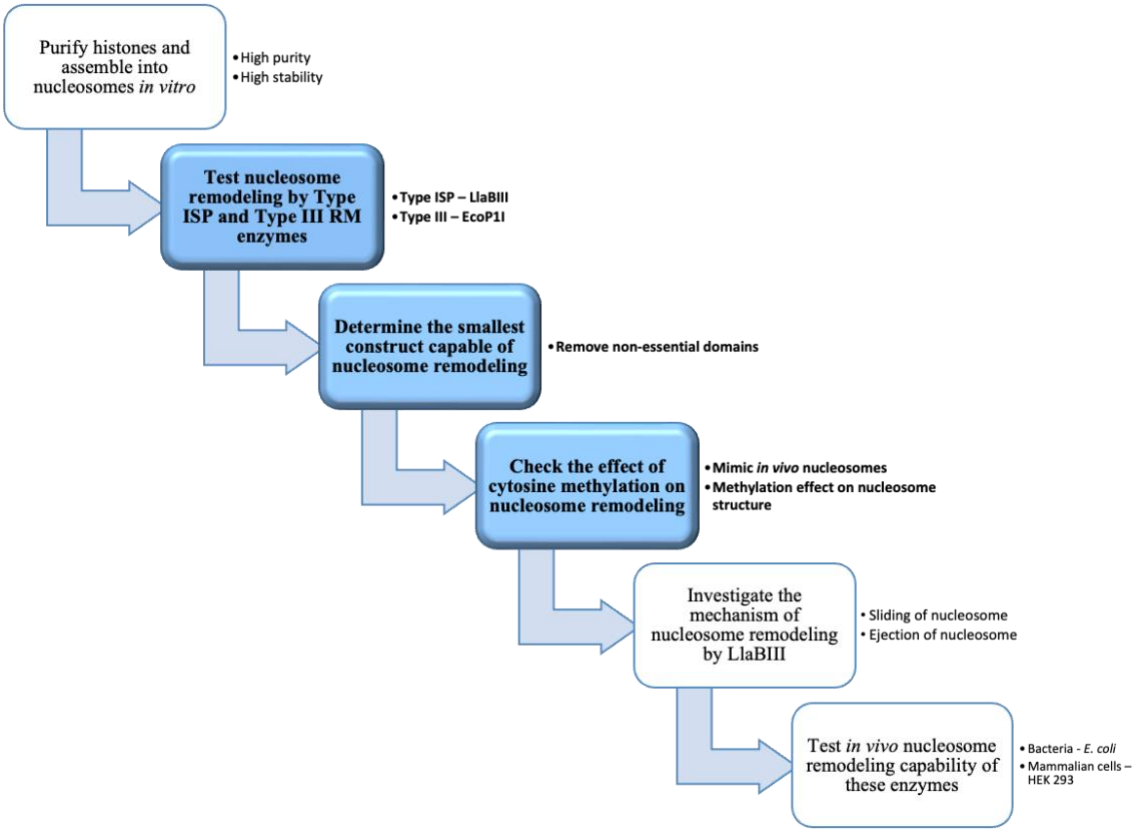

3.1 Introduction

A collective feature of the NTP dependent restriction enzymes is their ability to communicate between two distantly spaced target sites by moving along the DNA. Majority of these enzymes (Type I and Type III) fall into the Superfamily 2 (SF2) of helicases. All the helicases possess a RecA or AAA+ fold that is involved in transduction of energy from NTP hydrolysis (Singleton et al., 2007). There are a total of six superfamilies of helicases with most AAA+ motor proteins being included in the Superfamily 3 to 6 and proteins containing two tandem RecA like fold per monomer in superfamily 1 and 2 (Byrd & Raney, 2012; Singleton et al., 2007). Helicases were initially recognized as the enzymes that utilized NTP hydrolysis to bring about DNA or RNA strand unwinding (Gorbalenya & Koonin, 1993). Eventually it was found that there are many DNA translocases that were classified as helicase based on their motifs but did not unwind duplex nucleic acids. These enzymes used NTP hydrolysis to power their translocation on DNA. Hence, the helicase encompasses all the enzymes that use nucleoside 5'-triphosphate (NTP) hydrolysis to bring about a mechanical action towards remodeling nucleic acids or nucleic acid-protein complexes (Fairman-Williams et al., 2010; Singleton & Wigley, 2002). The RecA like ATPases included in superfamily 2 are further classified into ten families (Byrd & Raney, 2012; Fairman-Williams et al., 2010). As mentioned previously, the chromatin remodelers together constitute a family (Swi/Snf) under the SF2. The NTP dependent restrictions modification enzyme Type I and Type III RM enzymes collectively constitute another family (T1R) under of the SF2 helicases. Type I and Type III RM enzymes both recognize specific target sites in the DNA. Target recognition activates the enzymes for directional movement along the DNA which allows communication with a second enzyme bound or moving from another target site separated by several thousand base-pairs. The Type I RM enzymes have been shown to communicate between two target sites through active DNA translocation. On the contrary, the Type III RM enzymes, upon target recognition, have been shown to hydrolyze ATP to switch to a diffusion ready enzyme conformation. The activated enzyme thus diffuses downstream from the target site and interacts with an enzyme bound at a target site to bring about a double strand break. Hence, though the Type I and Type III enzymes are driven by the same conserved ATPase motor, the way these enzymes move along the DNA differs significantly.

Earlier we had shown that LlaBIII, a Type ISP RM enzyme can displace a nucleosome from its position on the DNA. A nucleosome is an intricate protein-DNA complex that LlaBIII could readily remodel. A nucleosome is the fundamental unit of the eukaryotic genome. Two monomers of each histone, H2A, H2B, H3 and H4 associate to form an octamer. The octamer associates with a 147bp DNA that forms 1.65 turns of left-handed super helical wrap around the histone octamer core to form a nucleosome (Davey et al., 2002; Luger et al., 1997). This wrapping of DNA makes the sequence within the nucleosome inaccessible to any DNA binding protein such as RNA polymerase, restriction enzymes, transcription factors and others. The inaccessibility of DNA may be partly due to the DNA distortion caused by histone octamer binding and partly due to the abundant protein-DNA interactions between the octamer and the DNA. The octamer-DNA complex is secured by numerous hydrogen bonds, salt bridges, non-polar interactions, and electrostatic interactions. About fourteen arginine residues (10 from the histone fold and 4 from histone tails) protrude into the DNA minor groove, into the phosphate backbone and form hydrogen bonds and non-polar interactions with the deoxy-ribose sugars (Davey et al., 2002; Harp et al., 2000; Luger et al., 1997). Additionally, the side chains as well as main chain amide nitrogen secure the DNA phosphates with hydrogen bonds. Most of these interactions either stabilize the phosphate backbone or the deoxyribose sugar (Davey et al., 2002; Luger et al., 1997). Although, the DNA sequence does influence the DNA flexibility and helicity, thus influencing the overall nucleosome stability. Also, there are certain specific (leucine with thymidine) and partly specific (arginine with pyrimidine) interactions between the histone residues and the DNA bases which further contribute towards nucleosome structural stability (Luger et al., 1997). Thus, sequences that contain a combination of these favorable base pair sequences can facilitate higher nucleosome stability and hence occupancy (Adhireksan et al., 2020; Chua et al., 2012; Vasudevan et al., 2010). An example of this partial sequence dependence is the Widom (601) sequence, which has been shown to have higher probability of nucleosome occupancy compared to most other sequences tested (Lowary & Widom, 1998). We have utilized the Widom sequence in our studies to allow optimal nucleosome stability and positioning. Here we further increased the complexity of the nucleosome substrate by duplicating the 601 sequence to assemble an array of two nucleosomes on the DNA substrate. We then tested the remodeling potential of LlaBIII with this dinucleosome, where the number of octamer-DNA contacts are doubled, and the enzyme encounters a more complex nucleosome substrate than a mononucleosome. We also investigated whether the Type

III RM enzyme EcoP1I, an ATP-dependent RM enzyme having an SF2 ATPase domain, can also remodel the dinucleosome.

3.2 Materials and methods

3.2.1 Preparation of DNA for dinucleosome assembly

The DNA required for dinucleosome assembly was prepared by PCR amplification. A 329 bp fragment was generated from a plasmid containing the 601 sequence using primers 329F and 329R. The 329F primer incorporated the target sites for enzymes LlaBIII and EcoP1I upstream of the 601 sequence in the amplified fragment. Next, two fragments each containing a 601 region were generated using 329 bp fragment as template. The first fragment was generated using primers 329F and R1 overlap. This incorporated a NdeI site at the 3' terminal of this DNA fragment. The second fragment was generated using primers F1 overlap and 329R. This incorporated a NdeI site at the 5' terminal in this fragment. Both the fragments were purified using a PCR Cleanup Kit (Qiagen, Cat. No. 28106) and subjected to digestion by NdeI (NEB, Cat. No. R0111S). The digested fragments were again purified using the PCR Cleanup Kit. Equimolar ratio of both the DNA fragments were ligated using the T4 DNA ligase (NEB, Cat. No. M0202S) according to the manufacturer's specifications. Upon ligation, the fragments were resolved on a 1% agarose gel, stained with ethidium bromide, and visualized under a UV transilluminator. The band corresponding to the 498 bp ligated product was excised from the gel and purified using a gel extraction kit (Qiagen, Cat. No. 28704). The purified 498 bp DNA was utilized as a template for further PCR amplification using primers 329F and 329R, to generate more DNA. After amplification, the DNA was purified from a native polyacrylamide gel as described previously in section 2.2.1. Subsequently, the gel purified DNA was used for dinucleosome assembly.

For preparation of the methylated DNA, the unmethylated 498 bp DNA was used as a template. Instead of the unmethylated cytosine, a dNTP mix with 5-methylcytosine was used in the PCR reaction. This led to amplification of a fully methylated 498 bp DNA, except for the ends where primers are incorporated, which were hemi-methylated. The methylated 498 bp DNA was also purified from native polyacrylamide gel as previously described and stored in -30°C until further requirement.

3.2.2 Purification of histones and assembly of histone octamer

Purification of histones and assembly of histone octamers was performed as described in sections 2.2.2 and 2.2.3 respectively.

3.2.3 Purification of LlaBIII WT, LlaBIII^{R564A} and LlaBIII n-

Purification of LlaBIII WT was performed as described in section 2.2.4. LlaBIII^{R564A} was purified as described in (Chand et al., 2020). LlaBIII n- cloning and purification has been previously described in PhD thesis by Dr. Mahesh Kumar Chand. Shortly, 1-165 amino acids that constitute the nuclease domain of LlaBIII were deleted from the full length *llaBiii* to obtain the construct expressing LlaBIII n-. The truncation of the nuclease domain was obtained by PCR amplification of the *llaBiii n-* from the full length *llaBiii* as template using primers LBΔN-pHIS-F and LB-PHIS-R. The ~4.3kb *llaBiii* n- fragment was cloned into NdeI and BamHI sites in pHIS17 vector through restriction-ligation cloning method and the clone having the correct sequence of *llaBiii* n- was further processed for protein expression. The protein was expressed in *E. coli* BL21-AI cells induced with 0.2% arabinose and purified following the same protocol as described for LlaBIII WT. All the proteins were stored at -80°C until further use.

3.2.4 Purification of EcoP1I^{E916A}

Purification of EcoP1I^{E916A} was performed by Dr. Ishtiyaq Ahmad and has been described in (Ahmad et al., 2018).

3.2.5 Reconstitution of dinucleosome and determination of nucleosome position on the DNA

Dinucleosome assembly was performed following the same protocol that was followed for mononucleosomes as mentioned in section 2.2.5. Dinucleosomes were reconstituted with un-methylated and methylated 498 bp DNA for the REAA.

The dinucleosome DNA possesses a NotI site at the beginning of the first 601 region, HhaI site in the center of each 601 regions and a NdeI site in the center of the linker region between the two 601 regions. Upon assembly, the dinucleosome was incubated with each of these enzymes

individually at 37°C for 2 hours in 1X Cutsmart buffer (NEB, Cat. No. B6004S). The reactions were stopped with 95 mM EDTA and 0.77% SDS at the end of incubation. 0.8 µL of 2 mg/mL Proteinase K (Invitrogen, Cat. No. AM2546) was added to all the reactions and incubated for 1 hour at 37 °C followed by heat inactivation at 65°C for 15 minutes. The samples were mixed with 3 ul of 6X Purple loading dye (NEB, Cat. No. B7025S) and loaded onto a 6% native PAGE run at 150 V for 55 minutes at room temperature. The PAGE gel was stained with ethidium bromide and scanned on Typhoon Trio+ Variable mode imager.

3.2.6 Restriction enzyme accessibility assay (REAA) with dinucleosome

All the remodeling assays were performed at 37°C for 2 hours in Cutsmart buffer at 1X concentration. Initially, 10-15 nM nucleosome and 100 nM enzyme (LlaBIII or EcoPI^{E916A}) were mixed on ice. The mixture was incubated on ice for 5-10 minutes. 0.5 µL HhaI (NEB, Cat. No. R0139S) or for methylated substrate, MseI (NEB, Cat. No. R0525S) was added to the relevant reactions. The reaction was started with addition of 2 mM ATP, and the samples were incubated at 37 °C for 2 hours. ATP (2 mM) was supplemented halfway through the incubation. The reactions were stopped with 95 mM EDTA and 0.77% SDS at the end of incubation. 0.8 µL Proteinase K (2 mg/mL) was added to all the reactions and incubated for 1 hour at 37°C followed by heat inactivation at 65°C for 15 minutes. The samples were mixed with 3 ul of 6X Purple loading dye and loaded onto a 6% native PAGE run at 150 V for 55 minutes at room temperature. The PAGE gel was stained with ethidium bromide and scanned on Typhoon Trio+ Variable mode imager. DNA bands were quantified using ImageJ software. GraphPad Prism 10 software was used for plotting graphs and statistical analysis.

3.3 Results

3.3.1 Preparation of dinucleosome

The DNA for dinucleosome reconstitution was designed to incorporate two 601 regions in the center separated by a 22 bp linker. A LlaBIII target site (TNAGCC) and an EcoP1I target site (AGACC) were incorporated adjacent to each other and upstream from the 601 regions. The dinucleosome DNA possessed a NotI site at the beginning of the first 601 sequence downstream of LlaBIII target site, a HhaI site in the center of both the 601 sequences and a NdeI site in the

center of the 22 bp linker separating the two 601 sequences (Fig. 3.1). Histones were purified and assembled into octamers as described in sections 2.2.2 and 2.2.3. The dinucleosomes were assembled following the salt dilution protocol (Dyer et al., 2003). Dinucleosomes were reconstituted with both the methylated and unmethylated DNA individually. Dinucleosomes were assembled in various DNA:octamer ratios and the quality of the preparations was analyzed on a 6% native polyacrylamide gel. The dinucleosome preparations containing minimum unbound DNA were utilized further for determination of nucleosome positions on the substrate DNA. The dinucleosome sample was incubated with NotI, HhaI and NdeI individually. After incubation, the sample was denatured by heating and analysed by native PAGE. The cleavage pattern obtained upon digestion with each of these enzymes indicated the occupancy of the respective DNA region by the octamer. The NotI site is present at the boundary of the octamer occupying region (601) and hence remains partially open. This results in partial access of NotI to its target site when the octamer is bound to the DNA. Hence, we observe partial cleavage of the DNA with NotI (Fig. 3.2b). On the other hand, the HhaI site is present in the center of the 601 region and hence would be completely occluded by the bound octamers. In the dinucleosome, as octamers occupied both the 601 regions, HhaI was unable to cleave the DNA at either of the two sites (Fig. 3.2c). Additionally, in an optimally assembled dinucleosome, the NdeI site that is present at the center of the linker between the two nucleosomes should be exposed completely in native state. In our assay, NdeI could completely cleave the dinucleosome DNA (Fig. 3.2d) indicating that the octamers were optimally placed in our preparations.

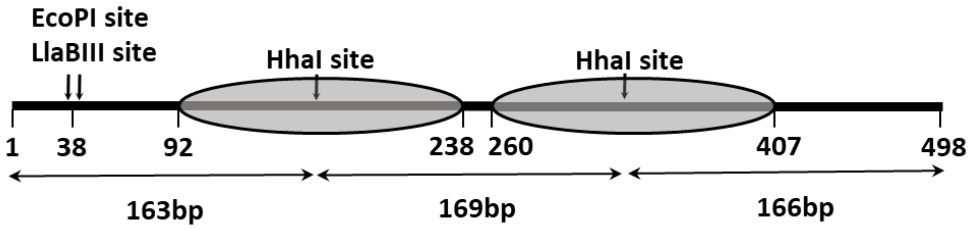

Figure 3.1: Design of the dinucleosome. The dinucleosome DNA was designed to have two 601 regions (grey line) separated by a 22 bp linker. Grey ovals represent the nucleosome occupancy regions (601). There is an HhaI target sequence in the center of each 601 region, a NotI target sequence at the beginning of the first 601 region and a NdeI target sequence in the center of the 22 bp linker. The LlaBIII target sequence is located 48 bp from the beginning of the first 601 region.

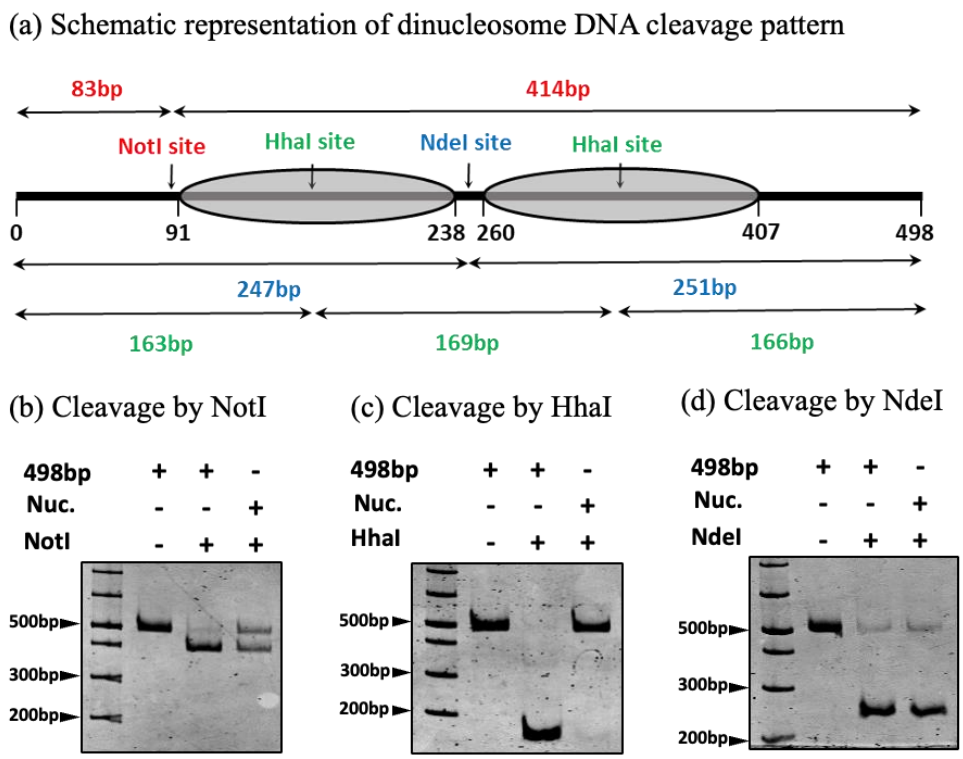

Figure 3.2: Nucleosome positioning check. The nucleosome occupancy on the substrate DNA was confirmed by digestion with the specified restriction enzymes and the cleavage fragments were analyzed on native PAGE. (a) Schematic representation of the dinucleosome substrate depicting the position of target sites for NotI (Red), HhaI (Green) and NdeI (Blue), and the fragments generated upon cleavage by these enzymes individually. Grey ovals represent the nucleosome occupancy. Representative native PAGE images showing the DNA cleavage pattern for free DNA and dinuclesosome upon cleavage by NotI (b), HhaI (c) and NdeI (d). N≥2

3.3.2 REAA with dinucleosome and LlaBIII WT

The dinucleosome that we prepared with the unmethylated DNA had one HhaI site in the center of each of the two 601 sequences. The 601 DNA forms the core of the nucleosome as it gets wrapped around the octamer in an optimally assembled nucleosome. When unaltered the nucleosomes occlude the HhaI sites and hence the DNA is completely protected from cleavage by HhaI as seen previously (Fig. 3.2c). We used this optimally assembled dinucleosome for testing the extent of remodeling potential of LlaBIII. The dinucleosome was incubated with LlaBIII in the absence and presence of ATP. The remodeling activity was monitored through cleavage of the 498

bp substrate DNA by HhaI. Exposure of and cleavage at either of the two HhaI sites was expected to yield ~335 bp and ~163 bp fragments, while cleavage at both the sites was expected to result in three fragments ~163 bp, ~169 bp and ~166 bp in length (Fig. 3.3a).

When resolved on a native PAGE, we observed that either in the absence of LlaBIII or ATP, the integrity of the DNA remained unaffected by the presence of HhaI (Fig. 3.3b & c, Lane 5 & 6). However, addition of LlaBIII, ATP and HhaI resulted in a prominent ~163 bp cleaved DNA fragment and a less prominent fragment that migrated just above 300 bp (Fig. 3.3b & c, Lane 7). The ~163 bp band was consistent with the DNA fragments obtained when HhaI cleaved at both its sites. As the size of the three fragments differed by only a few base pairs, they failed to be resolved into individual bands. The band near 300 bp was interpreted as the ~335 bp fragment produced when HhaI cleaved only at one site. This result clearly indicated that in the presence of LlaBIII and ATP, the two HhaI sites were exposed for cleavage. The occurrence of the ~335 bp fragment was suggestive of stepwise remodeling.

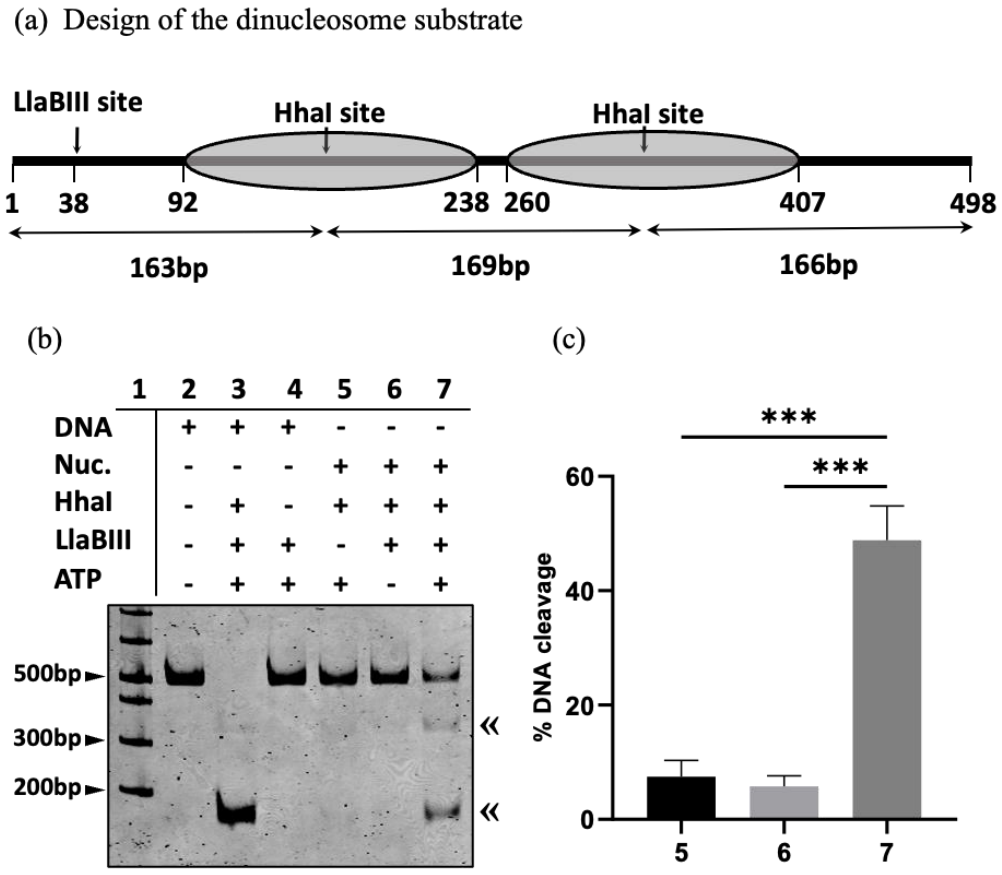

Figure 3.3: REAA with dinucleosome. (a) Schematic showing the positions of the HhaI target sites and the fragments generated upon DNA cleavage by HhaI. Gray ovals represent nucleosome occupancy region. (b) Representative native PAGE image accompanied by (c)-bar plots with percentage of DNA cleavage plotted on the Y-axis with corresponding lane numbers from the gel on X-axis. The arrows (**«**) mark the positions of the expected DNA cleavage products on the polyacrylamide gel. Error bars represent standard error mean for four separate trials. Statistical significance was assessed using the unpaired t-test (*P <0.05, **P <0.01, ***P <0.001). N≥4.

3.3.3 REAA with dinucleosome and EcoP1I

Having established that the Type ISP enzyme, LlaBIII, can dislodge histone octamers, we next asked if the SF2 ATPase in another closely related family of restriction enzymes, the Type III RM enzyme family, could do the same. For this we tested the nucleosome remodeling activity of EcoP1I, a Type III RM enzyme. In contrast to the LlaBIII ATPase, the SF2 ATPase in Type III RM enzymes translocates DNA for a short distance of less than 40 bp, and instead functions as a switch facilitating the 1D diffusion of the enzyme along the DNA and activating the nuclease (Schwarz et al., 2013; Ahmad et al., 2018; Sczelkun's recent paper in BioRxiv). We performed REAA using the same dinucleosome substrate, as it had a recognition sequence of the Type III RM enzyme EcoP1I, AGACC, adjacent to the LlaBIII recognition sequence (Fig. 3.4a). A nuclease-dead but ATPase-active mutant of EcoP1I (EcoP1I^{E916A}) was used for these experiments to prevent the enzyme from catalyzing the non-canonical single-site DNA cleavage (Ahmad et al., 2018). The REAA experiment clearly showed that, unlike LlalBIII, EcoP1I^{E916A} did not remodel the dinucleosome and expose the HhaI sites for cleavage in absence or presence of ATP (Fig. 3.4b & c, Lane 6 & 7).

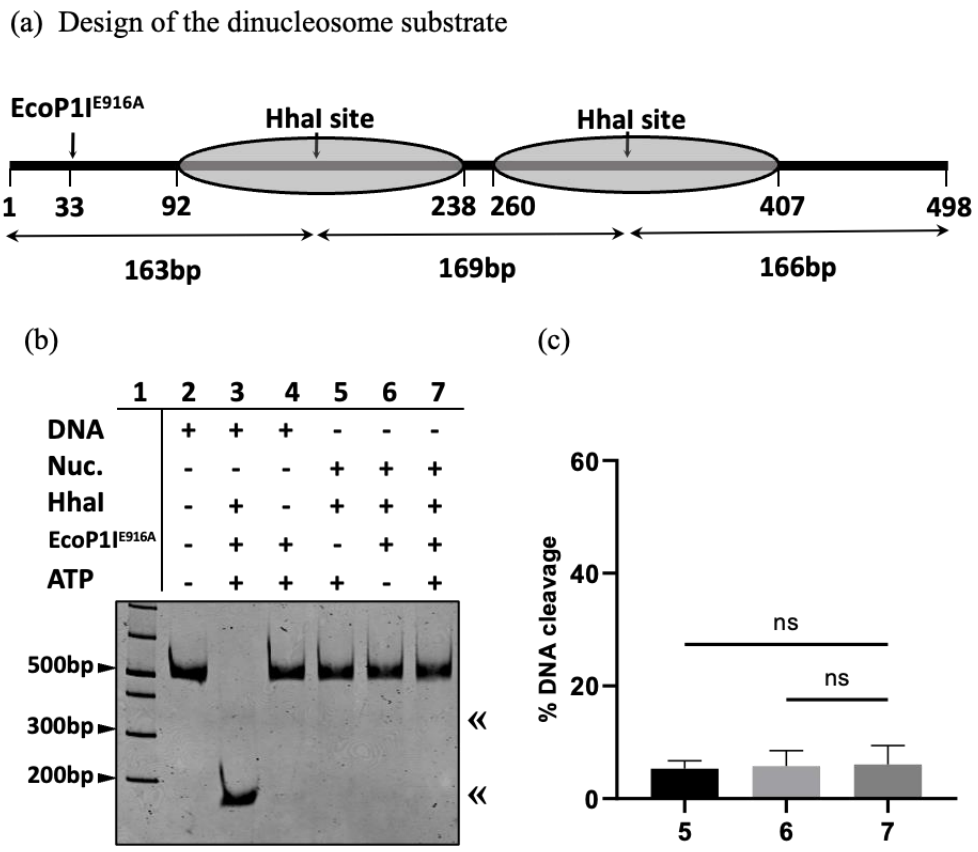

Figure 3.4: REAA with dinucleosome and EcoP1I^{E916A}. (a) Schematic showing the position of EcoP1I and HhaI sites and the DNA fragments that would be produced upon cleavage by HhaI. Grey ovals depict the nucleosome occupancy region. (b) Representative native PAGE image accompanied by (c)-bar plots with percentage of DNA cleavage plotted on the Y-axis with corresponding lane numbers from the gel on X-axis. The arrows («) mark the positions of the expected DNA cleavage products on the polyacrylamide gel. Error bars represent standard deviation for two separate trials. Statistical significance was assessed using the unpaired t-test (ns $P > 0.05$). N=2

3.3.4 REAA with dinucleosome and LlaBIII n-

We also tested if a deletion of the N-terminal nuclease domain of LlaBIII (LlaBIII n-) affected its ability to displace the histone particles. We had earlier shown that a similar nuclease-deleted construct of LlaGI, a close homologue of LlaBIII sharing ~80% sequence identity, is an active ATPase and translocase (Kulkarni et al., 2016). We performed remodeling assays with LlaBIII n-

and found that it was capable of nucleosome remodeling with similar efficiency as the wild-type enzyme (Fig. 3.5b & c, Lane 6 &7).

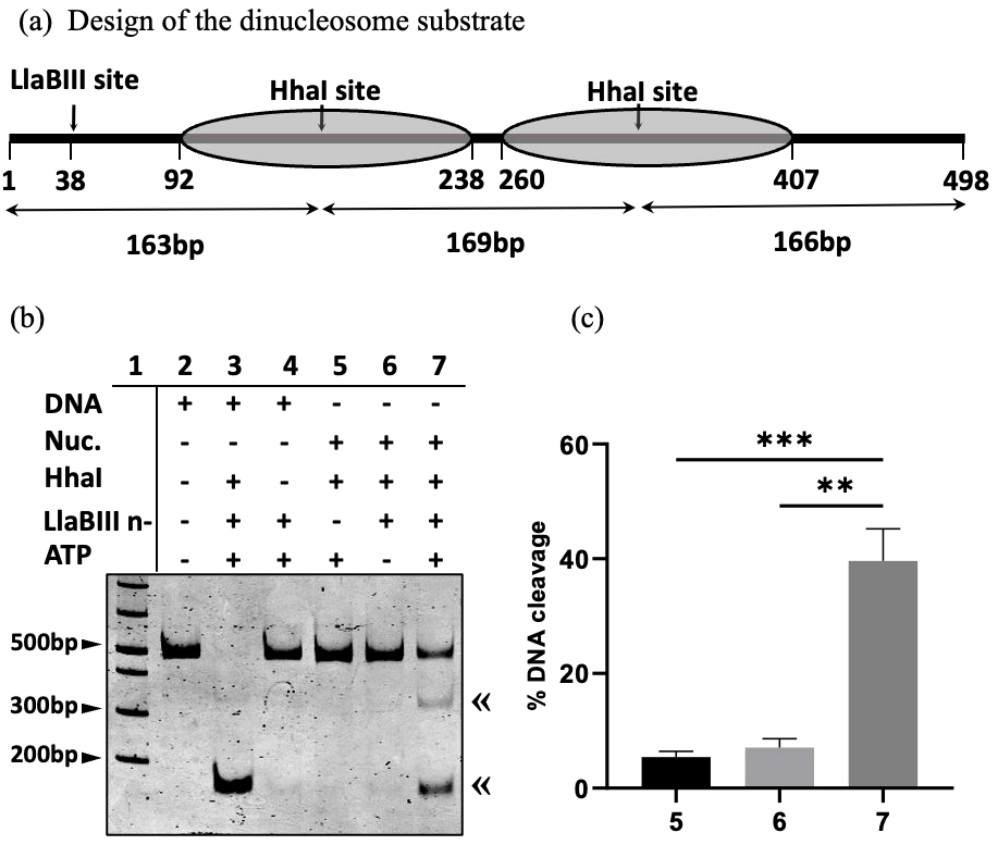

Figure 3.5: REAA with dinucleosome and LlaBIII n-. (a) Schematic showing the positions of the HhaI target sites and the fragments generated upon DNA cleavage by HhaI. Gray ovals represent nucleosome occupancy region. (b) Representative native PAGE image accompanied by (c)-bar plots with percentage of DNA cleavage plotted on the Y-axis with corresponding lane numbers from the gel on X-axis. The arrows («) mark the positions of the expected DNA cleavage products on the polyacrylamide gel. Error bars represent standard error mean for four separate trials. Statistical significance was assessed using the unpaired t-test (*P <0.05, **P <0.01, ***P <0.001). N≥4

3.3.5 REAA with dinucleosome and LlaBIII^{R564A}

Motif V is a functionally important motif of SF2 ATPases, which in ATP-dependent chromatin remodelers has been identified as a hot spot for cancer causing mutations (Medina & Sanchez-Cespedes, 2008). Studies have shown that mutation of motif V of SWI/SNF decouples ATPase from translocase activity, thus affecting chromatin remodeling (Smith & Peterson, 2005). To find if motif V of the ATPase domain of LlaBIII, which is similar but not identical to that in SWI/SNF has a similar mechanistic role, the highly conserved arginine-R564 was mutated to alanine. LlaBIII^{R564A} has been shown to be ATPase active with catalytic efficiency comparable to wild type enzyme but was shown to be deficient in cleavage activity (Chand et al., 2020). The translocation activity was also examined by triplex displacement assay. A time dependent triplex displacement assay revealed that the mutant was defective in its ability to displace the triplex oligomer as compared to wild type enzyme (Chand et al., 2020). As the mutant was found to be defective in triplex displacement, we wanted to examine if it is defective in nucleosome remodeling activity as well. We performed the nucleosome remodeling assay with LlaBIII^{R564A} under the same conditions as the wild type. Surprisingly LlaBIII^{R564A} could remodel the nucleosomes similar to the wild-type enzyme upon 2 hours incubation.

The reduced efficiency of triplex displacement by LlaBIII^{R564A} reflected a reduction in the translocation activity, which could have been due to a slower rate of translocation or a lower processivity. If the mutation had affected the processivity, we would have expected to see at least a feeble nucleolytic activity and a reduction in the remodeling activity. On the contrary, the mutation abolished the nuclease activity without affecting the enzyme's ability to remodel dinucleosome. This suggested that the mutant was a slower translocase, which could generate enough force to displace the nucleosome but not enough to activate the nuclease domains of the converging LlaBIII^{R564A}.

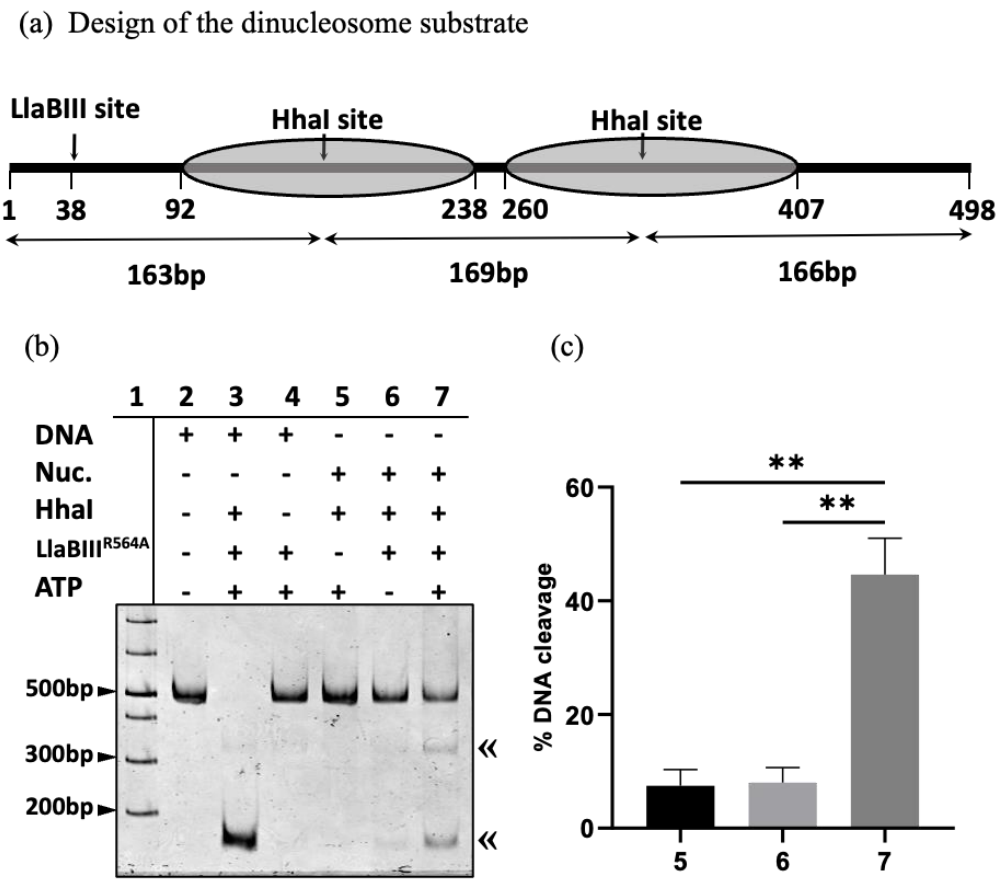

Figure 3.6: REAA with dinucleosome and LlaBIII^{R564A}. (a) Schematic showing the positions of the HhaI target sites and the fragments generated upon DNA cleavage by HhaI. The gray ovals represent nucleosome occupancy. (b) Representative native PAGE image accompanied by (c)-bar plots with percentage of DNA cleavage plotted on the Y-axis with corresponding lane numbers from the gel on X-axis. The arrows («) mark the positions of the expected DNA cleavage products on the polyacrylamide gel. Error bars represent standard error mean for four separate trials. N≥4. Statistical significance was assessed using the unpaired t-test (*P <0.05, **P <0.01, ***P <0.001).

3.3.6 REAA with methylated dinucleosome

Inside a cell, the DNA is almost always methylated, and the nucleosomes are always in association with the DNA containing methylated cytosine. In literature, there are contradictory reports about how the presence of methylated cytosines in the DNA affects the nucleosome structure in terms of the compaction, stability, and occupancy of nucleosome. There are several contrasting studies

where the effect of cytosine methylation on nucleosome occupancy has been considered. CpG methylation in human genome has been extensively linked to heterochromatin formation and gene silencing. The structural changes induced by DNA methylation could be the underlying cause of increased nucleosome stability and occupancy. Towards this, *in vitro* studies using human genome fragments have presented supporting data where in the presence of CpG dinucleotides were shown to directly correlate with the nucleosome enrichment upon methylation. CpG methylation was shown to directly lead to an increase in nucleosome occupancy in these regions (Collings et al., 2013). A single molecule and ensemble fluorescence study observed that the methylation of DNA with CpG resulted in tighter wrapping of DNA around the nucleosome core and hence increased the nucleosome stability. Another study shows that CpG methylation increases DNA rigidity and decreases DNA twisting leading the overwrapping of DNA in the nucleosome, therefore leading to an increase in the nucleosome occupancy (Lee & Lee, 2012). Several studies fortify the idea that DNA methylation in the CpGs increases the octamer-DNA contacts which in turn results in nucleosome compaction and rigidity (Choy et al., 2010; Li et al., 2022a). These studies indicate that cytosine methylation promotes nucleosome occupancy and stability. On the other hand, there are plenty of studies which propose that cytosine methylation affects DNA flexibility and architecture such that the octamer-DNA contacts are reduced, and the nucleosomes thus formed are lower in stability compared to those assembled on unmethylated DNA. 5-metylcytosine has been shown to enhance the unwrapping of DNA ends from the nucleosome core (Jimenez-Useche et al., 2013; Ngo et al., 2016). The effect of DNA methylation on DNA flexibility and how that affects the nucleosome stability is still unclear as there are numerous conflicting studies (Li et al., 2022b). Nevertheless, we decided to check whether remodeling of nucleosomes prepared from methylated DNA display any differences in the nucleosome remodeling. For this we prepared dinucleosomes with cytosine methylated DNA as described in the methods.

Nucleosome remodeling activity of LlaBIII was tested on methylated nucleosome. The REAA with methylated nucleosome utilized the two MseI restriction sites situated approximately in the center of the nucleosome occupying region (601) (Fig. 3.6a). Cleavage by MseI is unaffected by cytosine DNA methylation. LlaBIII was able to displace nucleosomes from the methylated substrate in presence of ATP. The extent of nucleosome displacement at the end of two hours was similar to that seen for unmethylated nucleosome (Fig. 3.6b & c). This suggests that the

interactions between the DNA and octamer might remain unaltered or increase upon cytosine methylation. We also tested if EcoP1I^{E916A} could remodel the methylated dinucleosomes. We observed that there was no indication of nucleosome displacement from the methylated DNA by EcoP1I^{E916A} (Fig. 3.6d & e). This indicated that the interaction between a methylated DNA and histone octamer was not significantly weakened to allow a DNA diffusing enzyme like EcoP1I^{E916A} to displace the octamer from its position on the DNA.

Next, we tested mutants of LlaBIII, LlaBIII^{R564A} and LlaBIII$^{\Delta N}$ for their remodeling activity with methylated dinucleosome. We found that both the translocase deficient mutant (LlaBIII^{R564A}) and the enzyme with nuclease domain deletion (LlaBIII$^{\Delta N}$), could displace nucleosomes at par with the wild-type enzyme. LlaBIII^{R564A} is a slower translocase compared to the wild-type enzyme, but its remodeling activity remained unchanged under the conditions tested (Fig. 3.6f & g). This suggests that either the methylation of DNA does not affect the nucleosome rigidity, or the mutant enzyme translocate at a rate that allows for the remodeling of nucleosomes. As the nuclease domain of LlaBIII is functionally not essential for DNA translocation, deletion of this domain does not hamper its remodeling activity even with methylated nucleosome (Fig. 3.6h & i).

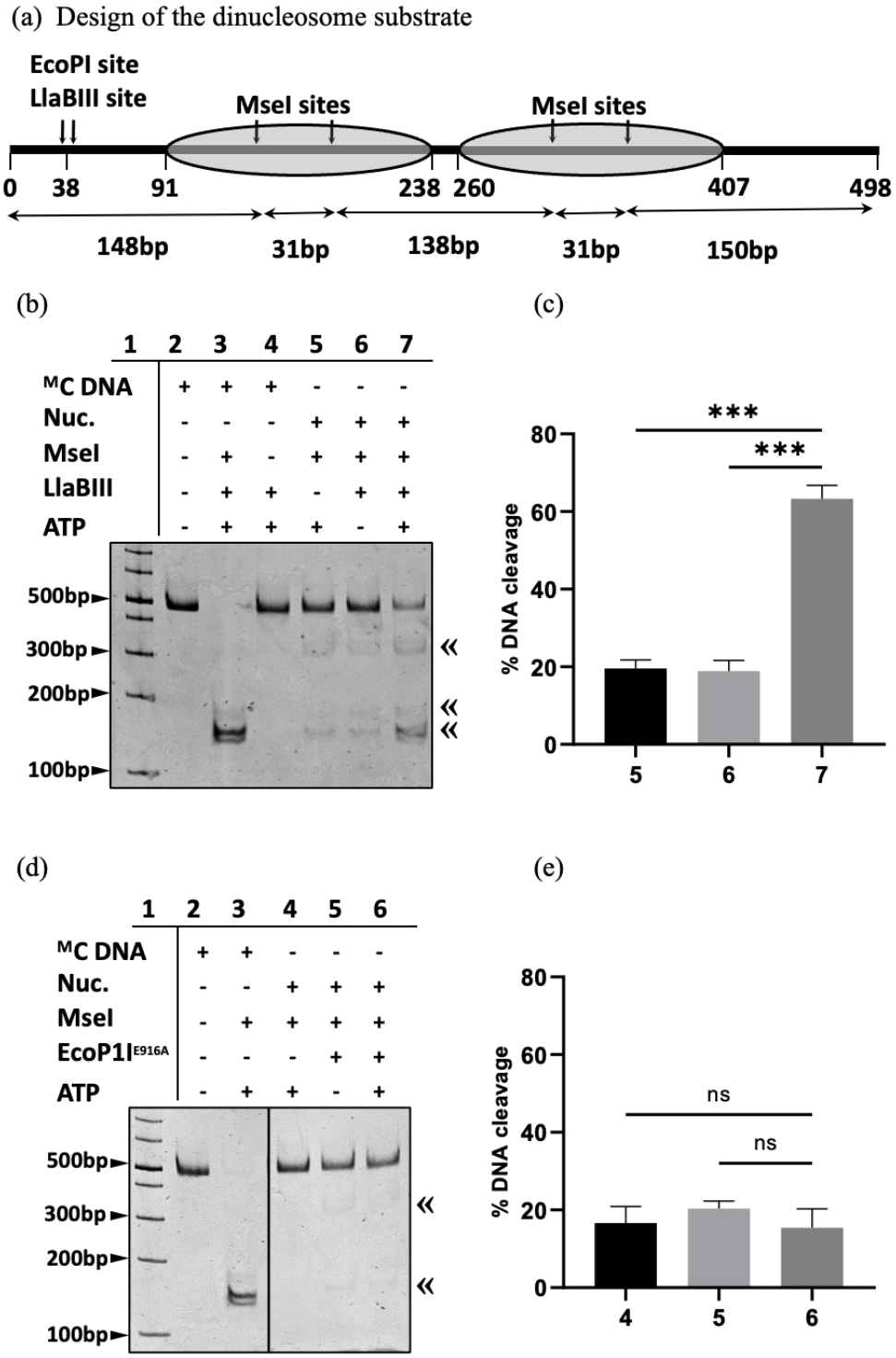
(a) Design of the dinucleosome substrate
EcoPI site
LlaBIII site
MseI sites
MseI sites
0
38
91
238
260
407
498
148bp
31bp
138bp
31bp
150bp
(b)
1 2 3 4 5 6 7
MC DNA + + + - - -
Nuc. - - - + + +
MseI - + - + + +
LlaBIII - + + - + +
ATP - + + + - +
500bp
300bp
200bp
100bp
(c)
% DNA cleavage
***
***
80
60
40
20
0
5
6
7
(d)
1 2 3 4 5 6
MC DNA + + - - -
Nuc. - - + + +
MseI - + + + +
EcoP1I E916A - - - + +
ATP - + + - +
500bp
300bp
200bp
100bp
(e)
% DNA cleavage
ns
ns
80
60
40
20
0
4
5
6

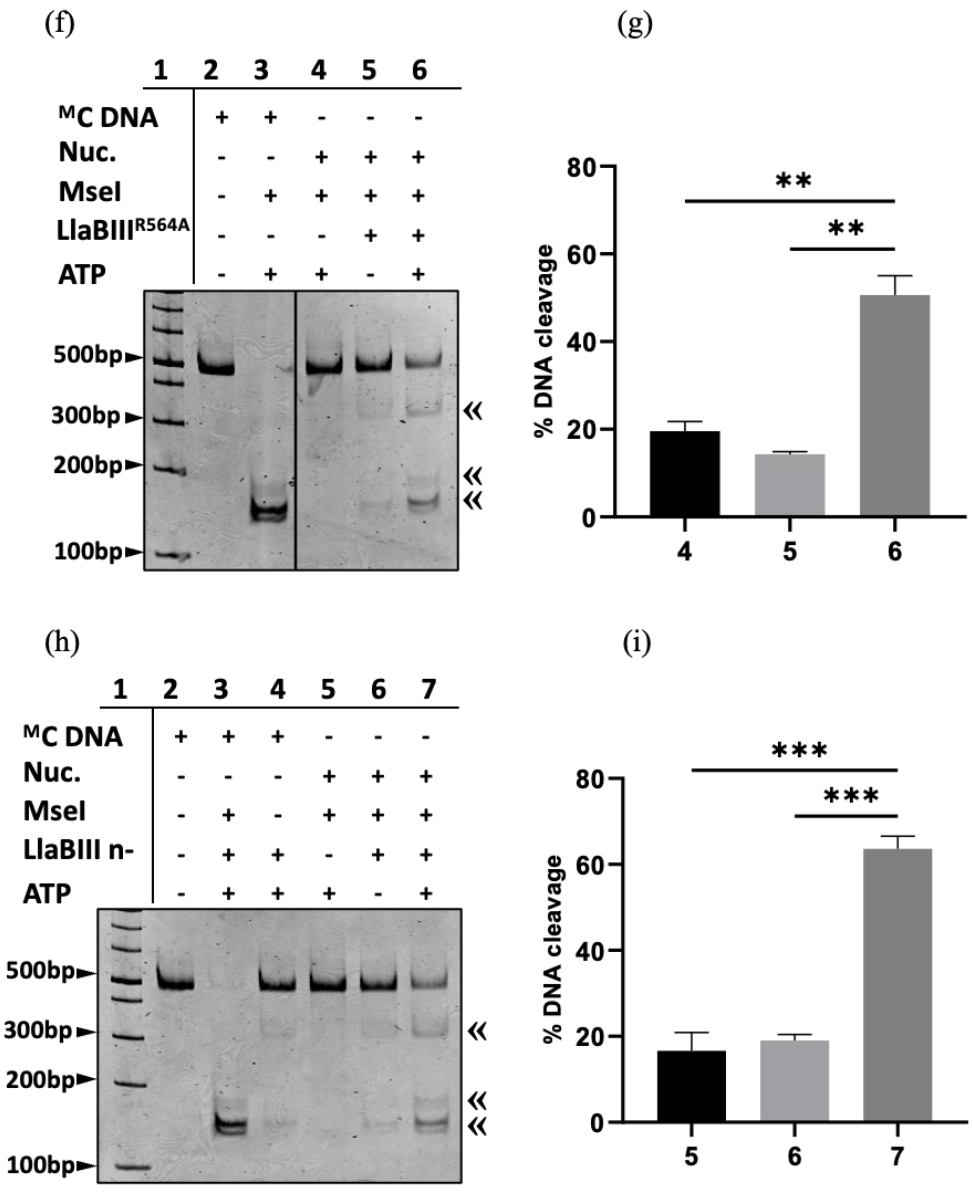

Figure 3.7: REAA with methylated dinucleosome. (a) Schematic showing the design of the dinucleosome assembled on methylated DNA. Gray ovals represent the nucleosome occupying region (601). Two MseI sites in each 601 region are marked and arrows depict the DNA fragments generated upon cleavage by MseI. Representative native PAGE images showing REAA with (b) LlaBIII (d) EcoP1I^{E916A} (f) LlaBIII^{R564A} (h) LlaBIII n-. The arrows («) mark the positions of the expected DNA cleavage products on the polyacrylamide gel. The images are accompanied by bar plots with percentage of DNA cleavage plotted on the Y-axis with corresponding lane numbers

from the gel image on X-axis. Statistical significance was assessed using the unpaired t-test (*P <0.05, **P <0.01, ***P <0.001). N≥3

3.4 Discussion

In the earlier chapter we showed that LlaBIII, by virtue of its conserved ATPase motor belonging to the superfamily 2 (SF2) of helicases, can displace a nucleosome from its position on the DNA, both from terminal and central positions. In this chapter we demonstrated the remodeling capacity of LlaBIII with a more complex nucleosome substrate. We increased the complexity of the nucleosome substrate by duplicating the nucleosome occupancy regions, hence the DNA now accommodated two nucleosomes in tandem separated by a short 22 bp linker DNA. We positioned the LlaBIII target sequence on one end of the DNA and performed the REAA as described before. Here we found that LlaBIII was able displace both the nucleosomes as observed from the DNA fragments generated upon cleavage at both HhaI sites which were otherwise occluded by the two nucleosomes. Cleavage at both HhaI sites will produce three smaller DNA fragments of approximately the same size that will co-migrate on native PAGE. Also, cleavage at either of the two HhaI sites will produce two larger DNA fragments of approximately the same size that will co-migrate on native PAGE. In REA assay with LlaBIII, a prominent band of the smaller fragments and a less prominent band of the larger fragment was observed. This suggested that LlaBIII displaced both the nucleosomes more often than just one. The larger fragment could be generated because of cleavage at either of the two HhaI sites, although cleavage at first site will separate the DNA containing LlaBIII target site from the second nucleosome and hence make it inaccessible to displacement by LlaBIII. In such a case we would see accumulation of larger DNA fragment. We saw a less prominent larger fragment band which indicates that the high processivity and translocation rate of LlaBIII allowed efficient displacement of nucleosomes from the DNA thereby freeing up both the HhaI sites for cleavage. Additionally, we found that the nuclease domain is completely dispensable for the nucleosome remodeling activity of LlaBIII. The nuclease truncated enzyme, LlaBIII n- was also able to displace nucleosomes as efficiently as LlaBIII wild-type. Thus, LlaBIII n- is the minimal construct of the nuclease-deleted LlaBIII that had the SF2 ATPase and the modules required for sequence recognition, i.e. the methyltransferase and target recognition domain(Chand et al., 2015; Kulkarni et al., 2016), and was also proficient in remodeling. In contrast, EcoP1I, a Type III RM enzyme which also belongs to the superfamily 2 of helicases and

possesses the RecA like motor domain, failed to remodel the dinucleosome. Although EcoP1I and LlaBIII are both powered by the same conserved ATPase, the SF2 ATPase in Type III enzymes is primarily a switch that activates 1D diffusion along the DNA, rather than a lomg-range translocase. Though a diffusing Type III RM enzyme may diffuse along the DNA in a directed manner and collide with the nucleosome, the force exerted does not appear to be sufficient for remodeling. These assays together demonstrated that the remodeling of the nucleosome required an SF2 ATPase, which was an active DNA translocase.

An important motif in the SF2 ATPase motor is the motif V. This motif has been shown to couple the ATPase activity to the DNA translocase in the Swi2/Snf2 chromatin remodeler (Smith & Peterson, 2005). Motif V in chromatin remodelers is known to be a hotspot for cancer causing mutations (Medina & Sanchez-Cespedes, 2008). In LlaBIII, mutation of the highly conserved motif V arginine, LlaBIII-R564, to alanine did not affect the ATPase activity but decreased the translocation efficiency, indicative of partial decoupling of the ATPase and translocase activities. Although this mutant was defective in DNA translocation, it could surprisingly remodel nucleosome at par with the wild-type enzyme. This implied that the force generated by the slower colliding mutant enzyme is sufficient for remodeling the dinucleosome. In this LlaBIII may differ from the chromatin remodelers. While in the former mutation in the motif V does not affect the nucleosome remodeling activity, in the latter mutation affects remodeling (Dürr et al., 2005b; C. L. Smith & Peterson, 2005b; Xia et al., 2016). This might be due to the difference in the rate of DNA translocation of LlaBIII and chromatin remodelers. LlaBIII is more than 10-fold faster (Šišáková et al., 2013) than SWI/SNF or RSC (Sirinakis et al., 2011). Also, the reduction in the efficiency of translocation of the remodeler RSC has been shown to result in sliding instead of ejection of the histone octamers (Clapier et al., 2016). Therefore, it is possible that the sliding or ejection of the histone octamer from the nucleosome can be affected by altering the translocation efficiency of LlaBIII by suitable mutations that modulate the coupling of the ATPase to the translocase activity. Hence, reduction in translocation rate does not have a significant effect on the nucleosome remodeling.

We also tested the remodeling potential of LlaBIII, its mutants and EcoP1I^{E916A} with methylated dinucleosome. Cytosine methylation has been implicated in contradicting effects on DNA flexibility and nucleosome stability. In the cell, DNA methylation has been related to high

nucleosome occupancy leading to formation of transcriptionally inactive regions of DNA. Several *in vitro* studies support this notion (Choy et al., 2010; Collings et al., 2013; Lee & Lee, 2012; Li et al., 2022a) whereas several others suggest DNA methylation weakens the octamer DNA interactions hence destabilize the nucleosome structure (Davey et al., 1997; Ngo et al., 2016). Nonetheless, it is clear that DNA methylation plays an important role in the nucleosome structure and stability. We found that DNA methylation did not affect the remodeling activity of LlaBIII and its mutants in the conditions tested. Furthermore, DNA methylation did not aid remodeling by EcoP1I which was ineffective in displacement of methylated nucleosomes as well. Thus, DNA methylation might affect the nucleosome structure and stability, but it may neither hinder the remodeling activity of an active translocase nor it can allow unrestricted displacement of nucleosomes by any protein that moves along the DNA. In summary, in this chapter I demonstrate that LlaBIII can function as a sequence-specific nucleosome remodeler and can remodel an array of dinucleosome.

3.5 References

Adhireksan, Z., Sharma, D., Lee, P. L., & Davey, C. A. (2020). Near-atomic resolution structures of interdigitated nucleosome fibres. *Nature Communications*, *11*(1), 4747. https://doi.org/10.1038/s41467-020-18533-2

Ahmad, I., Kulkarni, M., Gopinath, A., & Saikrishnan, K. (2018). Single-site DNA cleavage by Type III restriction endonuclease requires a site-bound enzyme and a trans-acting enzyme that are ATPase-activated. *Nucleic Acids Research*, *46*(12), 6229–6237. https://doi.org/10.1093/nar/gky344

Byrd, A. K., & Raney, K. D. (2012). Superfamily 2 helicases. *FBL*, *17*(6), 2070–2088.

Chand, M. K., Carle, V., Anuvind, K. G., & Saikrishnan, K. (2020). DNA-mediated coupling of ATPase, translocase and nuclease activities of a Type ISP restriction-modification enzyme. *Nucleic Acids Research*, *48*(5), 2594–2603. https://doi.org/10.1093/nar/gkaa023

Chand, M. K., Nirwan, N., Diffin, F. M., Van Aelst, K., Kulkarni, M., Pernstich, C., Szczelkun, M. D., & Saikrishnan, K. (2015). Translocation-coupled DNA cleavage by the Type ISP restriction-modification enzymes. *Nature Chemical Biology*, *11*(11), 870–877. https://doi.org/10.1038/nchembio.1926

Choy, J. S., Wei, S., Lee, J. Y., Tan, S., Chu, S., & Lee, T.-H. (2010). DNA Methylation Increases Nucleosome Compaction and Rigidity. *Journal of the American Chemical Society*, *132*(6), 1782–1783. https://doi.org/10.1021/ja910264z

Chua, E. Y. D., Vasudevan, D., Davey, G. E., Wu, B., & Davey, C. A. (2012). The mechanics behind DNA sequence-dependent properties of the nucleosome. *Nucleic Acids Research*, *40*(13), 6338–6352. https://doi.org/10.1093/nar/gks261

Clapier, C. R., Kasten, M. M., Parnell, T. J., Viswanathan, R., Szerlong, H., Sirinakis, G., Zhang, Y., & Cairns, B. R. (2016). Regulation of DNA Translocation Efficiency within the Chromatin Remodeler RSC/Sth1 Potentiates Nucleosome Sliding and Ejection. *Molecular Cell*, *62*(3), 453–461. https://doi.org/10.1016/j.molcel.2016.03.032

Collings, C. K., Waddell, P. J., & Anderson, J. N. (2013). Effects of DNA methylation on nucleosome stability. *Nucleic Acids Research*, *41*(5), 2918–2931. https://doi.org/10.1093/nar/gks893

Davey, C. A., Sargent, D. F., Luger, K., Maeder, A. W., & Richmond, T. J. (2002). Solvent Mediated Interactions in the Structure of the Nucleosome Core Particle at 1.9Å Resolution††We dedicate this paper to the memory of Max Perutz who was particularly inspirational and supportive to T.J.R. in the early stages of this study. *Journal of Molecular Biology*, *319*(5), 1097–1113. https://doi.org/https://doi.org/10.1016/S0022-2836(02)00386-8

Davey, C., Pennings, S., & Allan, J. (1997). CpG methylation remodels chromatin structure in vitro11Edited by T. Richmond. *Journal of Molecular Biology*, *267*(2), 276–288. https://doi.org/https://doi.org/10.1006/jmbi.1997.0899

Dürr, H., Körner, C., Müller, M., Hickmann, V., & Hopfner, K.-P. (2005). X-Ray Structures of the Sulfolobus solfataricus SWI2/SNF2 ATPase Core and Its Complex with DNA. *Cell*, *121*(3), 363–373. https://doi.org/10.1016/j.cell.2005.03.026

Dyer, P. N., Edayathumangalam, R. S., White, C. L., Bao, Y., Chakravarthy, S., Muthurajan, U. M., & Luger, K. (2003). Reconstitution of Nucleosome Core Particles from Recombinant Histones and DNA. In *Methods in Enzymology* (Vol. 375, pp. 23–44). Academic Press. https://doi.org/https://doi.org/10.1016/S0076-6879(03)75002-2

Fairman-Williams, M. E., Guenther, U.-P., & Jankowsky, E. (2010). SF1 and SF2 helicases: family matters. *Current Opinion in Structural Biology*, *20*(3), 313–324. https://doi.org/https://doi.org/10.1016/j.sbi.2010.03.011

Gorbalenya, A. E., & Koonin, E. V. (1993). Helicases: amino acid sequence comparisons and structure-function relationships. *Current Opinion in Structural Biology*, *3*(3), 419–429. https://doi.org/https://doi.org/10.1016/S0959-440X(05)80116-2

Harp, J. M., Hanson, B. L., Timm, D. E., & Bunick, G. J. (2000). Asymmetries in the nucleosome core particle at 2.5Å resolution. *Acta Crystallographica Section D*, *56*(12), 1513–1534. https://doi.org/10.1107/S0907444900011847

Jimenez-Useche, I., Ke, J., Tian, Y., Shim, D., Howell, S. C., Qiu, X., & Yuan, C. (2013). DNA Methylation Regulated Nucleosome Dynamics. *Scientific Reports*, *3*(1), 2121. https://doi.org/10.1038/srep02121

Kulkarni, M., Nirwan, N., van Aelst, K., Szczelkun, M. D., & Saikrishnan, K. (2016). Structural insights into DNA sequence recognition by Type ISP restriction-modification enzymes. *Nucleic Acids Research*, *44*(9), 4396–4408. https://doi.org/10.1093/nar/gkw154

Lee, J. Y., & Lee, T.-H. (2012). Effects of DNA Methylation on the Structure of Nucleosomes. *Journal of the American Chemical Society*, *134*(1), 173–175. https://doi.org/10.1021/ja210273w

Li, S., Peng, Y., Landsman, D., & Panchenko, A. R. (2022). DNA methylation cues in nucleosome geometry, stability and unwrapping. *Nucleic Acids Research*, *50*(4), 1864–1874. https://doi.org/10.1093/nar/gkac097

Li, S., Peng, Y., & Panchenko, A. R. (2022). DNA methylation: Precise modulation of chromatin structure and dynamics. *Current Opinion in Structural Biology*, *75*, 102430. https://doi.org/https://doi.org/10.1016/j.sbi.2022.102430

Lowary, P. T., & Widom, J. (1998). *New DNA Sequence Rules for High Affinity Binding to Histone Octamer and Sequence-directed Nucleosome Positioning*.

Luger, K., Mäder, A. W., Richmond, R. K., Sargent, D. F., & Richmond, T. J. (1997). Crystal structure of the nucleosome core particle at 2.8 Å resolution. *Nature*, *389*(6648), 251–260. https://doi.org/10.1038/38444

Medina, P. P., & Sanchez-Cespedes, M. (2008). Involvement of the chromatin-remodeling factor BRG1/SMARCA4 in human cancer. *Epigenetics*, *3*(2), 64–68. https://doi.org/10.4161/epi.3.2.6153

Ngo, T. T. M., Yoo, J., Dai, Q., Zhang, Q., He, C., Aksimentiev, A., & Ha, T. (2016). Effects of cytosine modifications on DNA flexibility and nucleosome mechanical stability. *Nature Communications*, *7*(1), 10813. https://doi.org/10.1038/ncomms10813

Schwarz, F. W., Tóth, J., van Aelst, K., Cui, G., Clausing, S., Szczelkun, M. D., & Seidel, R. (2013). The Helicase-Like Domains of Type III Restriction Enzymes Trigger Long-Range Diffusion Along DNA. *Science*, *340*(6130), 353–356. https://doi.org/10.1126/science.1231122

Singleton, M. R., Dillingham, M. S., & Wigley, D. B. (2007). Structure and Mechanism of Helicases and Nucleic Acid Translocases. *Annual Review of Biochemistry*, *76*(1), 23–50. https://doi.org/10.1146/annurev.biochem.76.052305.115300

Singleton, M. R., & Wigley, D. B. (2002). Modularity and Specialization in Superfamily 1 and 2 Helicases. *Journal of Bacteriology*, *184*(7), 1819–1826. https://doi.org/10.1128/jb.184.7.1819-1826.2002

Sirinakis, G., Clapier, C. R., Gao, Y., Viswanathan, R., Cairns, B. R., & Zhang, Y. (2011). The RSC chromatin remodelling ATPase translocates DNA with high force and small step size. *The EMBO Journal*, *30*(12), 2364–2372. https://doi.org/https://doi.org/10.1038/emboj.2011.141

Šišáková, E., Van Aelst, K., Diffin, F. M., & Szczelkun, M. D. (2013). The Type ISP Restriction-Modification enzymes LlaBIII and LlaGI use a translocation-collision mechanism to cleave non-specific DNA distant from their recognition sites. *Nucleic Acids Research*, *41*(2), 1071–1080. https://doi.org/10.1093/nar/gks1209

Smith, C. L., & Peterson, C. L. (2005a). A Conserved Swi2/Snf2 ATPase Motif Couples ATP Hydrolysis to Chromatin Remodeling. *Molecular and Cellular Biology*, *25*(14), 5880–5892. https://doi.org/10.1128/MCB.25.14.5880-5892.2005

Smith, C. L., & Peterson, C. L. (2005b). A Conserved Swi2/Snf2 ATPase Motif Couples ATP Hydrolysis to Chromatin Remodeling. *Molecular and Cellular Biology*, *25*(14), 5880–5892. https://doi.org/10.1128/MCB.25.14.5880-5892.2005

Vasudevan, D., Chua, E. Y. D., & Davey, C. A. (2010). Crystal Structures of Nucleosome Core Particles Containing the '601' Strong Positioning Sequence. *Journal of Molecular Biology*, *403*(1), 1–10. https://doi.org/https://doi.org/10.1016/j.jmb.2010.08.039

Xia, X., Liu, X., Li, T., Fang, X., & Chen, Z. (2016). Structure of chromatin remodeler Swi2/Snf2 in the resting state. *Nature Structural & Molecular Biology*, *23*(8), 722–729. https://doi.org/10.1038/nsmb.3259

Chapter 4 – Mechanism of nucleosome remodeling by LlaBIII

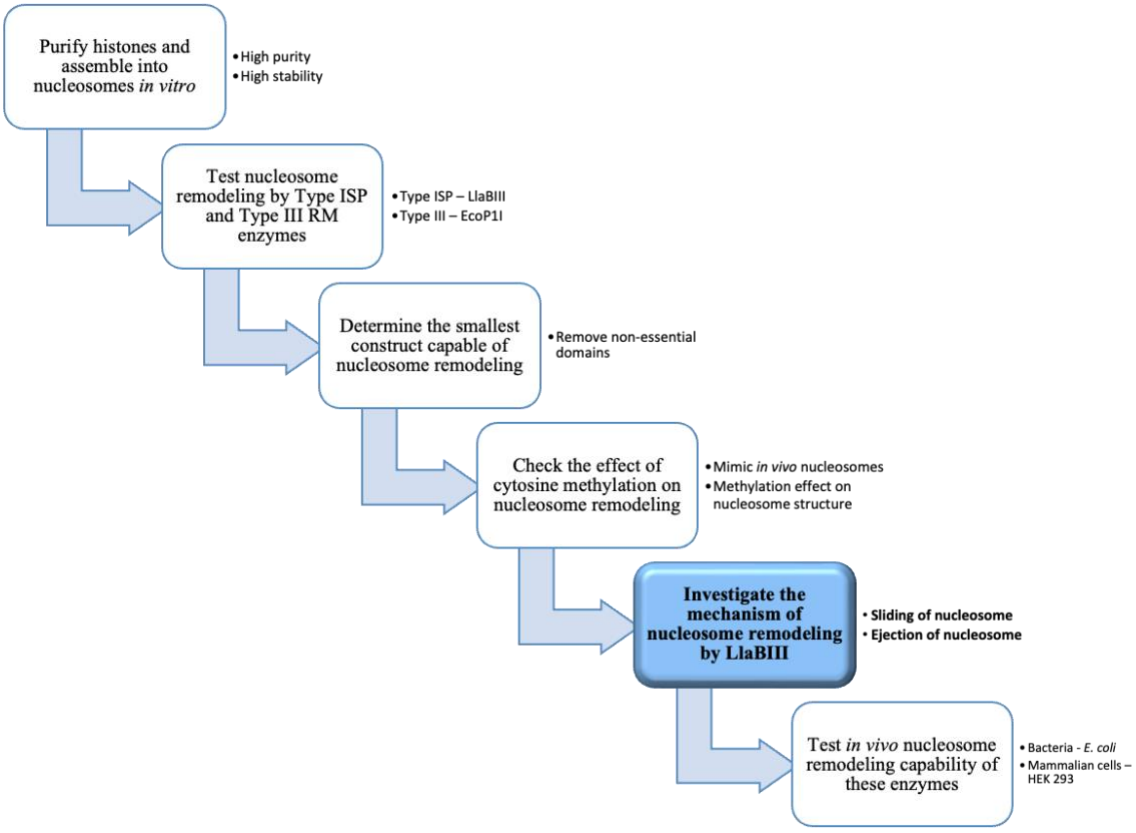

4.1 Introduction

In the previous chapter we discussed how a nucleosome is stabilized by the extensive protein-DNA interactions between the histone octamer and the DNA wrapped around it. Majority of these interactions are sequence independent and are formed between the sugar- phosphate backbone of the DNA and amino acid side chains as well as the histone main chain atoms. The nucleosomes are highly stable structures but they are far from static. They are highly dynamic complexes that change in response to the cellular environment. They can change conformations or positions in response to thermal fluctuations or as a result of specific enzymatic activities (N. Liu et al., 2011). Spontaneous unwrapping and re-wrapping of nucleosome DNA is also a common feature both *in vivo* and *in vitro* (G. Li et al., 2005; Polach & Widom, 1995c). DNA unwrapping begins progressively from one end of the nucleosome and lasts for only 10-50 ms (G. Li et al., 2005). This provides a window of opportunity for DNA binding proteins (DBPs) to gain access to the DNA wrapped at the ends. This access though, is modulated by the concentration of the DNA binding proteins, the number and position of binding sites on the DNA. The closer the site is to nucleosome ends, higher the access provided by nucleosome unwrapping. Although, the presence of the nucleosome structure on DNA imparts substantial changes in the DNA geometry which inherently inhibits binding of DBPs. Also, the spontaneous DNA unwrapping is fairly partial and the core of the nucleosome remains intact during these conformational changes thereby blocking the access to core nucleosome DNA (Poirier et al., 2008). The accessibility to core DNA is decreased so significantly that the required protein concentration for binding of the DBP, far exceeds the physiological protein concentration (Poirier et al., 2008). Hence, there exist the specialized class of ATP driven-molecular motors called chromatin remodelers, that are intertwined with the cellular signaling to assist nucleosome rearrangements which in turn may either facilitate or further restrict access of DBPs to the nucleosome occupied DNA.

The chromatin remodelers are a class of ATP powered complexes that in response to a cellular signal, rearrange, eject or modify nucleosomes at a specific region of the chromatin (Clapier & Cairns, 2009). These enzymes and the proposed mechanisms for nucleosome remodeling by these enzymes have been discussed in detail in chapter one. In short, these enzymes either change the DNA conformation by introducing a twist defect to mobilize the nucleosomes or they cause a loop to be formed in the nucleosome DNA wrap through ATP driven translocation, which travels

through the nucleosome to lead to a shift in the nucleosome position (Nodelman & Bowman, 2021). As discussed previously the chromatin remodelers are closely related to the Type I RM enzymes which also utilize ATP hydrolysis to translocate DNA. In the previous chapter, we demonstrated that a Type ISP RM enzyme, LlaBIII remodels nucleosomes *in vitro* similar to the chromatin remodelers. It should be noted that, not all DNA translocases can open the nucleosome core, not even the other DNA translocases of the same family as the chromatin remodelers. In this chapter, I have tried to understand the details of LlaBIII mediated nucleosome remodeling through *in vitro* time-dependent EMSA and REA assays.

4.2 Materials and methods

4.2.1 Preparation of Cy5-labelled DNA substrates for nucleosome assembly

The 5'-Cy5 labeled mononucleosome DNA substrates were prepared as described in chapter 2 section 2.2.1. In brief, the template for mononucleosome substrate DNA with LlaBIII target site at 5' end was generated from a plasmid (pUC18) carrying the 601 sequence. An adaptor sequence was incorporated at the 5' terminal which was used for incorporation of 5'-Cy5 label via PCR amplification. For terminally placed nucleosome DNA, 265 bp DNA was amplified using primers Cy5-F and 601R. For centrally placed nucleosomes, a 356 bp DNA was generated using primers Cy5-F and 329R. The DNA substrates were purified from native gel, concentrated, purified using PCR cleanup column and stored in refolding buffer (2 M NaCl, 10 mM Tris pH 7.5, 1 mM EDTA, 10 mM β-mercaptoethanol) at -30°C until required for nucleosome reconstitution.

To prepare 5'-Cy5 labelled dinucleosome substrate, the unlabeled 498 bp DNA, as described in chapter 3 section 3.2.1, was used as template for incorporation of an adaptor sequence at the 5' end using primers Cy5oligo-498-AdaptorF and 329R. A 489 bp DNA fragment was amplified, purified using PCR cleanup column and used as template for incorporation of 5'-Cy5 label in subsequent PCR amplification. A 5'-Cy5-525 bp fragment was amplified using primers Cy5-F and 329R. The 5'-Cy5-525 bp DNA was purified from native gel as described previously. The native gel extracts were concentrated and purified using PCR cleanup column. The DNA was eluted in refolding buffer (2 M NaCl, 10 mM Tris pH-7.5, 1 mM EDTA, 10 mM β-mercaptoethanol) and stored at -30°C until required for nucleosome reconstitution.

4.2.2 Mono and dinucleosome assembly

The histones and octamer were purified as described in chapter 2 sections 2.2.2 and 2.2.3. Both mono- and dinucleosomes were reconstituted using the salt dilution method as described in chapter 2, section 2.2.5, and chapter 3, section 3.2.5. The quality of nucleosomes was assessed through native gel electrophoresis. The reconstituted nucleosome samples were loaded onto a 6% native polyacrylamide gel that was pre-run at 150 V for 20 minutes at 4°C in 1X TBE. The nucleosome samples were resolved for 90 minutes at 150 V at 4°C in 1X TBE. The gel was imaged on Typhoon Biomolecular Imagers (Amersham) using the Cy5 filter. The reconstituted nucleosomes were stored at 4°C until required.

4.2.3 Electrophoretic mobility shift assay (EMSA)

The EMSA was performed over a maximum time period of 90 minutes. Just 5'-Cy5 DNA of appropriate lengths were used as controls to track mobility of the free DNA. The reactions were prepared without ATP, as indicated in the figures, and incubated on ice. The protein was mixed with the DNA or nucleosome and incubated on ice for 5 minutes before addition of ATP. ATP was added wherever indicated to start the reaction. The reactions for various time points were initiated in a staggered manner. All the reactions were stopped by addition of excess unlabeled competitor DNA (250 ng plasmid fragments with seven LlaBIII target sites and 1 uM 35 bp DNA with one LlaBIII site) and incubation on ice for 10 minutes before addition of 2 ul EDTA (0.5 M). The samples were mixed with 4 ul of 6X ST buffer (100 mM Tris pH-7.5, 40% w/v Sucrose) and loaded onto 6% native PAGE that was pre-run at 150 V for 20 minutes at 4°C in 1X TBE. The samples were resolved for 90 minutes at 150 V at 4°C in 1X TBE. The gel was imaged on Typhoon Biomolecular Imagers (Amersham) using the Cy5 filter.

4.2.4 Time-dependent REAA with HhaI and NdeI

The REAA assay was performed similar to as described before in chapter 2 section 2.2.6 with minor changes. The reaction mixes were prepared as indicated in the figures except addition of ATP. The protein and DNA or nucleosome were incubated on ice for 5 minutes. The reactions were started with addition of ATP and shifted to 25°C. The reactions were started in a staggered manner starting with the longest time point. At the end of incubation time, all the reactions were

stopped together with addition of unlabeled competitor DNA and excess ADP (10mM). After 10 minutes incubation on ice, the reaction mixture was split equally into three separate vials and the respective restriction enzymes (HhaI/ NdeI) were added to each vial as indicated. The reactions were incubated at 37°C for 1 hour. At the end of an hour, 2 ul EDTA (0.5 mM) and 0.8 ul 10% SDS was added followed by 1 ul of 20 mg/mL Proteinase K and the reactions were further incubated at 37°C for 30 minutes. At the end of incubation time the reactions were heated at 65°C for 20 minutes. The samples were mixed with 4 ul of 6X ST buffer (100 mM Tris pH-7.5, 40% w/v Sucrose) and loaded onto 6% native PAGE pre-run at 150 V for 20 minutes at room temperature in 1X TBE. The samples were resolved for 50 minutes at 150 V at room temperature in 1X TBE. The gel was imaged on Typhoon Biomolecular Imagers (Amersham) using the Cy5 filter. Gel images were analyzed using ImageJ software (C. A. Schneider et al., 2012).

4.3 Results

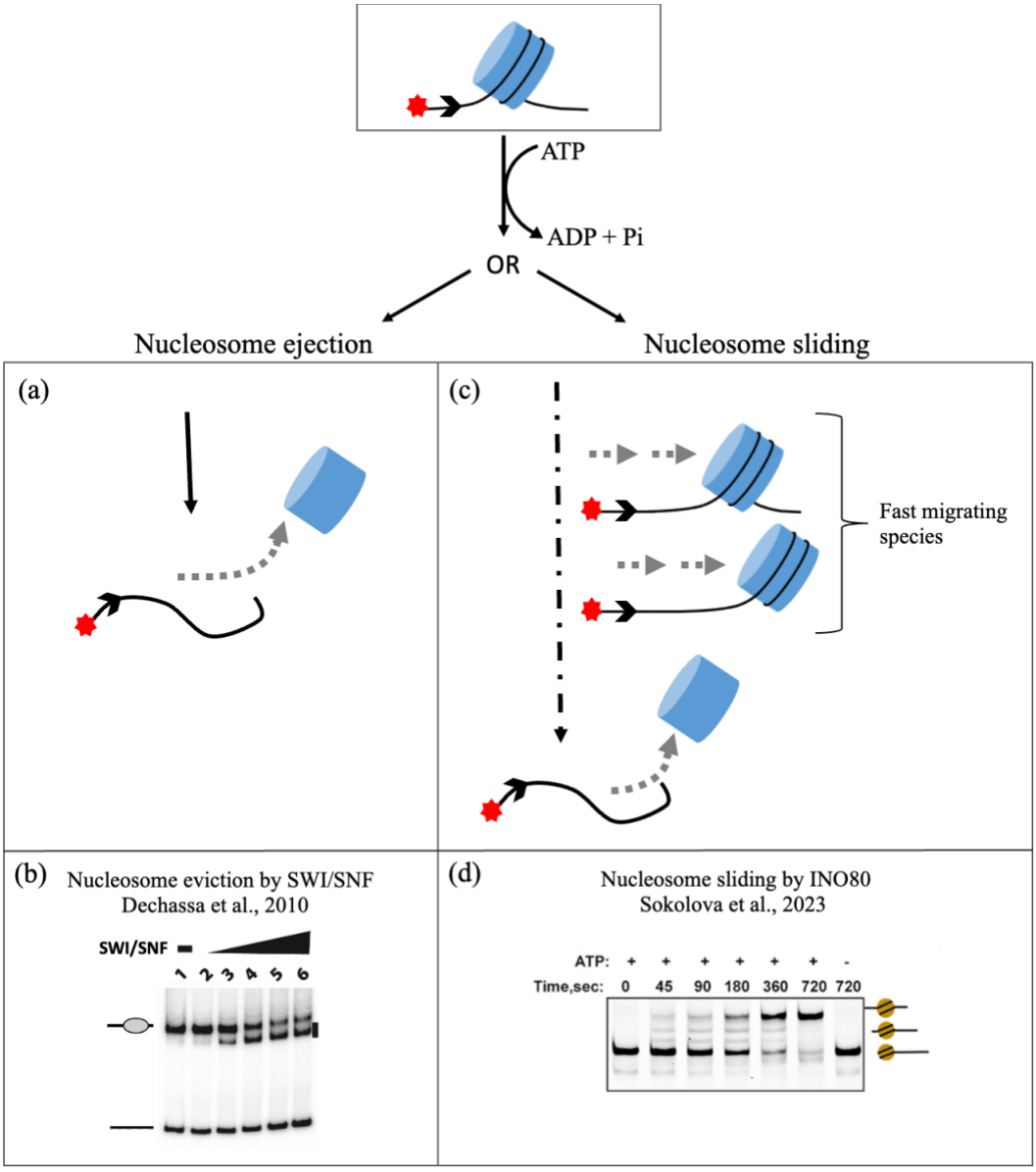

Figure 4.1: Possible mechanisms for nucleosome displacement by LlaBIII. (a) Schematic illustrating nucleosome ejection. (c) Schematic illustrating nucleosome sliding. (b) and (d) Examples mononucleosome displacement by canonical chromatin remodelers that either evict (SWI/SNF) or slide (INO80) the nucleosomes. EMSA gel images from the cited published articles adopted as examples for each mechanism.

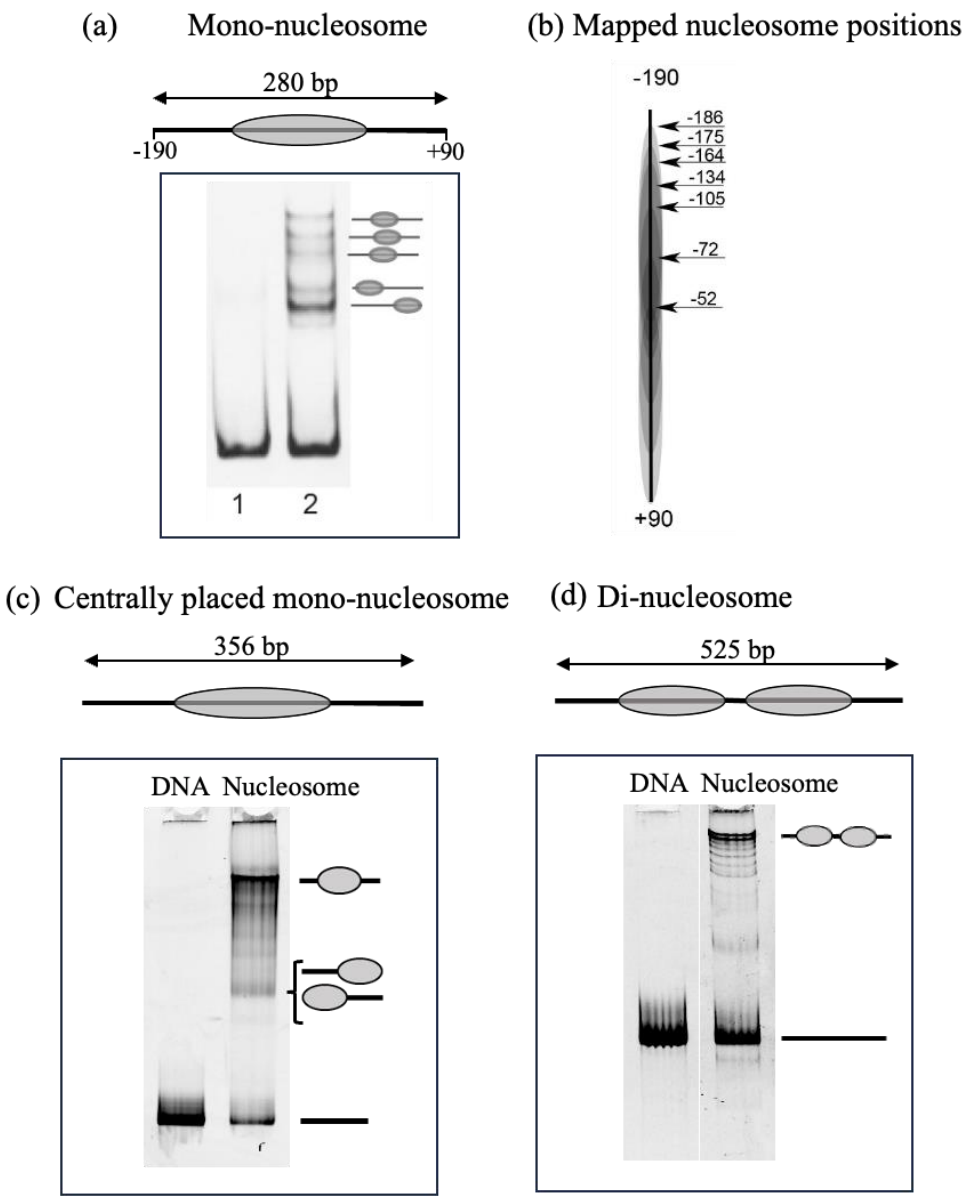

Figure 4.2: Nucleosome positions observed on native polyacrylamide gel. (a) and (b) adapted from (Manelyte et al., 2014). (a) Nucleosome assembled on the Cy5 labelled rDNA promoter (-190 to +90). (b) Schematic showing the identified nucleosome positions on the rDNA promoter fragment determined by Exonuclease III mapping. (c) Mononucleosome assembled on Cy5 labelled 356 bp DNA with 601 sequence positioned centrally. (d) Dinucleosome assembled on Cy5 labelled 525 bp DNA carrying two 601 sequences.

4.3.1 Time-dependent remodeling EMSA with mono and dinucleosomes

The canonical chromatin remodeler families are known to either predominantly slide the nucleosome on the DNA (CHD, ISWI and INO80) or known to predominantly eject the nucleosome from its position on the DNA (SWI/SNF) (Clapier et al., 2017; Clapier & Cairns, 2009; Dechassa et al., 2010; Sokolova et al., 2023). To understand which of these probable mechanism LlaBIII adopts to bring about nucleosome remodeling, we performed time dependent assays with mono- and dinucleosomes. For this the mono- or dinucleosomes were incubated with LlaBIII in presence of ATP and the remodeling products at various time points over a duration of 90 minutes were analyzed through native PAGE. Based on the octamer location on the DNA, the nucleosomes are known to migrate at different rates on native polyacrylamide gel, and separate into distinct bands. A centrally positioned nucleosome migrates slower than a terminally positioned octamer assembled on the same DNA (Fan et al., 2003; Hamiche et al., 1999b; Manelyte et al., 2014). Free DNA migrates faster than the octamer bound DNA. A nucleosome assembled on a DNA with 601 sequence and overhangs contains a mixture of nucleosomes with varied octamer occupancy with majority occupying the 601 sequence. Hence, when resolved through native PAGE, these individual populations of nucleosomes segregate accordingly, the most centrally oriented nucleosomes migrate slowly whereas the more terminally oriented nucleosomes migrate faster. Previously, many studies have systematically mapped these positions of nucleosomes on DNA through Exonuclease III or MNase mapping techniques (Fan et al., 2003; Hamiche et al., 1999b; Manelyte et al., 2014). An example is presented in figure 4.1 (a-b) (Manelyte et al., 2014). Manelyte et al. assembled a nucleosome on a 280bp DNA and mapped the positions of nucleosome positions in the preparation (Fig. 4.1 a-b). Fan et al. assembled and mapped octamer positions on a 202 bp DNA (Fig. 2.4 a). They were able to determine the difference in octamer occupancy in each nucleosome band seen on 5 percent native polyacrylamide gel to be ~10 bp. Thus, change in the banding pattern of a nucleosome preparation over time is indicative of change in octamer position and can be used to gauge the nucleosome remodeling mechanism. The ejection of the octamer from its position would lead to instantaneous freeing up of the DNA and the nucleosome would be rapidly converted to free DNA in a single step as seen with SWI/SNF (Fig. 4.1 a-b) (Dechassa et al., 2010). Whereas, sliding of the octamer would gradually decrease the centrally placed nucleosome (slow migrating) with a simultaneous increase

in more terminally placed nucleosomes (fast migrating) and free DNA as seen for nucleosome sliding by INO80 (Fig. 4.1 c-d) (Sokolova et al., 2023). We studied the change in the octamer occupancy over time through a time dependent electrophoretic mobility shift assay (EMSA). Fig. 4.2c and d show the mononucleosome and dinucleosome preparations used for the our EMSA studies. The DNA substrates used for nucleosome preparation were designed to possess a LlaBIII target site 48bp upstream of the 601 sequence. There is another LlaBIII target site located close to the 5' end of the DNA, although this site is too close to the DNA end (11bp) to allow LlaBIII translocation and can be ignored for the purpose of these assays. Controls were set up with unbound 5'-Cy5 labeled DNA (Fig. 4.3 b, lanes 1-3) to allow comparison between mobility of free DNA and DNA bound to LlaBIII. An unlabeled specific competitor DNA was added at the end of incubation (Fig. 4.3 b, Lane 3-13) to sequester LlaBIII that would otherwise remain bound to the free DNA or the nucleosome and alter its mobility in EMSA (Fig. 4.3 b, lane 2). The competitor DNA was able to sequester most of LlaBIII away from the labelled DNA. Nevertheless, a negligible amount remains bound (Fig. 4.3 b, lane 3). The mononucleosome preparation shows ~8 bands corresponding to 8 distinct octamer positions at the beginning (Fig. 4.3 b, bands 1-8). The mononucleosome was incubated with LlaBIII in absence of ATP to monitor any changes in the nucleosome stability during the reaction due to LlaBIII binding. We observed that addition of LlaBIII in the absence of ATP did not change the original banding pattern (Fig. 4.3 b-c, lane 5) but added extra bands that most likely correspond to the LlaBIII bound mononucleosome and LlaBIII bound free DNA as compared to the control lanes (Fig. 4.3 b, lane 2-3, bands 0). The reactions were started with addition of ATP and stopped with addition of excess unlabeled competitor DNA and EDTA at time points – 1, 2.5, 5, 10, 20, 30, 60, 90-minute time points. The EMSA reveals the shift from slow migrating centrally placed nucleosomes to fast migrating terminally placed nucleosomes as soon as ATP is added (Fig. 4.3 b-c, lane 6). There is also a simultaneous increase in the free DNA (Fig. 4.3 b-c, lane 6-13, band 9) as the slow migrating band intensities decrease over time (Fig. 4.3 b-c, lanes 6-13 bands 1-8). The unbound DNA increases drastically upon ATP addition (Fig. 4.3 d), indicating rapid displacement of octamer mediated by active DNA translocation by LlaBIII. LlaBIII DNA translocation on centrally placed nucleosome leads to octamer displacement such that it assumes terminal positions as seen by the increase in the number and intensity of fast migrating bands that appear over the course of 90 minutes. This suggests that the octamer is pushed from the center towards the terminal of the DNA from where

it can be completely removed from the DNA resulting in an increase in the free DNA. We also performed an EMSA with the dinucleosome substrate (Fig. 4.4 b and c). Upon ATP addition, a rapid increase in free DNA was observed (Fig. 4.4 b-c, lanes 5-6, 4.4 d). Emergence of intermediate dinucleosome bands corresponding to octamers moved towards the terminal end is more evident at later time points (Fig. 4.4 b-c, lanes 8-13). The slow migrating species do not resolve very well at the later time points. Nevertheless, the appearance of distinct bands corresponding to terminally positioned nucleosome reiterates the sliding of octamer by LlaBIII powered by ATP hydrolysis.

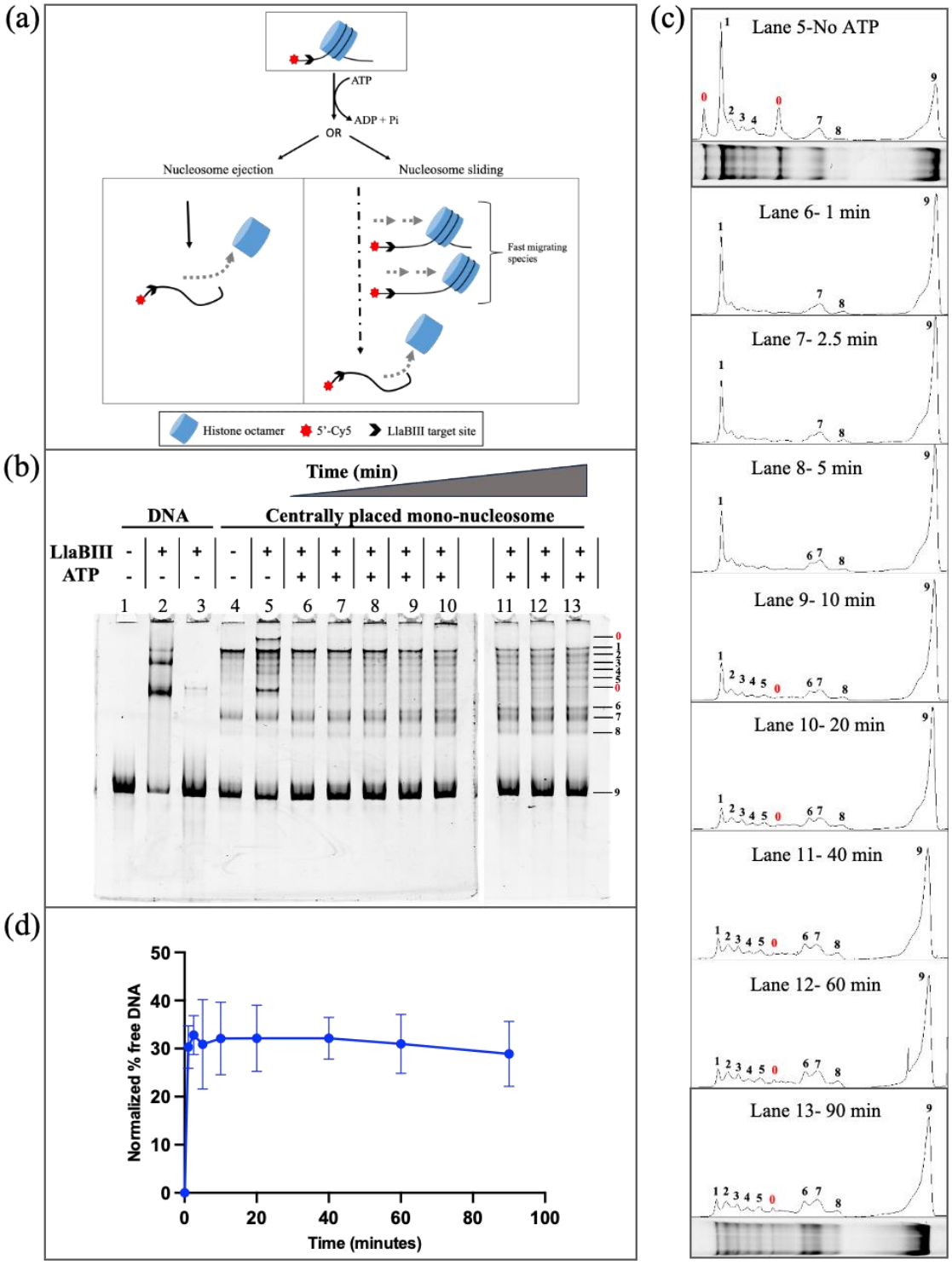
(a)
ATP
ADP + Pi
OR
Nucleosome ejection
Nucleosome sliding
Fast migrating species
Histone octamer
5'-Cy5
LlaBIII target site
(b)
Time (min)
DNA
Centrally placed mono-nucleosome
LlaBIII
ATP
1 2 3 4 5 6 7 8 9 10 11 12 13
0
1
2
3
4
5
0
6
7
8
9
(c)
Lane 5-No ATP
Lane 6- 1 min
Lane 7- 2.5 min
Lane 8- 5 min
Lane 9- 10 min
Lane 10- 20 min
Lane 11- 40 min
Lane 12- 60 min
Lane 13- 90 min
(d)
Normalized % free DNA
50
40
30
20
10
0
0
20
40
60
80
100
Time (minutes)

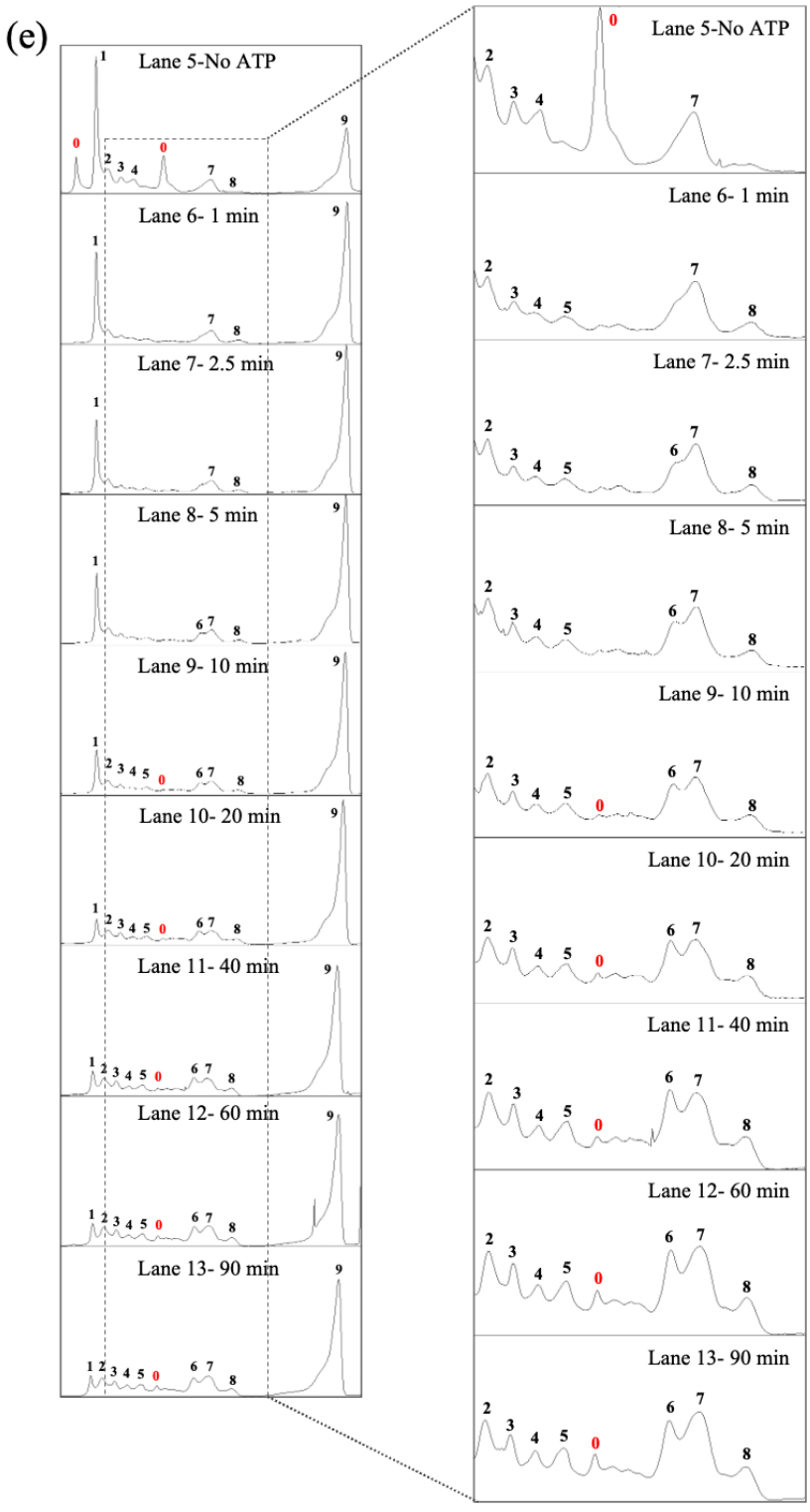

Figure 4.3: Time dependent EMSA with centrally placed mononucleosome and LlaBIII. (a) Graphical representation of possible outcomes of the reaction. (b) Representative gel image

showing the mobilization of nucleosome over time by LlaBIII in presence of ATP. Lanes 1-3 contain free DNA; with LlaBIII wherever indicated; Lanes 4-13 contain nucleosome; with LlaBIII and ATP wherever indicated. All the reactions were incubated at 25°C. All the controls (Lane 1 – Lane 5) were incubated for 90 minutes. The reactions were stopped by addition of excess unlabeled competitor DNA (except in lane 1 and 2), and EDTA at the end. Lane 2 – DNA with LlaBIII without competitor DNA. Lane 3 – DNA and LlaBIII with competitor DNA. Lane 4 – Mononucleosome. Lane 5 – Mononucleosome and LlaBIII without ATP. Lane 6 to Lane 13 – Mononucleosome with LlaBIII and ATP incubated for increasing time intervals (1 minute to 90 minute). Each nucleosome band has been labelled with a number (1-8). The free DNA is labelled as 9. The LlaBIII-nucleosome and LlaBIII-DNA bands are labelled as 0. (c and e) Intensity plot of the accompanying gel image. The peaks correspond to each of the bands as seen in the corresponding lane are labelled accordingly. Peak 1, corresponding to the centrally placed nucleosome decreases over time along with other slower migrating nucleosome species and there is a corresponding increase in the fast-migrating species, peaks 6-8 and free DNA (peak 9) over time. Each section of the plot shows bands in corresponding lane from top to bottom as peaks from left to right as indicated by accompanying lane images of lane 5 and lane 13. (d) Plot showing the increase in free DNA over time. The percentage of free DNA in each lane was calculated separately and normalized with reference to free DNA in nucleosome in lane 5 (LlaBIII without ATP). N=3

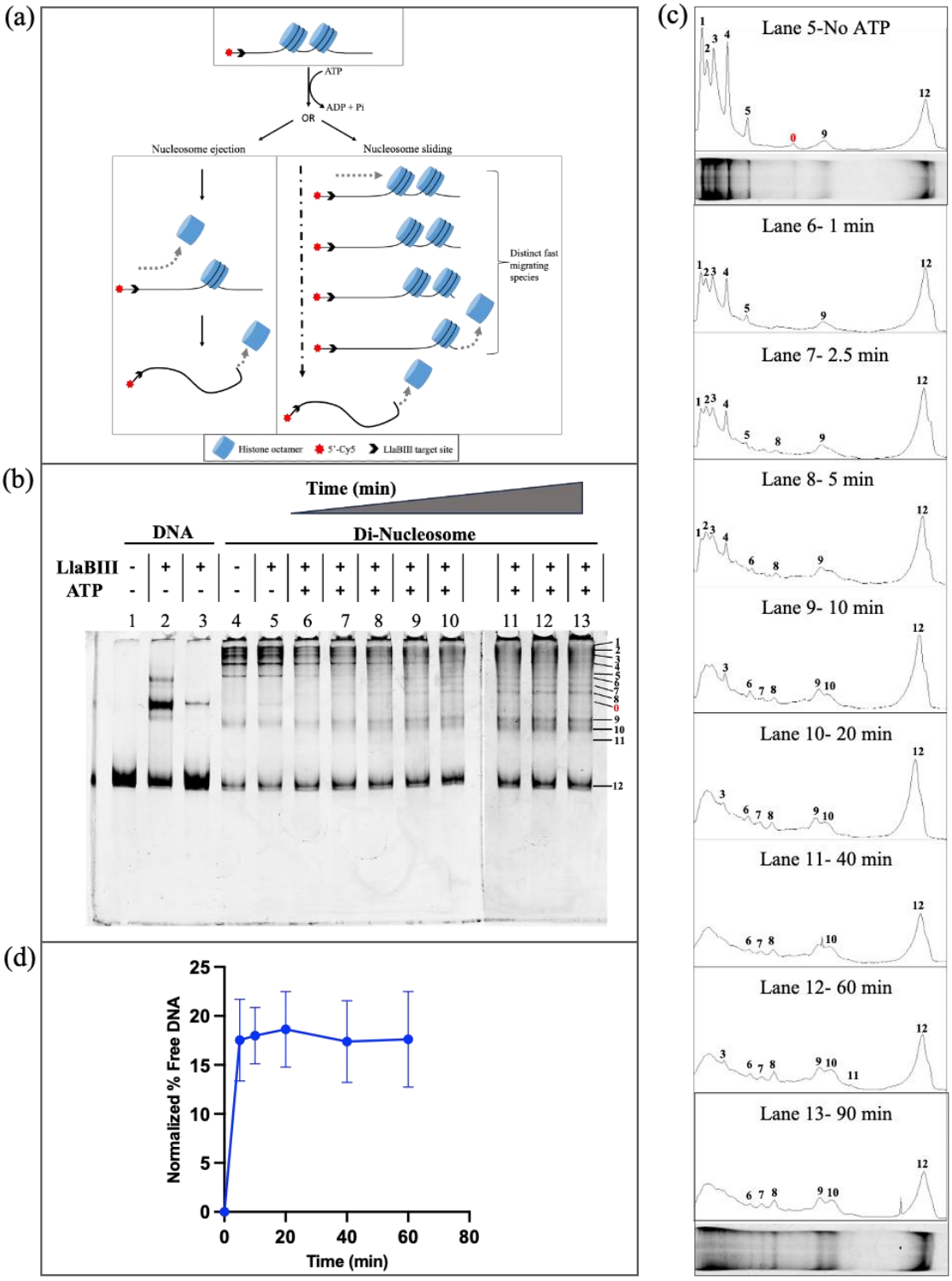
(a)
ATP
ADP + Pi
OR
Nucleosome ejection
Nucleosome sliding
Distinct fast migrating species
Histone octamer
5'-Cy5
LlaBIII target site
(b)
Time (min)
DNA
Di-Nucleosome
LlaBIII
ATP
1 2 3 4 5 6 7 8 9 10 11 12 13
(c)
Lane 5-No ATP
Lane 6- 1 min
Lane 7- 2.5 min
Lane 8- 5 min
Lane 9- 10 min
Lane 10- 20 min
Lane 11- 40 min
Lane 12- 60 min
Lane 13- 90 min
(d)
Normalized % Free DNA
Time (min)
0
5
10
15
20
25
0
20
40
60
80

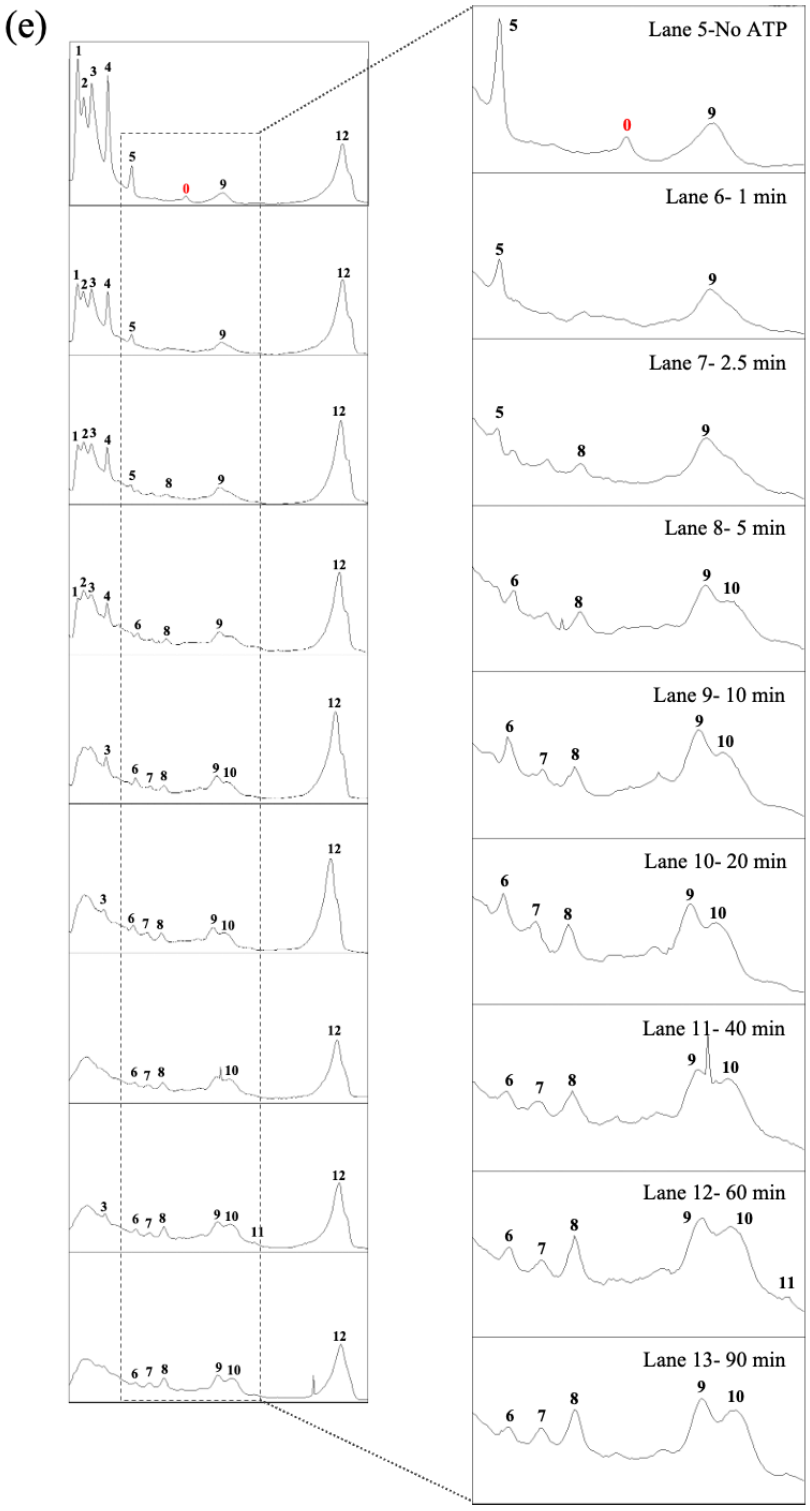

Figure 4.4: Time dependent EMSA with dinucleosome and LlaBIII. (a) Graphical representation of possible outcomes of the reaction. (b) Representative gel image showing the mobilization of

nucleosomes by LlaBIII over time. Lanes 1-3 contain free DNA with LlaBIII as indicated; Lanes 4-13 contain dinucleosome with LlaBIII and ATP as indicated. All the reactions were incubated at 25°C. All the controls (Lane 1 – Lane 5) were incubated for 90 minutes. The reactions were stopped by addition of excess unlabeled competitor DNA (except lane 1 and 2) and EDTA at the end. Lane 2 – DNA with LlaBIII without competitor DNA. Lane 3 – DNA and LlaBIII with competitor DNA. Lane 4 – Dinucleosome. Lane 5 – Dinucleosome incubated with LlaBIII and without ATP. Lane 6 to Lane 13 – Dinucleosome with LlaBIII and ATP was incubated for increasing time intervals (1 minute to 90 minute). Each nucleosome band has been labelled with a number (1-8) with free DNA labelled as 9. The persistent LlaBIII-DNA band has been labelled as 0. (c and e) Intensity plot of the accompanying gel image. The peaks correspond to each of the bands seen in each corresponding lane as labelled. The peaks 1-5 show the slower migrating nucleosome species prominent in lanes 4-5 that decrease upon ATP addition over time (lanes 6-13) with a corresponding increase in the fast-migrating species, peaks 6-11 and free DNA, peak 12. Each section of the plot shows bands in corresponding lane from top to bottom as peaks from left to right as indicated by accompanying lane images of lane 5 and lane 13. (d) Plot shows the increase in free DNA over time. The percentage of free DNA in each lane was calculated separately and normalized with reference to free DNA in in lane 5 (nucleosome + LlaBIII without ATP). N=4

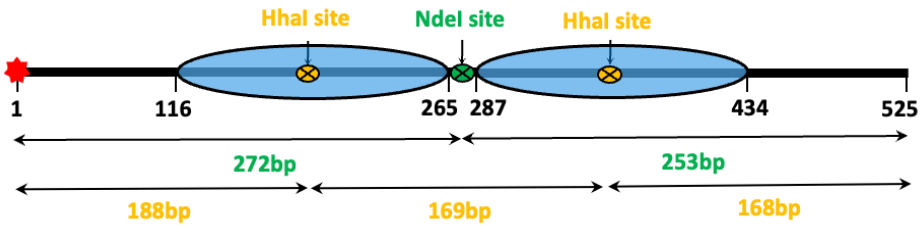

Figure 4.5: Graphical representation of the 5'-cy5 labeled dinucleosome construct. The HhaI target sites are indicated in yellow text and symbols (⊗). The DNA fragment sizes resultant of HhaI cleavage are indicated in blue text as well. The NdeI target site is indicated in green text and symbol (⊗). The sizes of the DNA fragment resulting from NdeI cleavage are indicated in green text.

4.3.2 Time-dependent REAA with dinucleosome - HhaI

The dinucleosome substrate was designed in such a way that it harbors restriction sites in the nucleosome occupying regions as well as the central and flanking regions (Fig. 4.5). There is a HhaI site at the center of each of the two 601 regions and a NdeI site in the center of the 22bp linker region connecting the two 601 regions. We utilized the presence of these target sites to track LlaBIII translocation mediated movement of the octamer on the DNA. For this we performed a time dependent REA assay separately with each of these restriction enzymes. The dinucleosome was incubated with LlaBIII and the reaction was started with addition of ATP. The remodeling activity was stopped with addition of excess competitor DNA and excess ADP. The samples at each time point were split into aliquots for restriction digestion with each of the specified enzymes. After restriction digestion and protein denaturation, the DNA cleavage products were analyzed on native PAGE.

Cleavage of the 5'-Cy5 labeled 525 bp DNA by HhaI at both the target sites results in three DNA fragments, and cleavage at either of the two sites result in two DNA fragments (Fig. 4.6 a). As we used Cy5 specific filter for scanning the native gel, we could detect only the fragments with 5'-Cy5. Hence, we were able to observe a 188 bp DNA fragment that resulted from cleavage at either both the HhaI sites or just at the first HhaI site downstream of the LlaBIII target site. The second fragment observed was the 357bp DNA obtained after cleavage exclusively at the second HhaI site due to incomplete DNA cleavage by HhaI or because the first HhaI site was occluded. HhaI cleavage of naked DNA resulted in occurrence of both the DNA fragments, although the 188bp fragment was the most predominant as cleavage happens typically at both the HhaI sites even in presence of LlaBIII (Fig. 4.6 b, lane 2-3). Although, there is a slight decrease in cleavage efficiency as a result of competitor DNA addition (Fig. 4.6 b, lane 3). Exposure of dinucleosome to HhaI in absence of LlaBIII resulted in cleavage of only the unbound DNA present in the nucleosome preparation whereas the octamer occupied DNA was protected (Fig. 4.6 b, lane 4). The addition of LlaBIII in absence of ATP showed similar result where most of the DNA was protected (Fig. 4.6 b-c, lane 5). Upon addition of ATP there was a rise in both the 188bp and 357bp fragment indicating that both the octamers get displaced promptly and almost simultaneously (Fig. 4.6 b-d). The rise in band intensities for the 188bp and 357bp fragments was comparable for the first 20 minutes when rapid nucleosome displacement would occur. The 357 bp fragment intensity

plateaued off, and the 188bp fragment intensity kept rising until 40 minutes before getting leveled off. After the initial cleavage, the 357 bp DNA gets further cleaved at the HhaI site to form the 188 bp DNA, hence its intensity kept rising. On the other hand, there was a steady decline in the intensity of the uncut DNA band and a rise in the total cut DNA fragment intensities (Fig. 4.6 b-c, lanes 6-13). There was an overall rise in the total DNA cleavage 40 minutes post ATP addition after which the cleavage leveled off (Fig. 4.6 e). Ideally all the nucleosome DNA should have been cleaved into smaller fragments, but we do not see an increase in DNA cleavage beyond the 40 minutes time point. We attribute this to the presence of the excess competitor DNA and the presence of displaced histones. The competitor DNA does inhibit cleavage of free DNA itself to some extent, in the nucleosome remodeling reactions, the increase in displaced histone proteins over time and LlaBIII might have enhanced the inhibition.

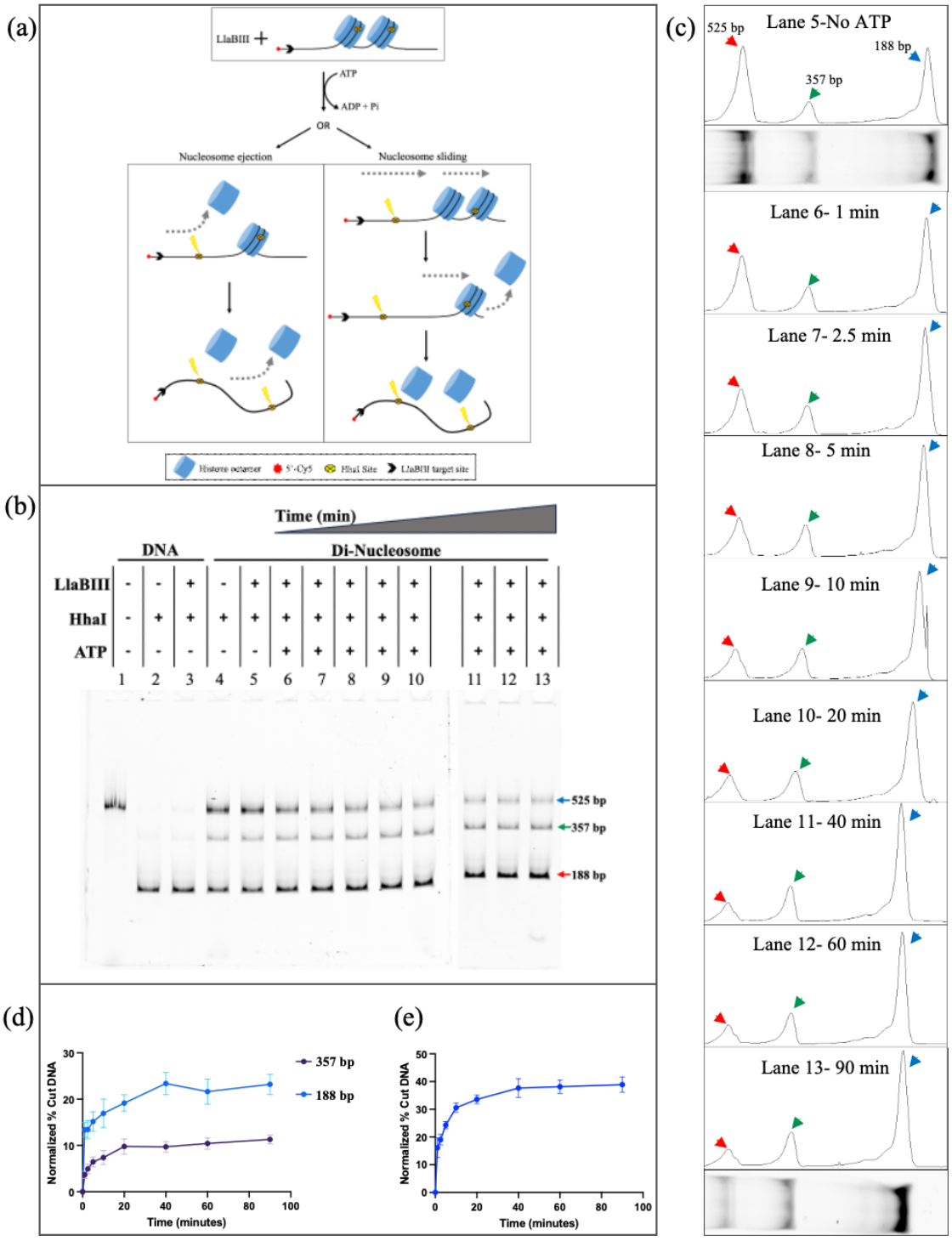

Figure 4.6: Time dependent REAA with HhaI and LlaBIII. (a) Graphical representation of the reaction set up and possible outcomes of the assay. (b) Representative gel image showing REAA with HhaI over 90 minutes. Lanes 1-3 contain free DNA; with LlaBIII and HhaI wherever

indicated. Lanes 4-13 contain dinucleosome; with LlaBIII, ATP and HhaI wherever indicated. All the controls (Lane 1 – Lane 5) were incubated at 25°C for 90 minutes then shifted to 37°C after HhaI addition. For lanes 6 – 13, the dinucleosome and LlaBIII were incubated with ATP at 25°C for given time points from 1 minute to 90 minutes. At the end of 90 minutes, unlabeled competitor DNA was added to all the reactions except the ones in lanes 1 and 2. The remodeling reaction was stopped by addition of excess ADP and the dinucleosome was exposed to HhaI for an hour at 37°C. The unbound nucleosome DNA gets cleaved into three fragments after cleavage at two HhaI target sites, otherwise occupied by the octamers. (c) Intensity plot of the accompanying REAA gel image. The peaks correspond to each of the bands seen in the corresponding lane as labelled. Red arrows show the peaks corresponding to the uncut (525 bp) dinucleosome DNA band and the blue arrows show the peaks corresponding to the band of 188 bp DNA fragments and green arrows show peaks corresponding to 357 bp DNA fragments. The uncut DNA band intensity decreases over time with a corresponding increase in the cut DNA bands. Each section of the plot shows bands in the corresponding lane from top to bottom as peaks from left to right as represented by accompanying lane images of lane 5 and lane 13. (d) Plot showing the changes in intensities of each of the cleavage fragment bands – 357bp and the 188bp. (e) Plot showing the increase in total DNA cut over time by HhaI. The percentage of each DNA fragment in every lane was calculated separately and normalized with reference to the DNA fragments produced from dinucleosome in presence of LlaBIII without ATP (lane 5). N=3

4.3.3 Time dependent REAA with dinucleosome – NdeI

The NdeI site is located at the center of the linker DNA that connects the two 601 regions (Fig. 4.5). This linker region remained unoccupied when the octamers were optimally assembled to form the dinucleosome (Fig. 4.7 a). The assay was performed similarly to the time dependent assay done with HhaI described above. If the nucleosomes are kicked off the DNA without sliding, the NdeI site would always be exposed for cleavage and it will remain unaffected over time. Whereas, if the nucleosomes are slid by LlaBIII, the first nucleosome will slide over the linker DNA and occlude the NdeI target site. Thus, in case of nucleosome sliding the DNA cleavage by NdeI would decrease (Fig. 4.7 a). Cleavage of the free DNA with NdeI resulted in two fragments and the 5'-Cy5 labelled fragment (272 bp) is detected in our experiments. The DNA cleavage was cleaved efficiently even in presence of LlaBIII (Fig. 4.7 b, lane 2-3). But presence of competitor DNA

decreased the NdeI cleavage efficiency slightly (Fig. 4.7 b, lane 3). When the dinucleosome was exposed to NdeI, the DNA was cleaved at the exposed target site to yield two DNA fragments and the 5'-Cy5 labeled fragment (272 bp) was detected (Fig. 4.7 b, lane 4). The intensity of the cleaved DNA band was much higher than the uncut DNA band (525 bp), indicating that a large fraction of the nucleosome bound DNA was cleaved. Presence of LlaBIII in absence of ATP did not affect this cleavage pattern (Fig. 4.7 b-c, lane 5). Addition of ATP lead to a steady increase in the uncut DNA band and a decrease in the cut DNA over time (Fig. 4.7 c-d). We interpret this as the occlusion of the NdeI target site by octamer displacement resulting from the octamers sliding in the direction in which LlaBIII translocates DNA (5'-3'). Occlusion of the NdeI site supports the nucleosome sliding mechanism as the NdeI site would always remain available for DNA cleavage in case of nucleosome ejection. As LlaBIII slides the nucleosomes, eventually the octamers are expected to be pushed off the DNA ends. Hence, when sufficient time is given, the NdeI site would be exposed to DNA cleavage. But we do not see an increase in NdeI cleavage over the course of 90 minutes. As we saw similar results with HhaI cleavage, we speculate that the presence of competitor DNA, increase in displaced histone proteins with time and LlaBIII together may contribute to inhibition of NdeI cleavage activity at later time points. Another possibility is a decrease in the LlaBIII nucleosome remodeling activity as the ATP decreases over time with the simultaneous increase in unbound histone proteins.

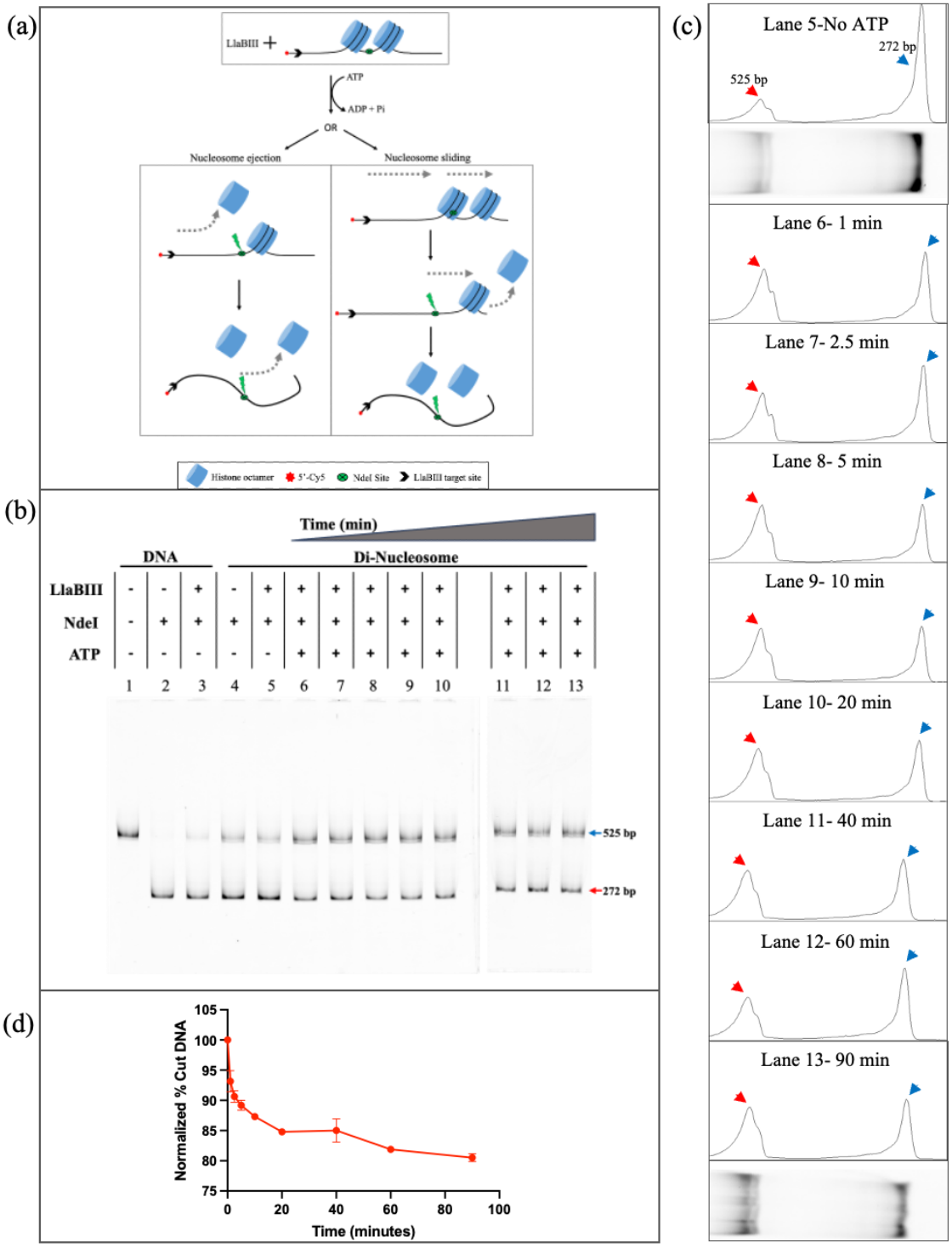

Figure 4.7: Time dependent REAA with NdeI and LlaBIII. (a) Graphical representation of the reaction set up and possible outcomes of the assay. (b) Representative gel image showing REAA with NdeI over 90 minutes. Lanes 1-3 contain free DNA with LlaBIII and NdeI wherever

indicated; Lanes 4-13 contain dinucleosome with LlaBIII, ATP and NdeI wherever indicated. All the controls (Lane 1 – Lane 5) were incubated at 25°C for 90 minutes then shifted to 37°C after NdeI addition. For lanes 6 – 13, the dinucleosome and LlaBIII were incubated with ATP at 25°C for given time points from 1 minute to 90 minutes. At the end of 90 minutes, unlabeled competitor DNA was added to all the reactions except the ones in lanes 1 and 2. The remodeling reaction was stopped by addition of excess ADP and the dinucleosome was exposed to NdeI for an hour at 37°C. The unbound as well as bound nucleosome DNA was cleaved into two fragments after cleavage at a single NdeI target site located symmetrically between the two nucleosome occupying regions (601) that remained exposed when octamers were unperturbed (Lane 4 and 5). Cleavage decreased as the octamers moved along the direction of the translocation of LlaBIII and occupied the region with NdeI target site (Lanes 6 to 13) (c) Intensity plot of the accompanying REAA gel image. The peaks correspond to each of the bands as seen in each corresponding lane as labelled. Red arrows show the peaks corresponding to the uncut dinucleosome DNA band and the blue arrows show the peaks corresponding to the bands of cleaved DNA fragment. The intensity of uncut DNA band (525 bp) increased over time with a corresponding decrease in the intensity of the cut DNA (272 bp). Each section of the plot shows bands in corresponding lane from top to bottom as peaks from left to right as represented by accompanying lane images of lane 5 and lane 13. (d) Plot showing the decrease in total DNA cut over time by NdeI. The percentage of each DNA fragment in every lane was calculated separately and normalized with reference to DNA fragments produced from dinucleosome in presence of LlaBIII without ATP (lane 5). N=3

4.4 Discussion

So far, we had established the remodeling potential of LlaBIII, a Type ISP RM enzyme. It was able to displace mononucleosomes and dinucleosome in an ATP dependent manner. In this chapter, we aimed to understand the mechanism of nucleosome remodeling by this translocase. LlaBIII is a distant prokaryotic relative of the typical eukaryotic chromatin remodelers. The chromatin remodelers have evolved to displace, eject or modify nucleosomes while sensing the cellular cues. There are two probable mechanisms proposed for the various chromatin remodelers with minor differences at mechanistic levels depending on the remodeler family (Clapier & Cairns, 2009; Längst & Becker, 2004; Nodelman & Bowman, 2021; Zhang et al., 2006). These are the twist defect model and the loop propagation model (Längst & Becker, 2004; Nodelman & Bowman,

2021). Both of these models have supporting or conflicting evidence with various remodeler families as discussed previously in chapter one. Sliding of octamer by a remodeler is possible with either of these mechanisms. The remodelers are also active DNA translocases like LlaBIII, although they act in a target independent manner. They interact with DNA or nucleosomes in a sequence independent manner and are known to interact with the nucleosome DNA such that they modify the octamer-DNA interactions to enable nucleosome sliding. LlaBIII on the other hand is simply a DNA translocase that recognizes specific target sites, translocates and cleaves DNA. It is not known to specifically interact with the nucleosome dyad and change DNA conformation to induce a twist defect or to incorporate a loop. Nevertheless, it is unique in its ability to displace nucleosomes, as not all DNA translocases can slide octamers. Another exception is RNA polymerase which translocate DNA and have also been shown to reposition nucleosomes in the direction opposite to the polymerase translocation (Studitsky et al., 1994, 1997). The RNA polymerases are thought to do so through loop propagation as the polymerase unwraps the DNA from the nucleosome ahead of it, while it traverses transcribing the DNA in the loop formed and eventually the DNA rewraps as the RNA polymerase passes through (Kulaeva et al., 2009). The nucleosomes are repositioned over ~75-80 bp from their original positions (Studitsky et al., 1994, 1997). On the other hand, in our *in vitro* experiments, the octamers are displaced significantly and they are moved along the direction of LlaBIII translocation. Looking carefully at the time dependent EMSAs and the REA assays, we were able to establish that LlaBIII displaces the nucleosomes to more terminal positions before sliding them off the ends to free up the DNA completely. LlaBIII is able to displace nucleosome, but the mechanism by which it is achieved may not be very similar to the proposed mechanisms for chromatin remodelers. As for the twist defect model where DNA distortion is a essential, we do not know if LlaBIII translocation distorts the DNA. DNA distortion is one of the main drivers of the twist defect model. Nucleosome displacement via loop translocation by an enzyme that is not a standard chromatin remodeler, also seems unlikely as it involves a far more complex mechanism involving multiple domains specialized to open up a loop at nucleosome dyad which is further propagated to slide the nucleosome. RNA polymerase II forms and propagates a small intranucleosomal loop but does not displace the nucleosomes in doing so (Kulaeva et al., 2009). It is likely that LlaBIII utilizes a unique mechanism that depends on the ATP intensive DNA translocation activity that might be able to generate enough force to push the nucleosomes and enable nucleosome sliding.

4.5 References

Chand, M. K., Carle, V., Anuvind, K. G., & Saikrishnan, K. (2020). DNA-mediated coupling of ATPase, translocase and nuclease activities of a Type ISP restriction-modification enzyme. *Nucleic Acids Research*, *48*(5), 2594–2603. https://doi.org/10.1093/nar/gkaa023

Chand, M. K., Nirwan, N., Diffin, F. M., Van Aelst, K., Kulkarni, M., Pernstich, C., Szczelkun, M. D., & Saikrishnan, K. (2015). Translocation-coupled DNA cleavage by the Type ISP restriction-modification enzymes. *Nature Chemical Biology*, *11*(11), 870–877. https://doi.org/10.1038/nchembio.1926

Clapier, C. R., & Cairns, B. R. (2009). The Biology of Chromatin Remodeling Complexes. *Annual Review of Biochemistry*, *78*(1), 273–304. https://doi.org/10.1146/annurev.biochem.77.062706.153223

Fan, H.-Y., He, X., Kingston, R. E., & Narlikar, G. J. (2003). Distinct Strategies to Make Nucleosomal DNA Accessible. *Molecular Cell*, *11*(5), 1311–1322. https://doi.org/10.1016/S1097-2765(03)00192-8

Hamiche, A., Sandaltzopoulos, R., Gdula, D. A., & Wu, C. (1999). ATP-Dependent Histone Octamer Sliding Mediated by the Chromatin Remodeling Complex NURF. *Cell*, *97*(7), 833–842. https://doi.org/10.1016/S0092-8674(00)80796-5

Li, G., Levitus, M., Bustamante, C., & Widom, J. (2005). Rapid spontaneous accessibility of nucleosomal DNA. *Nature Structural & Molecular Biology*, *12*(1), 46–53. https://doi.org/10.1038/nsmb869

Liu, N., Balliano, A., & Hayes, J. J. (2011). Mechanism(s) of SWI/SNF-Induced Nucleosome Mobilization. *ChemBioChem*, *12*(2), 196–204. https://doi.org/https://doi.org/10.1002/cbic.201000455

Manelyte, L., Strohner, R., Gross, T., & Längst, G. (2014). Chromatin Targeting Signals, Nucleosome Positioning Mechanism and Non-Coding RNA-Mediated Regulation of the Chromatin Remodeling Complex NoRC. *PLOS Genetics*, *10*(3), e1004157-. https://doi.org/10.1371/journal.pgen.1004157

Nodelman, I. M., & Bowman, G. D. (2021). Biophysics of Chromatin Remodeling. *Annual Review of Biophysics*, *50*(1), 73–93. https://doi.org/10.1146/annurev-biophys-082520-080201

Poirier, M. G., Bussiek, M., Langowski, J., & Widom, J. (2008). Spontaneous Access to DNA Target Sites in Folded Chromatin Fibers. *Journal of Molecular Biology*, *379*(4), 772–786. https://doi.org/https://doi.org/10.1016/j.jmb.2008.04.025

Polach, K. J., & Widom, J. (1995). Mechanism of Protein Access to Specific DNA Sequences in Chromatin: A Dynamic Equilibrium Model for Gene Regulation. *Journal of Molecular Biology*, *254*(2), 130–149. https://doi.org/https://doi.org/10.1006/jmbi.1995.0606

Schneider, C. A., Rasband, W. S., & Eliceiri, K. W. (2012). NIH Image to ImageJ: 25 years of image analysis. *Nature Methods*, *9*(7), 671–675. https://doi.org/10.1038/nmeth.2089

Studitsky, V. M., Clark, D. J., & Felsenfeld, G. (1994). A histone octamer can step around a transcribing polymerase without leaving the template. *Cell*, *76*(2), 371–382. https://doi.org/https://doi.org/10.1016/0092-8674(94)90343-3

Studitsky, V. M., Kassavetis, G. A., Geiduschek, E. P., & Felsenfeld, G. (1997). Mechanism of Transcription Through the Nucleosome by Eukaryotic RNA Polymerase. *Science*, *278*(5345), 1960–1963. https://doi.org/10.1126/science.278.5345.1960

Chapter 5 – Effect of LlaBIII on protein-DNA interactions in bacterial and mammalian cells

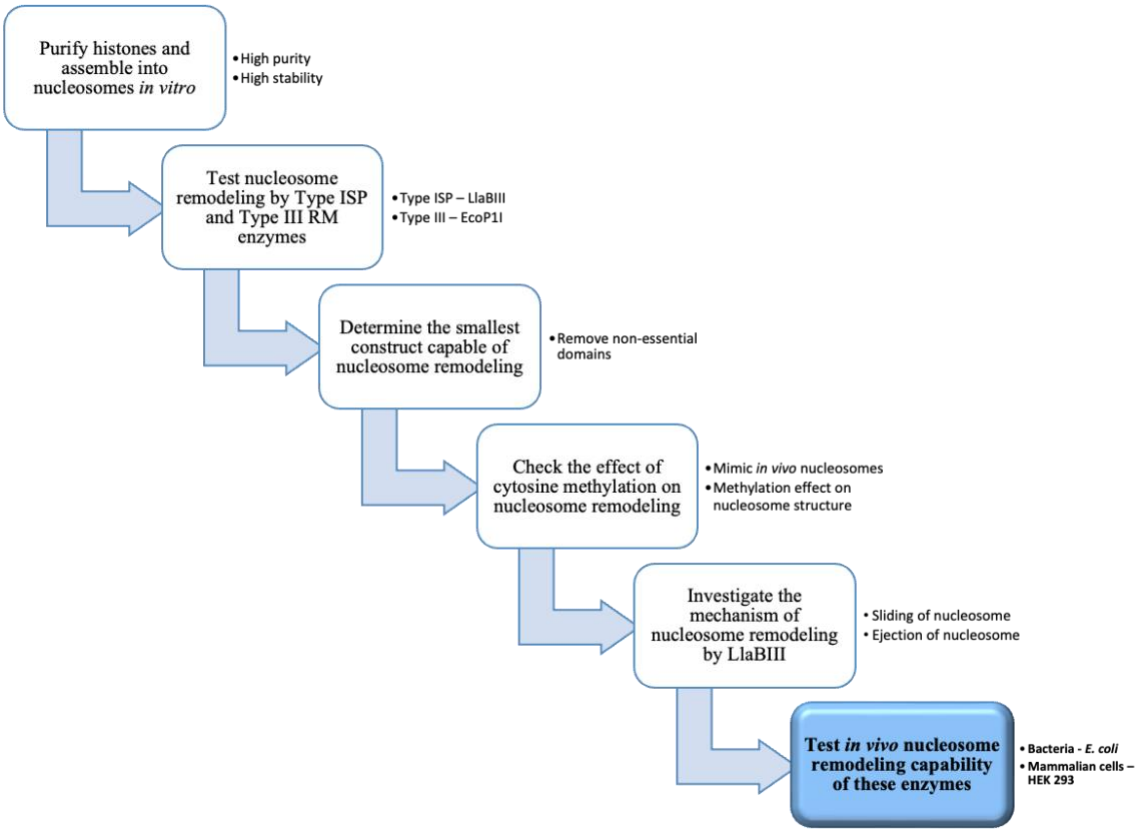

5.1 Introduction

LlaBIII is a multidomain, multifunctional, single polypeptide RM enzyme that recognizes a specific target sequence of DNA, either methylates an adenine in its target site or translocates DNA and ultimately coordinates with another translocating LlaBIII to cleave double stranded DNA (Šišáková et al., 2013). It binds to the DNA sequence – TNAGCC, and flips the adenine (A) opposite the thymidine (T) into a catalytic pocket in the methyltransferase domain. If the adenine is methylated, the enzyme does not activate DNA translocation. If the adenine is unmethylated, the methyltransferase either transfers a methyl group from s-adenosyl methionine (SAM) to the N6 position of the adenine or the motor is activated which couples ATP hydrolysis with DNA translocation. The methylation of adenine aids the bacteria to protect its own genomic DNA from cleavage by LlaBIII, whereas the invading phage DNA that does not carry this methylation mark would be targeted for cleavage. For DNA cleavage the translocating enzymes have to collide head on. As LlaBIII moves unidirectionally, the target sites have to be positioned in a head-to-head orientation (Chand et al., 2015; Šišáková et al., 2013). Also, upon head-to-head collision, LlaBIII likely undergoes a conformational change that activates the nucleases on both the enzymes to nick one DNA strand each (van Aelst et al., 2013, 2015). A head-to-tail interaction on the other hand would not lead to activation of both the enzyme units, and even if it does, they would both nick the same DNA strand, thereby preventing a double strand break (Šišáková et al., 2013; Smith et al., 2009b). Additionally, only the interaction between two Type ISP RM enzymes leads to nuclease activation and DNA cleavage, a random protein roadblock is unable to activate the nuclease for cleavage (van Aelst et al., 2013).

LlaBIII translocation plays an important role in regulating the enzyme activity *in vivo*. The long-range communication between two asymmetric target sites that need to be positioned in a preferred orientation (head-to-head), allows the bacteria to protect the nucleoid from self-cleavage. The motor domain is constituted by the highly conserved arrangement of two RecA-like folds in tandem that power the ATP driven DNA translocation (Chand et al., 2015). Upon recognition of an unmethylated target sequence, the enzyme begins unidirectional translocation while utilizing ~1-2 ATP per base pair translocated (Šišáková et al., 2013; R. M. Smith et al., 2009c; Van Aelst et al., 2013). The DNA translocation happens at ~300 bp/sec (Chand et al., 2020; Šišáková et al., 2013), therefore ATP is also processed at significant rates. Active DNA translocation at such speed

can affect DNA binding by other proteins in its path as we have observed for the histone octamers. In this chapter we test the effects of LlaBIII translocation in bacteria as well as in mammalian cells. Using *E. coli* as a prokaryotic model system and HEK293 cells as eukaryotic model system, we have tried to understand the downstream effects of disruption of protein-DNA contacts by LlaBIII.

5.2 Materials and methods

5.2.1 Cloning of LlaBIII mutants

To make a *LlaBIII* nuclease-truncated methyltransferase mutant, site directed mutagenesis was performed to mutate asparagine 1018 to alanine (N1018A). The mutation was incorporated in the gene in two steps by PCR amplification using pHis17-*LlaBIII* $n^-m^+a^+$ (1-165 amino acid residues deleted from WT) as template. The first gene fragment was generated using primers LB-N1017D-F and T7-R. The PCR product was used as a primer with T7-F for extension of the full length *LlaBIII* n^-m^-. The PCR product was purified using PCR cleanup kit (Qiagen, Cat. No. 28106). The mutation incorporated a BamHI site in the gene, therefore to incorporate the mutation in the clone pHis17-*LlaBIII* n^-, two internal EcoRV sites were used. Restriction digestion and ligation was performed to incorporate the mutated gene fragment in pHis17-LlaBIII $n^-m^+a^+$ to get pHis17-LlaBIII $n^-m^-a^+$.

To make *llaBiii* nuclease-truncated, methyltransferase inactive, ATPase inactive mutant, site-directed mutagenesis was performed. Lysine 209 was mutated to alanine (K209A) using pHis17-*llaBiii* $n^-m^-a^+$ as template. The mutated gene product was amplified as described above in two steps of PCR amplification using primers T7-F and LB-WalkerA-R for the first PCR. Product from the first PCR was used as primer with T7-R for the second PCR extension to get *llaBiii n-m-a-* gene. The gene was incorporated into pHis17 plasmid through restriction cloning method using the NdeI and HindIII sites. All the genes were subcloned by restriction cloning method into pHis17 (Kan^R) vector which carries resistance marker for kanamycin instead of ampicillin.

For expression in mammalian cells, the mutant *llaBiii* genes were cloned into pCMV10 vector (a gift from Dr. Sanjeev Galande Lab). The genes were PCR amplified using primers LBdN-pCMV10-F and LBdN-pCMV10-R. The forward primer added sequences for N-terminal 3xFlag

epitope tags and a simian virus 40 (SV40) nuclear localization signal sequence linked in frame to the gene by a three amino acid linker. The PCR amplified gene products were cloned into the pCMV10 vector through restriction cloning method using HindIII and BamHI sites.

5.2.2 Methylation assay

The plasmids pHis17-*llaBiii* $n^-m^+a^+$, pHis17-*llaBiii* $n^-m^-a^+$, pHis17-*llaBiii* $n^-m^-a^-$ and pHis17-*MBdN* were propagated in *E. coli* cells [BL21 (DE3), BL21-AI, DH5α, MG1655]. Single colonies were inoculated for each and incubated at 37°C until OD reaches 0.4-0.6. Cultures of lab strains (DH5α, MG1655) were incubated as it is. For overexpression strains [BL21 (DE3), BL21-AI], the culture was split into two separate sterile vials. Culture in one of the vials was induced either with 0.5 mM IPTG [BL21(DE3)] or with 1 percent arabinose w/v (BL21-AI). Both the cultures, uninduced and induced, are incubated for 3 hours at 37°C. Post incubation, the cells are harvested by centrifugation at 4000 rpm at 4°C and plasmids are isolated using plasmid prep kit (Qiagen, Cat. No. 27104). The plasmids were linearized using HindIII and purified using PCR cleanup kit (Qiagen, Cat. No. 28106). The linearized plasmids were incubated with LlaBIII WT and ATP as indicated, at 25°C for 30 minutes. The reactions were stopped by addition of 2 µl EDTA (500 mM) and 1 µl of 10% SDS. The reactions were heated at 65°C for 20 minutes and mixed with 4 µl ST buffer (100 mM Tris-HCl pH 7.5, 40% w/v sucrose) before loading onto 0.8% agarose gel run at 80 V until the DNA fragments resolved.

5.2.3 Microscopy

The *Escherichia coli* MG1655-HUαGFP strain used for the microscopic studies, was a kind gift from Dr. Itzhak Fishov, Ben-Gurion University of the Negev, Israel. The strain carries a single chromosomal copy *hupA-egfp-ampR* fusion under the native promoter (Abebe et al., 2017). The plasmids (pHis17 Kan^R-*llabiii* $n^-m^+a^+$, $n^-m^-a^+$ and $n^-m^-a^-$) were transformed into this *E. coli* strain and transformants were selected on LB agar plates with 100 µg/mL Ampicillin and 20 µg/mL Kanamycin. Single colony was inoculated in LB media supplemented with the given antibiotic concentrations. The cultures were incubated at 37°C for the indicated time and cells were harvested through centrifugation at 4000 rpm for 10 minutes. The cell pellet was resuspended in 1X Phosphate Buffered Saline (PBS) and centrifuged at 4000 rpm at 4°C. The supernatant was

discarded and the cell pellet was again resuspended in 1X PBS. The cell suspension was mixed with equal parts 5 ug/mL 4′,6-diamidino-2-phenylindole (DAPI) for 15 minutes at 37°C. The cells were centrifuged at 4000 rpm and the supernatant was discarded. The cell pellet was washed with 1X PBS before to remove excess DAPI. After centrifugation the cell pellets were resuspended in 1X PBS and 2 µl of the suspension was spotted onto 1% Agarose pads prepared on glass slides. The cells were imaged using Optima XE epifluorescence microscope using 100X oil immersion objective.

5.2.4 Culture and transfection of HEK293 cells

The HEK293 cells were cultured in Dulbecco's Modified Eagle Medium (DMEM) (Gibco; Cat.no. 11966025) supplemented with 10% fetal bovine serum and penicillin-streptomycin (Gibco; Cat.no.15140122); and maintained at 37°C under a 5% CO2 atmosphere. The cells were passaged upon reaching 70% confluence using 0.05% trypsin. For transfection, the HEK293 cells were passaged in a 6 well tissue culture plate. Sterile coverslips were placed in each well. The coverslips were sterilized by soaking in 100% methanol for a couple of hours. The methanol-soaked coverslips were placed in the wells (one in each well) and washed with sterile 1X PBS and air dried under UV for 30 minutes. HEK293 (70-80% confluent) culture was treated with 0.05% trypsin for 1 minute at 37°C to dislodge the cells. Fresh DMEM was added and the cells were transferred to a sterile vial and centrifuged at 1000 g for 5 minutes. The supernatant was discarded and the cell pellet was resuspended in 1 mL DMEM supplemented with 10% FBS. Cell number was estimated manually using a Neubauer's chamber. 2 mL media was added to each well of the 6-well plate containing the coverslips and 0.6 x 10^6 cells were seeded in each well. The cultures were incubated at 37°C for until 60-70% confluency was reached. For transfection, Lipofectamine 3000 (Invitrogen, Cat. No. L3000001) was used. The procedure was carried out according to the manufacturer's instructions. The plasmid and reagent mixtures were prepared with OptiMEM (Gibco; Cat.no 31985062) as per the given protocol. The spent culture media was discarded and replaced with1.5 mL of fresh media. The transfection mixture was gently overlayed on top of the cells and the cultures were incubated at 37°C under a 5% CO_2 atmosphere. 24 hours post transfection; the cell health was assessed by microscopy and the media was changed if cell death was observed.

5.2.5 Fluorescent *in-situ* hybridization

The cells grow over the coverslip and adhere to its surface, forming a layer of cells on the coverslips. 72 hours post transfection, the coverslips were recovered from the culture plates. Each coverslip was transferred to a petri dish and treated with 4% paraformaldehyde (PFA) for 10 minutes. The PFA was washed off gently with 1 X PBS using a micropipette. The cells were then treated with 1 mL of 0.1% Triton X. After 10 minutes incubation at room temperature, the cells were gently washed thrice with 1X PBS. The coverslips were then incubated for an hour with 2 mL of 3 % bovine serum albumin (BSA) solution. At the end of the incubation, the BSA solution was discarded and 50 ul of anti-Flag antibody (1:100 dilution) was aliquoted onto a parafilm piece kept in a petri dish. A coverslip was picked up by forceps and placed onto the antibody drop such that the cells were directly in contact with it. Pieces of wet tissue paper were placed adjacent to the parafilm and the petri dishes were incubated overnight at 4°C. Post incubation, the coverslips were transferred to a clean dish and washed thrice with 1X PBS. After washing the process is repeated with Alexa 568 tagged secondary antibody (1:250 dilution). The coverslips were incubated with the secondary antibody for an hour at room temperature. At the end of an hour, they were transferred to a clean dish and washed thrice with 1X PBS. The coverslips were transferred to a clean glass slide for microscopy. The coverslip edges were sealed to prevent dehydration of the cells. The cells were imaged using the Leica TCS SP8 X laser scanning confocal microscope was used for imaging the cells.

5.2.6 Immunoblotting

The cells were harvested 72 hours post transfection. Cell pellets were resuspended in lysis buffer [50 mM Tris pH 7.4, 1% SDS, 150 mM NaCl, 1% nonyl phenoxypolyethoxylethanol (NP-40)] containing 1× protease inhibitors cocktail (Roche) and phenylmethylsulfonyl fluoride (PMSF) (Sigma, commodity No. 10837091001). The lysates were centrifuged at 13000 rpm at 4°C for 30 min, to eliminate the cellular debris. The supernatant was collected in fresh microcentrifuge tube. The concentration of protein was determined by performing bicinchoninic acid (BCA) assay (Thermo Fisher Scientific, Cat. No. A65453). Equal amounts of protein lysates were boiled in 1× Laemmli buffer (0.5 M Tris-HCl [pH 6.8], 28% glycerol, 9% SDS, 5% β-mercaptoethanol, 0.01% bromophenol blue) for 10 to 15 min and resolved through electrophoresis on a polyacrylamide gel.

The resolved protein bands were transferred onto a polyvinylidene difluoride (PVDF) membrane (Millipore) by wet transfer method at 0.6 A for 3 hours at 4 °C. After the transfer, non-specific sites on the membrane were blocked using 5% skimmed milk. The membranes were then incubated overnight at 4°C with the primary antibodies (anti-Flag) prepared in 5% BSA. The membranes were washed three times with the buffer containing 20 mM Tris buffer (pH 7.4), 500 mM NaCl, and 0.1% Tween 20 (TBST) the next day and incubated with the appropriate secondary antibodies conjugated with horseradish peroxidase (HRP) for an hour at room temperature. After an hour the membranes were washed three times with TBST buffer. The blots were developed using Clarity Western ECL substrate (Biorad) and detected using ImageQuant LAS 4000 (GE Healthcare).

5.2.7 RNA extraction and cDNA synthesis

Total RNA was extracted using the TRIzol reagent (Invitrogen, Cat No. 15596026) according to the manufacturer's protocol. DNase treatment was performed as per the protocol provided by the manufacturer (Promega, Cat No. M6101) using 1 - 2 µg of RNA. DNase treated RNA was subjected to PCR amplification using GAPDH primers to ensure DNA elimination from the RNA samples. RNA samples free from DNA were used for cDNA synthesis using reverse transcriptase kits (Applied Biosystems) and random hexameric primers. Additionally, minus-reverse transcriptase (RT) control was also set up to verify the efficiency of DNase treatment. The synthesized cDNA was used to set up quantitative real-time PCR (qRT-PCR).

5.2.8 Quantitative real-time PCR

Quantitative real-time PCR was performed using SYBR green chemistry (Roche) with the set of primer pairs given in Table 5.1 using the ViiA7 thermal cycler (Applied Biosystems). Changes in threshold cycles (CT) were calculated by subtracting the CT values of the gene of interest from that of housekeeping control [CT (target genes) – CT (HEXIM1)]. ΔCT values of specific target genes from the experimental samples were then subtracted from their respective control samples to generate ΔΔCT values. The fold changes were calculated using the following formula: 2^ (−ΔΔCT value).

5.3 Results

5.3.1 LlaBIII methylates an adenine in its target site, *in vivo*

The methyltransferase (MTase) domain of LlaBIII has a structural fold similar to that of the γ-class N6-adenine MTase as seen in the typical Type I RM enzymes. The LlaBIII-MTase transfers a methyl group from the cofactor s-adenosyl methionine (SAM) to the exocyclic amino group of an adenine in its target site, forming m6A. In turn, presence of methyl group on the specific adenine in the target site prevents cleavage of the DNA by LlaBIII. The Type ISP enzymes have a MTase as well as a nuclease activity. *In vivo*, the cofactors necessary for both (SAM, ATP, Mg2+) are available. Consequently, binding of the enzyme with an unmethylated target site can lead to either methylation or activation of DNA translocation which would lead to DNA cleavage when two unmethylated head-to-head target sites are present. As LlaBIII recognizes a short target site, TNAGCC, this DNA sequence can occur at high frequency in a given length of DNA. Thus, in the *E. coli* genome, it is highly likely that head-to-head LlaBIII target sites occur frequently. Additionally, majority of these sites would be unmethylated, as the *E. coli* DNA adenine methyltransferase (DAM), can methylate only a subset of all the LlaBIII target sites in the genome. Hence, majority of LlaBIII target sites were expected to be susceptible to DNA cleavage by LlaBIII which in turn would kill the cell. Although, when LlaBIII was expressed in *E. coli* BL21(DE3), we found that the cells survived. This indicated that, *in vivo*, the LlaBIII methyltransferase activity was stimulated rather than the DNA translocation and nuclease activity. We tested this hypothesis through an *in vitro* DNA cleavage assay using the plasmid (pET28a-LlaBIII) extracted from *E. coli* BL21(DE3). The plasmid carried the LlaBIII wild-type gene and contained eleven LlaBIII target sites that formed at least seven direct combinations of head-to-head site orientations. The plasmid was linearized using the BamHI site and subjected to LlaBIII DNA cleavage assay as given by (Chand et al., 2020). A PCR amplified DNA substrate (1085 bp) containing a pair of head-to-head LlaBIII target sites was used as a control to monitor the LlaBIII cleavage activity. The 1085 bp DNA substrate contained unmethylated target sites, and so, was cleaved by LlaBIII in presence of ATP (Fig. 5.1 a, lane 3) but the linearized plasmid DNA was completely protected from DNA cleavage even in presence of ATP (Fig. 5.1 a, lane 6). This indicated that the LlaBIII target sites in the plasmid that was extracted from the bacteria were methylated. Also, the complete lack of cleavage suggested that all the eleven target sites were methylated, however only one of the eleven sites coincided with DAM target site. Hence, the blanket methylation of LlaBIII target sites strongly indicated that LlaBIII methylated its target sites *in vivo*. Although, *in vitro*, LlaBIII methylation activity has been found to be extremely poor (Šišáková et al., 2013), in the cell, the

target site methylation by LlaBIII appeared to take precedence over DNA cleavage. Also, the subsequent binding to these methylated target sites would prevent DNA translocation by LlaBIII. For nucleosome remodeling, the translocation activity is a pre-requisite. Therefore, for remodeling of nucleosome or protein-DNA *in vivo*, we needed to restrain the MTase activity of LlaBIII.

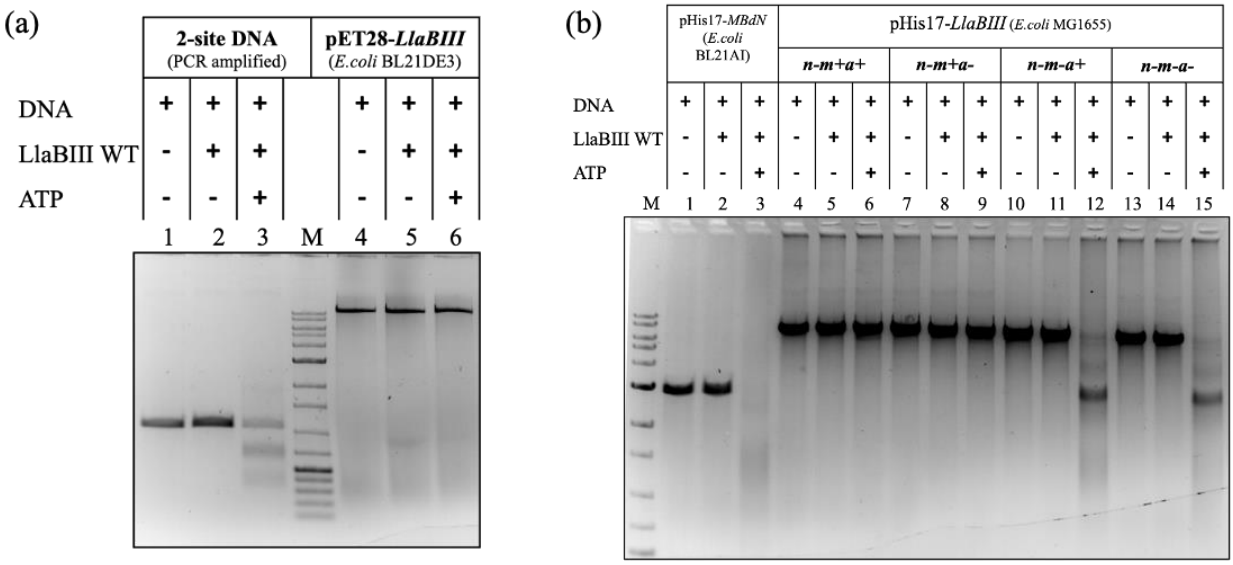

Figure 5.1: MTase activity of LlaBIII WT and mutants in different *E. coli*. All plasmids were isolated from the indicated *E. coli* strains, linearized and purified prior to the experiment. All the plasmids contain at least one set of LlaBIII target sites in head-to-head orientation. (a) Lanes 1-3, PCR generated DNA with two LlaBIII target sites in head-to-head orientation. M – DNA marker. Lanes 4-6, Linearized pET28a-LlaBIII isolated from *E. coli* BL21(DE3) subjected to cleavage by LlaBIII *in vitro.* (b) LlaBIII nuclease truncated methylase dead and ATPase mutants' plasmids isolated from *E. coli* MG1655 were subjected to cleavage by LlaBIII *in vitro* to determine the presence or absence of methyltransferase activity. Lanes 4-9 - methyltransferase active mutants (m^+), the plasmid DNA remains uncleaved by LlaBIII even in presence of ATP. Lanes 10-15 - methyltransferase inactive mutants (m-), the plasmid DNA is cleaved by LlaBIII in presence of ATP. N>2

Accordingly, we prepared a methyltransferase mutant of LlaBIII for our experiments with bacterial and mammalian cells. There are nine conserved motifs (I to VIII and X) in the N6-adenine MTases

that bind to SAM, bind specific DNA and transfer methyl groups from SAM to DNA. Out of these we chose to mutate motif IV [(D/N)PP(Y/F)], which catalyzes the transfer of the methyl group from SAM to the N6 position of the adenine base (Klimasauskas et al., 1989; Willcock et al., 1994). In EcoKI, a Type I RM enzyme, mutation of asparagine (N) to aspartic acid (D) in this motif did not affect binding of SAM with the MTase but severely hampered the methyltransferase activity (Willcock et al., 1994). A similar result was observed for another RM enzyme, BcgI. Mutation of the motif IV asparagine (N) to alanine (A)/glycine (G)/aspartic acid (D) completely abolished the methyltransferase activity (H. Kong & Smith, 1997). Therefore, we mutated motif IV asparagine (N) in LlaBIII nuclease truncated construct (*LlaBIII* n^-) to aspartic acid (D). Its methyltransferase activity was tested in *E. coli* lab strains.

Furthermore, we prepared a LlaBIII mutant that was defective in its ATPase activity. For this we mutated the lysine (K), that is a part of the Walker A motif [G(x4)GK(T/S)], to alanine (A). This motif stabilizes the β-phosphate of the bound ATP and mutation of this lysine residue has been shown to greatly decrease ATP hydrolysis and, in some cases, also disrupt ATP binding (Hall & Matson, 1999; Hanson & Whiteheart, 2005). The ATPase activity of this mutant was tested alongside the unmutated enzyme. The mutant failed to show ATPase activity comparable to the ATPase unmutated enzyme even with specific DNA substrate (Fig. 5.2). This mutant was thus utilized as a control for the subsequent *in vivo* experiments.

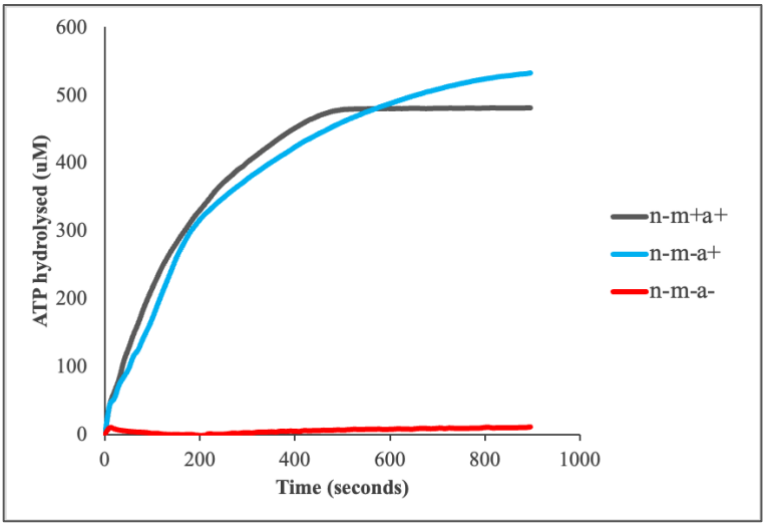

Figure 5.2: ATPase activity of LlaBIII mutants – LlaBIII $n^-m^+a^+$, LlaBIII $n^-m^-a^+$ and LlaBIII $n^-m^-a^-$. The ATPase assay was performed in presence of specific DNA substrate as given by (Chand et al., 2020). N=1

Combinations LlaBIII MTase and ATPase mutants with the nuclease truncated construct were made and their MTase activity was tested as described in methods. Briefly, the plasmids were propagated in *E. coli*, followed by plasmid extraction. The plasmids were linearized using a restriction site on the plasmids and exposed to LlaBIII in absence and presence of ATP. Cleavage by LlaBIII indicated presence of unmethylated target sites whereas absence of cleavage indicated *in vivo* methylation of target sites. We tested *in vivo* methylation activity of LlaBIII in the commonly used *E. coli* lab strains. An example is shown in the figure 5.1 b where we performed the methy-tansferase (MTase) assay with *E. coli* MG1655 strain, which has been used for further experiments. We found that even with a basal level expression in this strain, the MTase active LlaBIII ($n^-m^+a^+$) (Fig. 5.1 b, Lanes 4-9) could methylate and thus protect all the sites from cleavage, whereas when the MTase was mutated ($n^-m^-a^+$, $n^-m^-a^-$) (Fig. 5.1 b, Lanes 10-15), the sites were unmethylated and the DNA was cleaved. We also tested this in *E. coli* DH5α and the protein overexpression lab strains – *E. coli* BL21(DE3) (IPTG inducible) and *E. coli* BL21-AI (arabinose inducible). We saw a similar result with all the strains tested, with and without overexpression, LlaBIII MTase active construct ($n^-m^+a^+$) show protection from LlaBIII mediated DNA cleavage and the MTase mutants ($n^-m^-a^+$, $n^-m^-a^-$) showed complete susceptibility to DNA cleavage by LlaBIII upon addition of ATP. To ensure that the MTase activity that we were observing was only due to LlaBIII expression in these cells we also separately tested a plasmid construct expressing McrB mutant as a control. The McrB plasmid was susceptible to cleavage by LlaBIII (Fig. 5.1 b, Lanes 1-3).

5.3.2 Effect of LlaBIII on bacterial nucleoid

Once it was established that LlaBIII can disrupt protein-DNA interactions *in vitro*, we investigated the effect of LlaBIII translocation on bacterial nucleoid associated protein, HU. To do so, LlaBIII was expressed in an *E. coli* strain expressing HU-GFP fusion protein at physiological levels. This strain carries a single chromosomal copy of *hupA-egfp* fusion under the native promoter. Using these cells allowed us to microscopically observe the localization of HU. The bacterial nucleoid

was observed by staining with Hoechst stain, a stain that binds DNA. In the untransformed cells, a compact nucleoid arrangement was observed that was more central in position. The HU signal coincided with the nucleoid indicating that majority of the HU in the cell was bound to the nucleoid (Fig. 5.3 and 5.4 a). A similar observation was made for empty vector transformed cells (Fig. 5.3 and 5.4 b). The nucleoid was compact and HU co-localized with the DNA. In both of these samples, the cells displayed normal *E. coli* cell size wherein ~85 % cells were under 3 μm in length (Fig. 5.5 a-b). The distance of the brightest focus from the cell center for each cell was plotted against cell length. The plots for untransformed and vector transformed cells (Fig. 5.5 a-b), indicated near center localization of both HU-GFP and Hoechst signals in these samples. Also, the brightest foci for both signals largely coincided reiterating HU localization with the nucleoid in these cells. When LlaBIII mutants were expressed, the nucleoid morphology changed from compact to more dispersed such that it almost completely occupied the cell space. HU on the other hand was no longer exclusively localized with the nucleoid (Fig. 5.3 and 5.4 c-d). The HU foci were distant from the cell center and assumed a sub-polar localization. The plot with distance of brightest focus from cell center plotted against the cell length showed a more scattered distribution of HU foci in these cells (Fig. 5.5 c-d). The distance between HU-GFP and Hoechst foci was plotted against cell length to better gauge the extent of HU displacement from the nucleoid. The distance is minimum for controls (Fig. 5.6 a-b) whereas in presence of LlaBIII there is a drastic increase in this distance (Fig. 5.6 c-d). Moreover, the number of longer cells increased in these samples as more than ~30 percent cells were over 3 μm in length as compared to <15 percent in control. An important point to note here is that the expression of LlaBIII ATPase dead mutant (a-) also showed an effect on the HU localization and morphology. The mutant was designed to serve as a negative control to delineate the effect of LlaBIII DNA translocation from the effect of DNA binding by LlaBIII. However, under the conditions tested here, the mere binding of LlaBIII to DNA seemed adequate for disruption of HU-DNA interaction. Perhaps a DNA binding mutant of LlaBIII can allow us better understanding of whether simply LlaBIII binding itself affects HU localization in *E. coli* or that effect seen here due to the experimental protocols followed. Here we do not use a tightly regulated inducible expression system for our experiments but depend on the leaky expression of LlaBIII in *E. coli* MG1655 strain. Thus, the cells, from the beginning of the experiment (cell transformation), express LlaBIII and we do not regulate the expression

quantitatively or temporally. LlaBIII could thus be produced at such levels given the time that it is present at a significant cellular concentration to out-compete HU for DNA binding. Hence, any experiments in the future may need a change in the protocols and controls based on these findings.

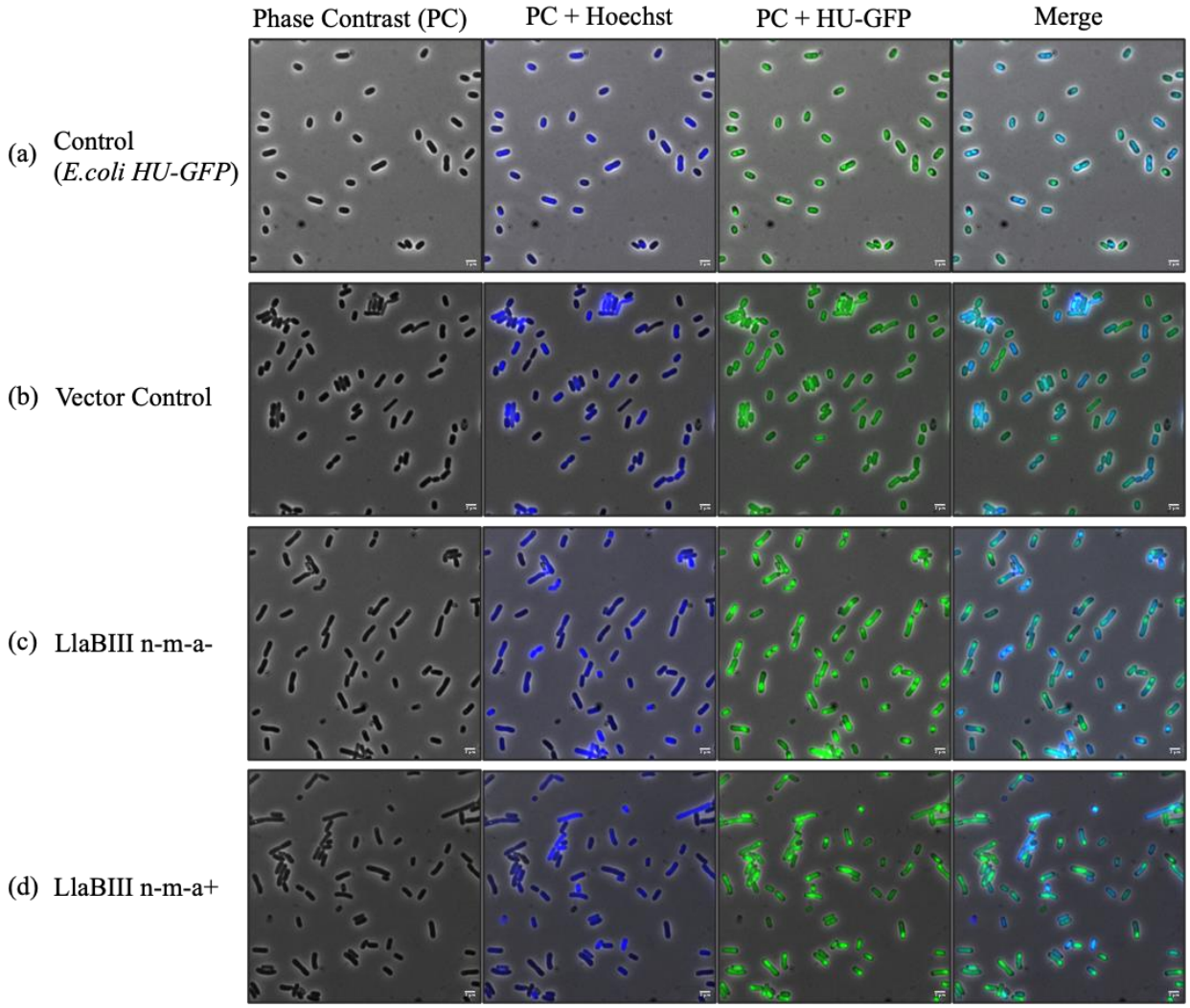

Figure 5.3: Effect of LlaBIII mutants on bacterial nucleoid and HU localization. Epifluorescence microscopy images of *E. coli* HU-GFP (a) Untransformed and transformed with (b) *pHIS17* (empty vector) (c) *pHIS17-llabiii* $n^-m^-a^-$ (d) *pHIS17-llabiii* $n^-m^-a^+$. Each row shows representative images of the transformants using channels – Phase contrast (PC), PC overlay with Hoechst, PC overlay with HU-GFP and merge of PC, Hoechst and HU-GFP. N>2

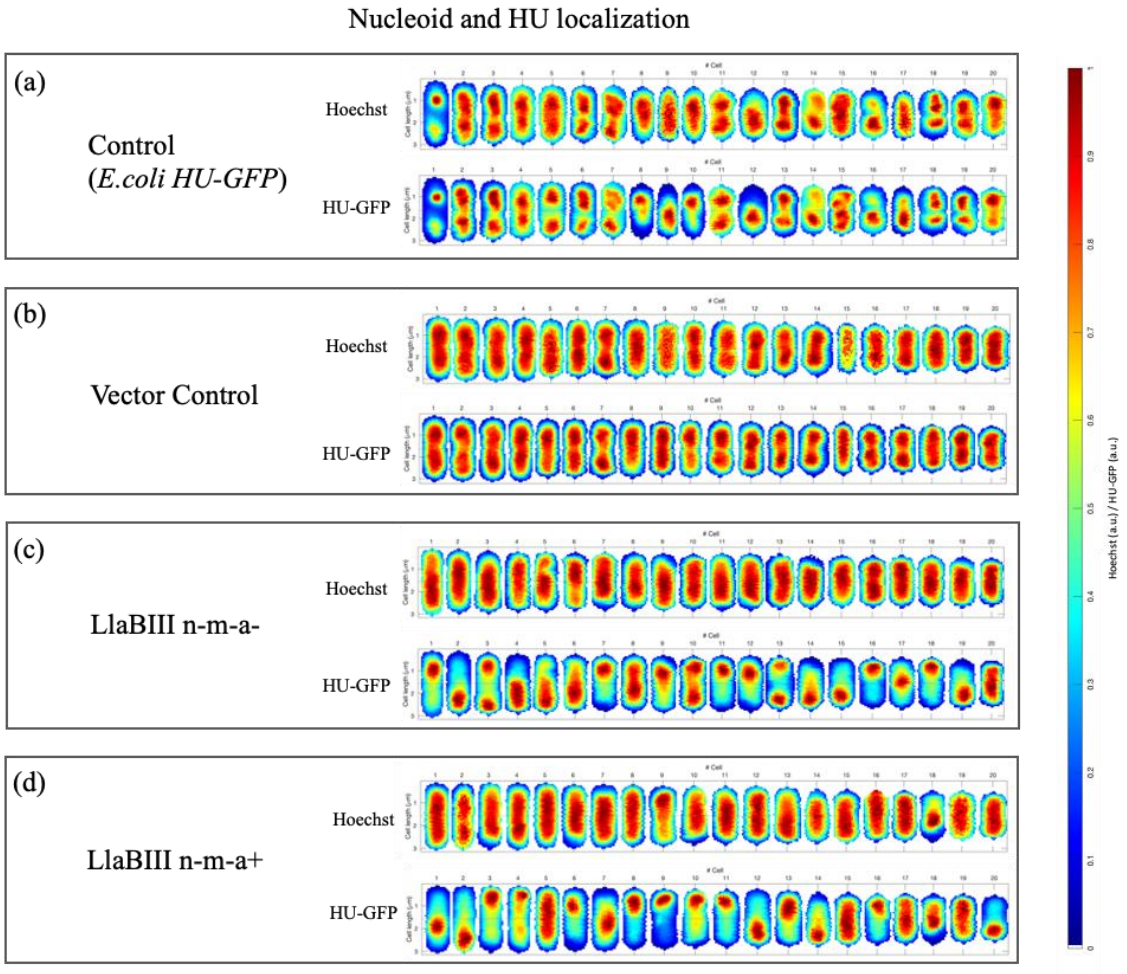

Figure 5.4: Bacterial nucleoid morphology and HU localization. Demograph of 20 cells of ~3 um length from the epifluorescence microscopy images. Background subtraction and intensity normalization performed using the published matlab program – Backstalk (Hartmann et al., 2020). (a) Untransformed, transformed with- (b) *pHIS17* (empty vector) (c) *pHIS17-llabiii* $n^-m^-a^-$ (d) *pHIS17-llabiii* $n^-m^-a^+$.

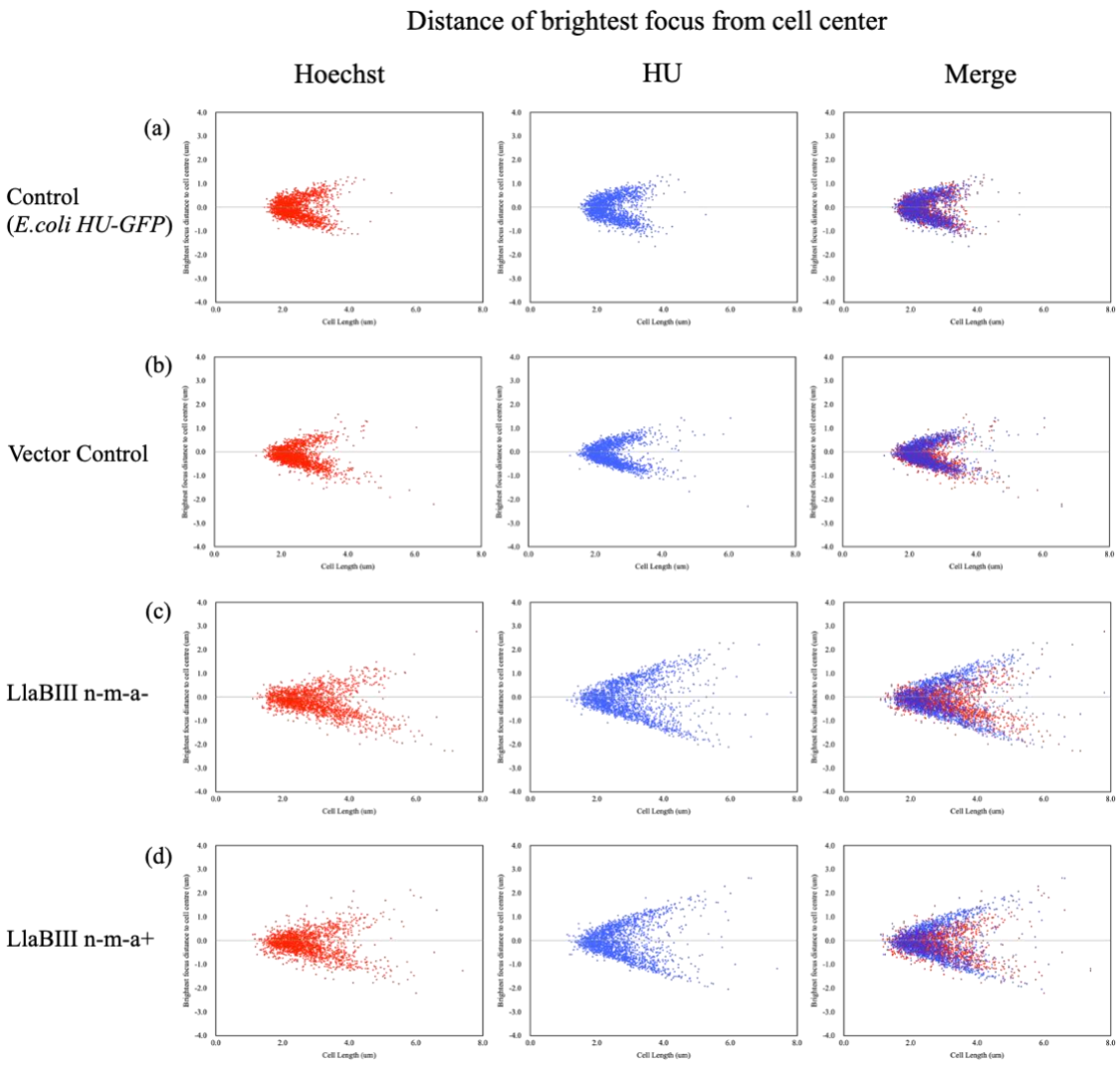

Figure 5.5: Quantitation of HU localization. Distance of brightest foci of either Hoechst (red) or HU (blue) from the cell center plotted against cell length. Each plot displays values from 2000 cells from each sample - *E. coli* HU-GFP (a) Untransformed and transformed with (b) *pHIS17* (empty vector) (c) *pHIS17-llabiii* $n^{-}m^{-}a^{-}$ (d) *pHIS17-llabiii* $n^{-}m^{-}a^{+}$. The third column (merge) shows the overlay of Hoechst and HU plots indicating the proximity of the two foci in the cell. N=2

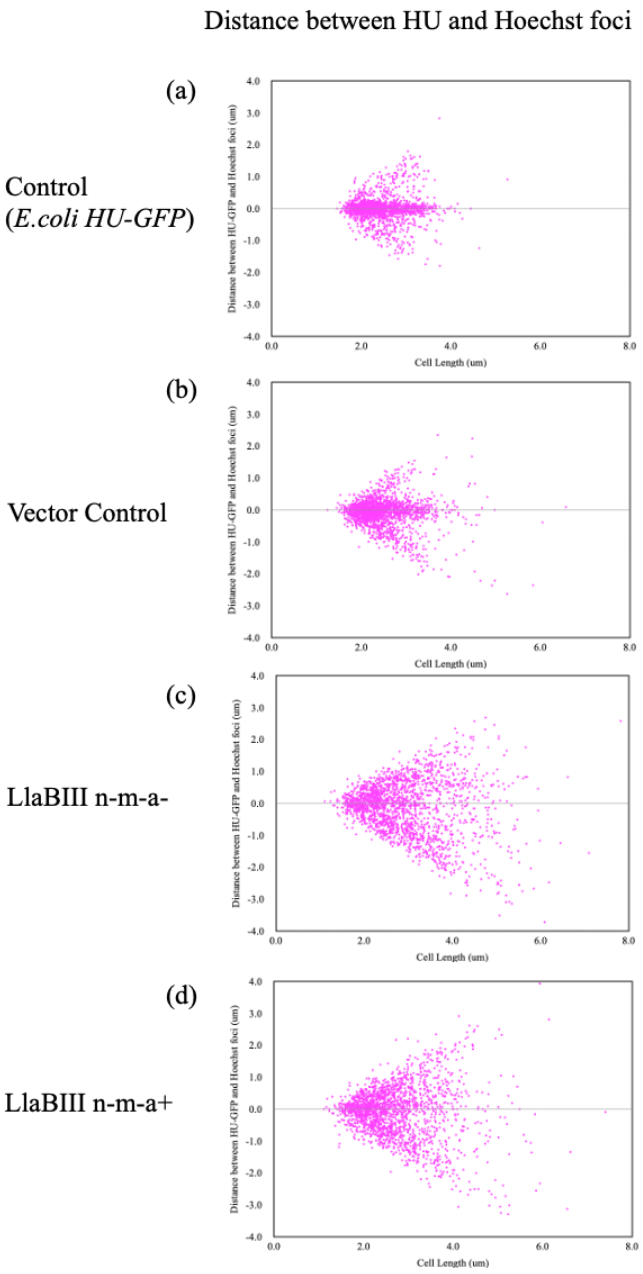

Figure 5.6: Quantitation of HU displacement from the nucleoid. Distance between Hoechst and HU foci was plotted against cell length. The plots show how well the HU foci coincides with the Hoechst foci in each cell as given in figure 5.5. N=2

5.3.3 Expression of LlaBIII constructs in HEK293 cells

An N-terminal 6xFlag tagged LlaBIII construct carrying the SV40 NLS under CMV promoter was transfected into HEK293 cells. LlaBIII expression was monitored 72 hours post transfection,

through fluorescent *in-situ* hybridization (FISH) and immunoblotting. Anti-Flag antibodies were used for detection of LlaBIII. Analysis of microscopic images after FISH showed a strong signal for LlaBIII in the nucleus of cells (Fig. 5.7). We could thus conclude that LlaBIII was expressed and successfully transported to the nucleus. Though, the transfection efficiency was poor and only ~10-15% cells showed the signal for Flag-tagged protein. This could be due to inefficient uptake of the large plasmid (10.5 Kbp) by the cells or inefficient transcription-translation of the high molecular weight protein-LlaBIII n^- (~160 KDa) or due to poor heterologous expression of the bacterial protein in mammalian cells. Another challenge was the mis-interpretation due to the presence of Flag tag at the N-terminus of the protein. Essentially, the Flag signals could be detected from even partially translated, truncated versions of LlaBIII. To ensure that the full-length enzyme was being produced in these cells, we probed for LlaBIII in the cell lysates through Western blotting technique. A ~160 KDa band corresponding to the molecular weight of LlaBIII $n^-m^+a^+$ and LlaBIII $n^-m^-a^+$ was detected in the respective cell lysates (Fig. 5.8). Also, this band was absent in the lysate from empty vector transfected cells. This confirmed that the signal observed in FISH was indeed that of LlaBIII and protein was successfully expressed and transported to nucleus in HEK293 cells.

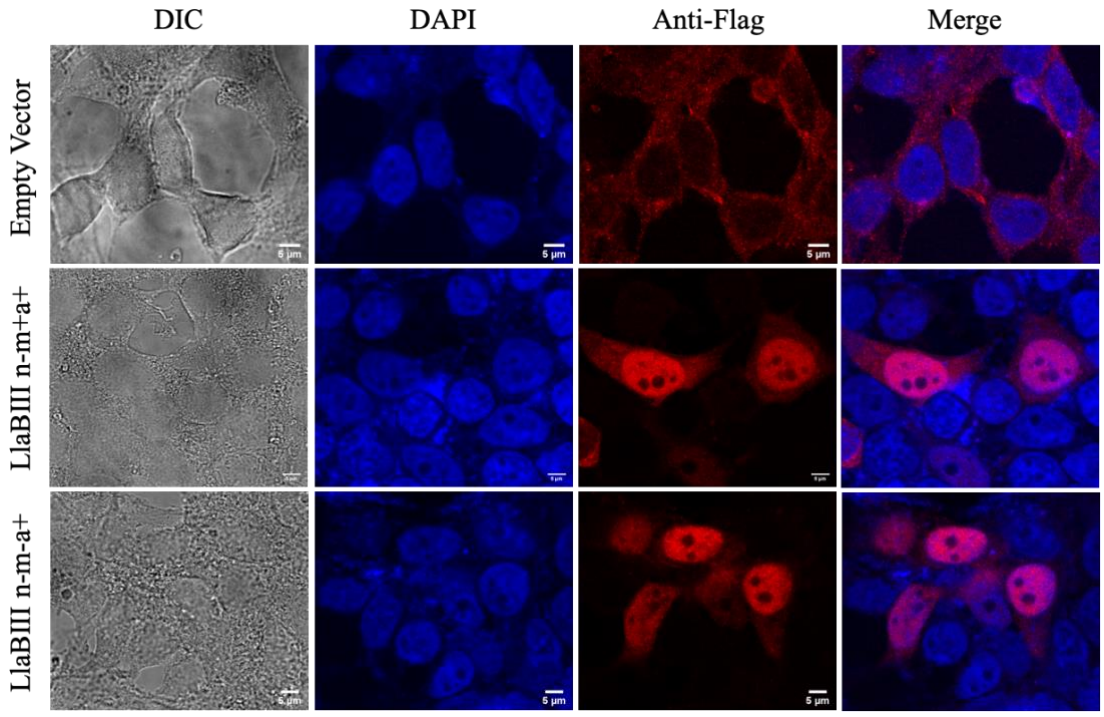

Figure 5.7: Localization of LlaBIII mutants in HEK293 cells. Representative confocal microscopy images of HEK293 cells transfected with empty vector (*pCMV10*), *pCMV10-llabiii* $n^{-}m^{+}a^{+}$ and *pCMV10-llabiii* $n^{-}m^{-}a^{+}$. Each row shows images sequentially as labelled, DIC, DAPI, anti-Flag (LlaBIII) and merge. N=2

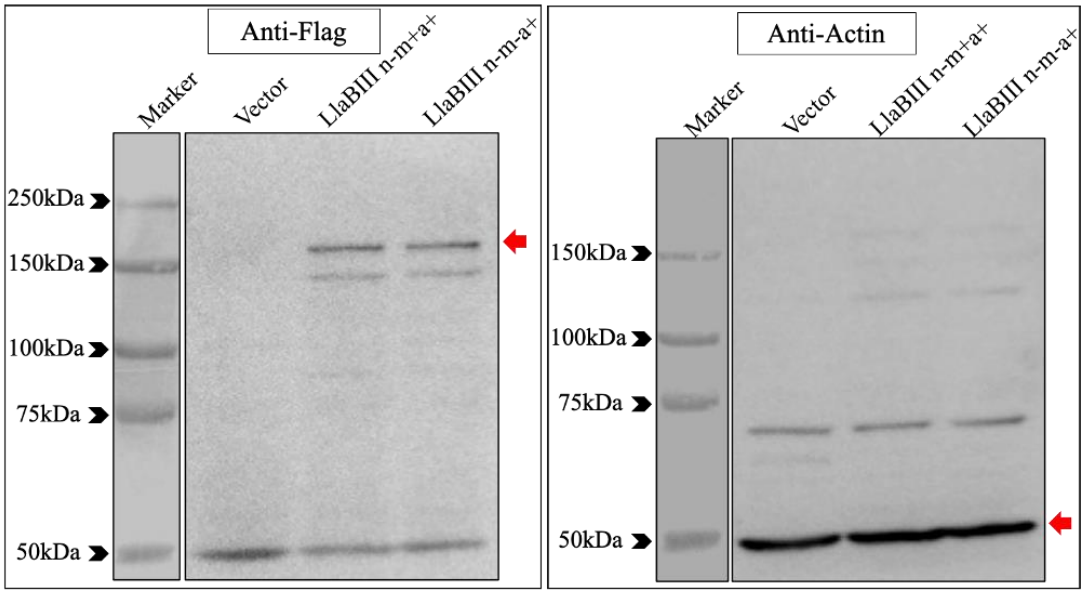

Figure 5.8: Immunoblots showing full length expression of LlaBIII mutants in HEK293 cells. The blot was probed with anti-Flag antibody for LlaBIII constructs and anti-actin antibody for actin. Red arrows indicate the bands of interest in each blot. N=2

5.3.4 Quantitative RT-PCR to monitor changes in transcription from the specific gene loci

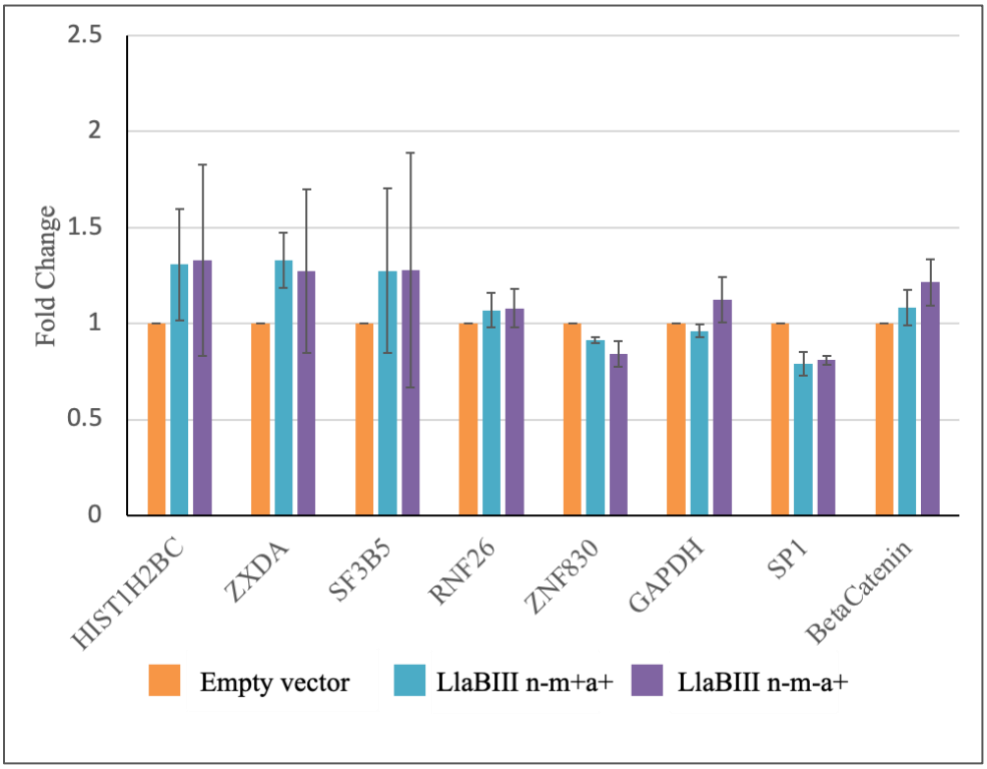

Figure 5.9: Quantitative RT-PCR showing gene transcription in LlaBIII mutants' transfected HEK293 cells. N=2

LlaBIII target sites (TNAGCC) are abundant in the human genome and occur at high frequency. The LlaBIII $n^{-}m^{+}a^{+}$ and $n^{-}m^{-}a^{+}$, produced and transported to nucleus of HEK293 cells, was expected to encounter many of these target sites and translocate DNA upon binding to unmethylated target sites. It is therefore highly likely that DNA translocation by LlaBIII leads to nucleosome displacement downstream of its target sites in the genome. When the target sites are close to gene regulatory or coding regions, it is likely to perturb transcription of those genes. Thus, nucleosome remodeling by LlaBIII in HEK293 cells can be monitored by correlating the changes in gene transcription profile, in presence and absence of LlaBIII, and the presence of target sites in the vicinity of gene loci. For this we selected seven single exon housekeeping genes and mapped all the LlaBIII sites in the coding region, the 5' UTR (2 Kbp) and 3' UTR (1 Kbp) regions. Quantitative RT-PCR was performed to monitor any changes in the transcription profiles of these genes in presence and absence of LlaBIII. As all the selected genes were housekeeping genes, the

transcript levels were normalized with reference the gene (HEXIM1) which showed almost no variance (Ct values) between vector control and test samples. We did not observe any significant differences in the fold change for the selected genes in test samples when compared to the control (Fig. 5.9). The lack of difference here does not necessarily indicate lack of nucleosome remodeling, and could rather be due to lack of enrichment of transfected cells. As the transfection efficiency was low, the effect of nucleosome remodeling cannot be observed in the entire cell population. The signal from the transfected cells can get masked by the majority of un-transfected cells. In future experiments, the transfected cells need to be enriched in the samples using suitable strategies (FACS or selectable marker), before processing them for quantitative RT-PCR.

5.4 Discussion

Previously, we had established the ability of LlaBIII to modulate protein-DNA interactions *in vitro*. In this section we tried to assess the effect of LlaBIII translocation on protein-DNA interactions in live cells – bacterial and mammalian cells. In order to do so we first created a mutant of LlaBIII lacking the nuclease and methyltransferase activity leaving the target recognition and DNA translocation activities unperturbed (LlaBIII $n^-m^-a^+$). We also created an ATPase defective mutation (LlaBIII $n^-m^-a^-$). These mutants were created to serve as controls for the LlaBIII mediated remodeling experiments *in vivo*. In *E. coli*, we looked at the effect of LlaBIII on localization of an important nucleoid associated protein, HU. We hypothesized that LlaBIII translocation on bacterial genomic DNA might have an effect on its interaction with nucleoid associated proteins such as HU. In turn, their localization should be disrupted by the presence of LlaBIII. We used an *E. coli* strain that expressed GFP-tagged HU from the genome at physiological levels. We found that HU is usually bound to the nucleoid which remains in a compact state in stationary phase. Introduction of LlaBIII translocase active (LlaBIII $n^-m^-a^+$) and defective constructs (LlaBIII $n^-m^-a^-$) in these bacterial cells disrupted the nucleoid structure making it more dispersed rather than compact. HU localization also changed from entirely coating the nucleoid to forming sub-polar foci where an accumulation of the protein can be observed. Whether the HU foci coincide with a part of the nucleoid is unclear yet but there is clear disruption of usual HU-nucleoid interaction which may have led to the change in nucleoid architecture as well. It still remains to be investigated whether the effect is specific to LlaBIII binding to the nucleoid or there is an effect of LlaBIII DNA translocation that leads to removal of HU from the DNA.

Next, we looked at the effect of LlaBIII expression on mammalian cells. We were able to transiently express full length LlaBIII n^- constructs in HEK293 cells. Addition of NLS tag ensured that the expressed protein was successfully transported to the nucleus of these cells. Being a large protein, the size of the plasmid constructs was fairly large, which possibly affected the transfection procedure and hence resulted in low transfection efficiency, wherein less than ~10-15 percent cells expressed these proteins. LlaBIII target site (TNAGCC) is fairly abundant in the human genome and would often be in close proximity to nucleosome occupying regions. Any changes in the nucleosome occupancy in these regions would have a direct effect on the gene transcription from nearby gene loci. Thus, we aimed to gauge the effect of LlaBIII mediated nucleosome remodeling in these cells by monitoring the effects on gene expression from selected gene loci. Single exon genes with multiple combinations of LlaBIII target sites in their 5'- and 3'-UTR were selected for monitoring the effect of LlaBIII expression in these cells. Quantitative RT-PCR analysis for these genes show no change in gene expression from these gene loci. This lack of change may be attributed to the masking of an effect, if any, in minority of transfected cells by majority of un-transfected cells in the samples. An attempt to prepare stable HEK293 cell line also failed. This could possibly be because stable expression of LlaBIII might be hazardous to the cellular homeostasis hence result in cell death. To overcome these issues, a way of enriching transfected cells has to be found before processing the cells for qRT-PCR in future.

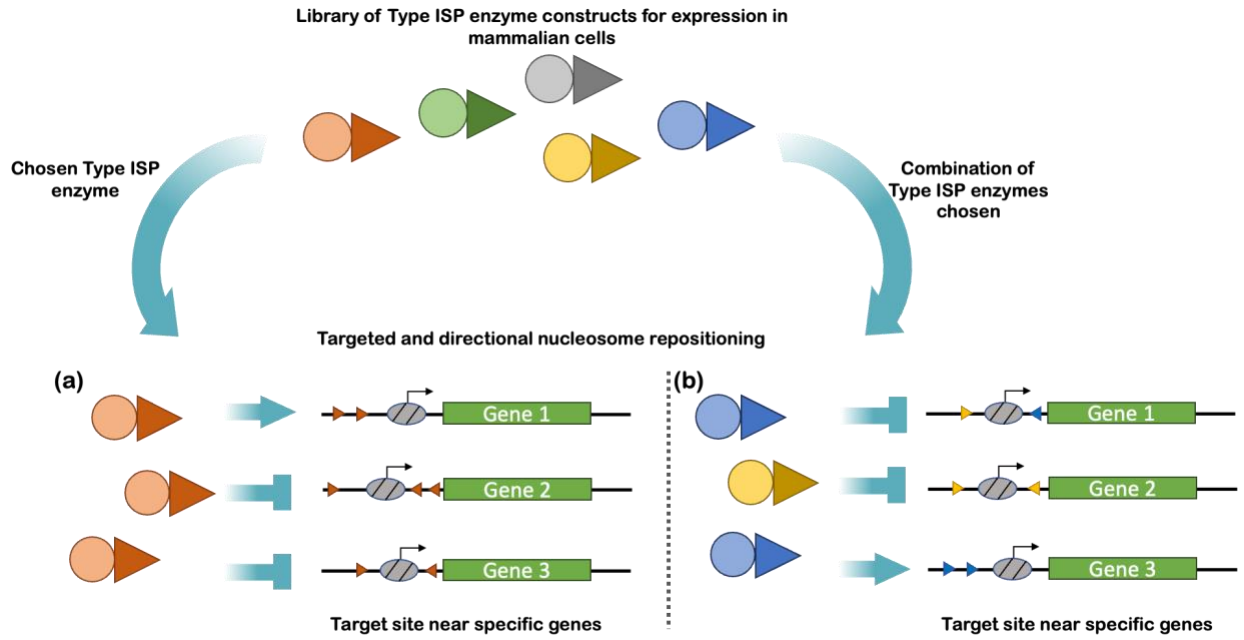

Figure 5.10: Schematic elaborating possible applications of Type I RM enzymes as targeted chromatin remodelers. A library of Type I RM enzymes can be made available, each recognizing a specific target sequence, can be used as target dependent chromatin remodelers in live cells. (a) Potential use of a single target specific enzyme for regulation of different target genes. Nucleosome occupancy could be modulated by presence of multiple specific target sites and their orientation in and around gene coding regions causing increase or decrease in DNA accessibility to transcription factors and RNA polymerase. (b) Potential use for two enzymes recognizing two different target sites for differential gene regulation at various gene loci depending on the target site availability and their orientations with respect to the gene body or gene regulation elements and relative nucleosome occupancy in the given regions. Nucleosomes can either be slid off these elements to promote gene expression or their sliding can be prevented to inhibit gene expression.

A successful demonstration of LlaBIII as a chromatin remodeler in live cells would be a significant finding in the field of targeted chromatin remodelers. LlaBIII is essentially a target dependent enzyme that can also remodel nucleosomes. This is a distinguishing characteristic of LlaBIII, as there are not any reports of such a simple, direct and naturally occurring DNA target-dependent chromatin remodeler in the literature. There are a few studies that report development of a system for DNA-targeted chromatin modulation. Most of these studies utilize the catalytic domain of a

canonical chromatin remodeler and fuse it to a specific or non-specific DNA binding domain (DBD) derived from either a transcription regulator or an engineered DBD (Donovan et al., 2019; McKnight et al., 2011b, 2016; Patel et al., 2013). Additionally, there are other strategies that have been tested to achieve chromatin remodeling at desired loci in the genome. For example, the engineered zinc finger proteins were fused with catalytic subunits of eukaryotic ATP-dependent chromatin remodelers Swi-Snf, RSC and Ino80 to create fusion proteins that could thus be targeted to specific regions in the genome (Keung et al., 2014). Alternatively, there are numerous studies that aim to specifically modify the targeted regions of the chromatin to trigger downstream chromatin remodeling machinery which may either activate or suppress gene expression from that region. These utilize fusions of chromatin modifying or regulatory enzymes with either nuclease dead Cas9 (Hilton et al., 2015; Kearns et al., 2015; Perez-Pinera et al., 2013) or engineered zinc finger proteins (Nunna et al., 2014; Rivenbark et al., 2012; Snowden et al., 2002) or TALE proteins (Mendenhall et al., 2013). The DNA regulators used in these are generally DNA or histone modification enzymes that either add or remove a methyl or acetyl group and hence indirectly affect gene expression from the targeted loci (Donovan et al., 2019; Hilton et al., 2015; Mendenhall et al., 2013; Perez-Pinera et al., 2013). The interaction between engineered protein like SpyCatcher with SpyTag epitope (Zakeri et al., 2012) has also been utilized for targeted gene regulation. Here the SpyTag epitope is linked to a DBD like a transcription factor, and the SpyCatcher is fused to a chromatin remodeler catalytic domain (Donovan et al., 2019). Although specific to a certain degree, these strategies involve extensive gene engineering for creating gene fusions or multiple gRNA or epitope fusions expression in cells for them to function efficiently. These studies have either used a homologous protein or used a fusion construct to overcome the complexities of the cellular conditions when utilizing an engineered enzyme system. Most of these strategies involve direct competition with endogenous factors for binding sites and also affect the stability of the interaction once the DBD bind to its target. The effect of these engineered chromatin remodelers is limited to close proximity of the binding site thus limiting its utility depending on the binding site availability near target chromatin regions. Since majority of these strategies utilize an endogenous DBD and chromatin remodeler, these have to be extensively tailored for every target gene and cell line. A heterologous chromatin remodeler like LlaBIII, that recognizes a short target sequence, can overcome these limitations. It is unaffected by the cellular signaling cascades and the target sites are not in direct competition for binding with other endogenous factors. This

remodeler does not require extensive protein engineering or gene modifications in the cells to perform targeted nucleosome rearrangements. Moreover, being entirely heterologous, it can be employed in many cells lines without making significant changes. It can also be easily incorporated into the cellular networks allowing temporal control over its expression and chromatin remodeling. There are numerous Type ISP RM enzymes that recognize a specific target sequence and translocate DNA. All these enzymes have the potential to be developed into a targeted chromatin remodeling tool thus providing us with a library of chromatin remodeling enzymes. A single enzyme can be used to target multiple genes or multiple enzymes can be employed in combination to upregulate or down regulate different genes based on target site availability in the gene vicinity (Fig. 5.10). Once successfully tested in live cells, these enzymes would provide an easily accessible modular library of proteins that require minimal tweaking to be used as sequence specific chromatin remodelers in multiple cell types and organisms. A single enzyme can be used to target multiple genes or multiple enzymes can be employed in combination to upregulate or down regulate different genes based on target site availability in the gene vicinity (Fig. 5.10). Once successfully tested in live cells, these enzymes would provide an easily accessible modular library of proteins that require minimal tweaking to be used as sequence specific chromatin remodelers in multiple cell types and organisms. As elaborated in figure 5.10, the Type I RM enzyme constructs can be developed for expression in eukaryotic cells. As each of these enzymes recognize a unique target sequence, they can be targeted to specific genes that need to be modulated. Available sequencing data would allow mapping of target sites at specific target gene loci and allow selection of enzymes from this library based on user requirements. The number and orientation of target sites in and around the gene body and gene regulatory elements (promoter, enhancer, transcription start site) would allow to either deplete these regions of nucleosomes so that gene transcription can be enhanced or preserve nucleosome occupancy such that gene transcription is inhibited.

5.5 References

Abebe, A. H., Aranovich, A., & Fishov, I. (2017). HU content and dynamics in Escherichia coli during the cell cycle and at different growth rates. *FEMS Microbiology Letters*, *364*(19), fnx195. https://doi.org/10.1093/femsle/fnx195

Chand, M. K., Carle, V., Anuvind, K. G., & Saikrishnan, K. (2020). DNA-mediated coupling of ATPase, translocase and nuclease activities of a Type ISP restriction-modification enzyme. *Nucleic Acids Research*, *48*(5), 2594–2603. https://doi.org/10.1093/nar/gkaa023

Chand, M. K., Nirwan, N., Diffin, F. M., Van Aelst, K., Kulkarni, M., Pernstich, C., Szczelkun, M. D., & Saikrishnan, K. (2015). Translocation-coupled DNA cleavage by the Type ISP restriction-modification enzymes. *Nature Chemical Biology*, *11*(11), 870–877. https://doi.org/10.1038/nchembio.1926

Donovan, D. A., Crandall, J. G., Banks, O. G. B., Jensvold, Z. D., Truong, V., Dinwiddie, D., McKnight, L. E., & McKnight, J. N. (2019). Engineered Chromatin Remodeling Proteins for Precise Nucleosome Positioning. *Cell Reports*, *29*(8), 2520-2535.e4. https://doi.org/10.1016/j.celrep.2019.10.046

Hall, M. C., & Matson, S. W. (1999). Helicase motifs: the engine that powers DNA unwinding. *Molecular Microbiology*, *34*(5), 867–877. https://doi.org/https://doi.org/10.1046/j.1365-2958.1999.01659.x

Hanson, P. I., & Whiteheart, S. W. (2005). AAA+ proteins: have engine, will work. *Nature Reviews Molecular Cell Biology*, *6*(7), 519–529. https://doi.org/10.1038/nrm1684

Hartmann, R., van Teeseling, M. C. F., Thanbichler, M., & Drescher, K. (2020). BacStalk: A comprehensive and interactive image analysis software tool for bacterial cell biology. *Molecular Microbiology*, *114*(1), 140–150. https://doi.org/https://doi.org/10.1111/mmi.14501

Hilton, I. B., D'Ippolito, A. M., Vockley, C. M., Thakore, P. I., Crawford, G. E., Reddy, T. E., & Gersbach, C. A. (2015). Epigenome editing by a CRISPR-Cas9-based acetyltransferase activates genes from promoters and enhancers. *Nature Biotechnology*, *33*(5), 510–517. https://doi.org/10.1038/nbt.3199

Kearns, N. A., Pham, H., Tabak, B., Genga, R. M., Silverstein, N. J., Garber, M., & Maehr, R. (2015). Functional annotation of native enhancers with a Cas9–histone demethylase fusion. *Nature Methods*, *12*(5), 401–403. https://doi.org/10.1038/nmeth.3325

Keung, A. J., Bashor, C. J., Kiriakov, S., Collins, J. J., & Khalil, A. S. (2014). Using Targeted Chromatin Regulators to Engineer Combinatorial and Spatial Transcriptional Regulation. *Cell*, *158*(1), 110–120. https://doi.org/10.1016/j.cell.2014.04.047

Klimasauskas, S., Timinskas, A., Saulius, M., Butkienè, D., Butkus, V., & Janulaitis, A. (1989). Sequence motifs characteristic of DNA[cytosine-N4]methyltransferases: similarity to adenine and cytosine-C5 DNA-methylases. *Nucleic Acids Research*, *17*(23), 9823–9832. https://doi.org/10.1093/nar/17.23.9823

Kong, H., & Smith, C. L. (1997). Substrate DNA and cofactor regulate the activities of a multi-functional restriction-modification enzyme, BcgI. *Nucleic Acids Research*, *25*(18), 3687–3692. https://doi.org/10.1093/nar/25.18.3687

McKnight, J. N., Jenkins, K. R., Nodelman, I. M., Escobar, T., & Bowman, G. D. (2011). Extranucleosomal DNA Binding Directs Nucleosome Sliding by Chd1. *Molecular and Cellular Biology*, *31*(23), 4746–4759. https://doi.org/10.1128/MCB.05735-11

McKnight, J. N., Tsukiyama, T., & Bowman, G. D. (2016). Sequence-targeted nucleosome sliding in vivo by a hybrid Chd1 chromatin remodeler. *Genome Research*, *26*(5), 693–704. https://doi.org/10.1101/gr.199919.115

Mendenhall, E. M., Williamson, K. E., Reyon, D., Zou, J. Y., Ram, O., Joung, J. K., & Bernstein, B. E. (2013). Locus-specific editing of histone modifications at endogenous enhancers. *Nature Biotechnology*, *31*(12), 1133–1136. https://doi.org/10.1038/nbt.2701

Nunna, S., Reinhardt, R., Ragozin, S., & Jeltsch, A. (2014). Targeted Methylation of the Epithelial Cell Adhesion Molecule (EpCAM) Promoter to Silence Its Expression in Ovarian Cancer Cells. *PLOS ONE*, *9*(1), e87703-. https://doi.org/10.1371/journal.pone.0087703

Patel, A., Chakravarthy, S., Morrone, S., Nodelman, I. M., McKnight, J. N., & Bowman, G. D. (2013). Decoupling nucleosome recognition from DNA binding dramatically alters the properties of the Chd1 chromatin remodeler. *Nucleic Acids Research*, *41*(3), 1637–1648. https://doi.org/10.1093/nar/gks1440

Perez-Pinera, P., Kocak, D. D., Vockley, C. M., Adler, A. F., Kabadi, A. M., Polstein, L. R., Thakore, P. I., Glass, K. A., Ousterout, D. G., Leong, K. W., Guilak, F., Crawford, G. E., Reddy, T. E., & Gersbach, C. A. (2013). RNA-guided gene activation by CRISPR-Cas9–based transcription factors. *Nature Methods*, *10*(10), 973–976. https://doi.org/10.1038/nmeth.2600

Rivenbark, A. G., Stolzenburg, S., Beltran, A. S., Yuan, X., Rots, M. G., Strahl, B. D., & Blancafort, P. (2012). Epigenetic reprogramming of cancer cells via targeted DNA methylation. *Epigenetics*, *7*(4), 350–360. https://doi.org/10.4161/epi.19507

Šišáková, E., Van Aelst, K., Diffin, F. M., & Szczelkun, M. D. (2013). The Type ISP Restriction-Modification enzymes LlaBIII and LlaGI use a translocation-collision mechanism to cleave non-specific DNA distant from their recognition sites. *Nucleic Acids Research*, *41*(2), 1071–1080. https://doi.org/10.1093/nar/gks1209

Smith, R. M., Diffin, F. M., Savery, N. J., Josephsen, J., & Szczelkun, M. D. (2009). DNA cleavage and methylation specificity of the single polypeptide restriction-modification enzyme LlaGI. *Nucleic Acids Research*, *37*(21), 7206–7218. https://doi.org/10.1093/nar/gkp790

Smith, R. M., Josephsen, J., & Szczelkun, M. D. (2009). The single polypeptide restriction-modification enzyme LlaGI is a self-contained molecular motor that translocates DNA loops. *Nucleic Acids Research*, *37*(21), 7219–7230. https://doi.org/10.1093/nar/gkp794

Snowden, A. W., Gregory, P. D., Case, C. C., & Pabo, C. O. (2002). Gene-Specific Targeting of H3K9 Methylation Is Sufficient for Initiating Repression In Vivo. *Current Biology*, *12*(24), 2159–2166. https://doi.org/10.1016/S0960-9822(02)01391-X

Van Aelst, K., Saikrishnan, K., & Szczelkun, M. D. (2015). Mapping DNA cleavage by the Type ISP restriction-modification enzymes following long-range communication between DNA sites in different orientations. *Nucleic Acids Research*, *43*(21), 10430–10443. https://doi.org/10.1093/nar/gkv1129

Van Aelst, K., Šišáková, E., & Szczelkun, M. D. (2013). DNA cleavage by Type ISP Restriction-Modification enzymes is initially targeted to the 3′-5′ strand. *Nucleic Acids Research*, *41*(2), 1081–1090. https://doi.org/10.1093/nar/gks1210

Willcock, D. F., Dryden, D. T., & Murray, N. E. (1994). A mutational analysis of the two motifs common to adenine methyltransferases. *The EMBO Journal*, *13*(16), 3902-3908–3908. https://doi.org/https://doi.org/10.1002/j.1460-2075.1994.tb06701.x

Zakeri, B., Fierer, J. O., Celik, E., Chittock, E. C., Schwarz-Linek, U., Moy, V. T., & Howarth, M. (2012). Peptide tag forming a rapid covalent bond to a protein, through engineering a bacterial adhesin. *Proceedings of the National Academy of Sciences*, *109*(12), E690–E697. https://doi.org/10.1073/pnas.1115485109